PONTIFICIA
UNIVERSIDAD
CATÓLICA
DE CHILE

FACULTAD DE CIENCIAS BIOLÓGICAS
DEPARTAMENTO DE BIOLOGÍA CELULAR Y MOLECULAR

uLSD1/neuroLSD1 ratio is a molecular sensor of dopaminergic transmission and a regulator of the immediate-early gene Nur77

By

Montserrat Olivares Costa

Thesis submitted to the Pontificia Universidad Católica de Chile in partial compliance with the requirements for the Ph.D. in Biological Sciences with a mention in Cellular and Molecular Biology.

Thesis Advisor: Dra. María Estela Andrés Coke

November 2020
Santiago, Chile

A dos de las personas que más han influido en mi vida. Mi madre quien, con una valentía y abnegación admirables, me dio la vida en dos ocasiones. Gianluca Merello, quien con su amistad cambió mi vida.

Agradecimientos

Este fue un proceso largo en el que mucha gente linda se cruzó por mi camino y no es necesario plasmar el nombre de cada una de ellas aquí, porque me he asegurado de que sepan lo agradecida que les estoy y, sobre todo, porque es algo que nunca van a leer. Sin embargo, no puedo dejar de mencionar a las personas que han estado involucradas directamente en este trabajo. Mi tutora, la Dra. Estela Andrés, quién me ha tenido una paciencia infinita y me ha apoyado y guiado durante la gran cantidad de etapas que pasé para llegar a terminar este escrito.

Carlos, Verónica, Fabián, Julián, Natalia, Angélica, son solo algunas de las personas que pasaron por este laboratorio y que de una u otra forma contribuyeron a este proyecto y a mi bienestar, les agradezco enormemente el buen ambiente y la disposición a ayudar que siempre han mostrado. Mención aparte para la Marce, sin quien gran parte de esta tesis no sería posible, también reconocer el apoyo muchas veces silencioso de la Señora Sole, la Señora Bárbara y Don Héctor. Por último, mencionar quienes se convirtieron en grandes amigos, a mis queridos Cristian Arredondo, Duxan Arancibia, Daniel Verbel y Gianluca Merello, de quienes he aprendido mucho, dentro y fuera de la cancha.

Table of contents

Agradecimientos 2
Table of contents 3
Table of figures 6
Table index 8
Resumen 9
Abstract 11
Introduction 13
1.- Immediate early genes 13
1.1 IEGs structural features. 14
1.2 IEGs expression in neurons 15
2. The immediate-early gene *Nur77* 17
2.1 Nur77 protein structure and DNA binding 18
2.2 Nur77 as a reader of dopaminergic transmission 19
3. LSD1, an epigenetic modifier 21
3.1 LSD1 expression and splicing regulation 23
3.2 LSD1 as a regulator of IEG in brain 24
Hypothesis 26
General aim 26
Specifics aims 26
LSD1 microexon E8a as a synaptic dopamine sensor and negative regulator of LSD1 expression 27
Abstract 29
Significance statement 30
Introduction 31
Materials and Methods 33
Animals 33
Drug treatments 33
Exon Inclusion Frequency by Relative Quantity Fluorescent-PCR (rqf-PCR) and q-PCR. 34
SDS-PAGE immunoblot 35
Fast Scan cyclic voltammetry 35

Locomotor sensitization 36

Statistical analyses 37

Results 38

Transient modulation of LSD1-RCOR1 protein levels and of H3K4me2 after acute administration of AMPH 38

Repeated administration of AMPH decreases LSD1 in mice brain by a neuroLSD1-dependent negative feedback. 41

Selective D2 receptor modulation alters LSD1 alternative splicing in the striatum. 44

Wild-type and neuroLSD1 null mice display similar locomotor response to AMPH administration. 47

neuroLSD1 null mice exhibit reduced release and faster reuptake of dopamine in response to AMPH 50

Discussion 54

References 57

Supplementary data 59

Annex 1 62

rqf-PCR standardization 62

Chapter II 66

Transactivation of IEGs by neuroLSD1, a mechanism dependent on phosphorylation state of an exclusively neuronal-expressed threonine. 66

Abstract 68

Significance statement 69

Introduction 70

Materials and Methods 72

Animals 72

qPCR and rqf-PCR 72

Characterization of the *NR4A1* promoter region 73

Cell lines culture conditions 74

Transient transfection and reporter gene assays 74

Chromatin immunoprecipitation (ChIP) assays 74

Primary culture and bicuculline treatment 75

Immunofluorescence 76

Statistical analyses 76

Results 77
Structure and characterization of *NR4A1* promoter region 77
LSD1 and neuroLSD1 but not the phosphomimetic neuroLSD1 mutant increase *NR4A1* promoter activity 80
Similar induction of *NR4A1* and cFOS in wild-type and neuroLSD1 null mice cultured neurons. 83
Discussion 86
References 89
Supplementary data 92
Discussion 94
References 98
Annex 2: 105
A bioinformatics approach reveals Nur77-regulated genes common to the nervous and immune systems 105
Abstract 106
Introduction 107
Methods 110
Data acquisition 110
Nur77 binding site characterization 110
Microarray analyses 111
Ontology analysis 111
Results and discussions 112
Characterization of Nur77 binding sites throughout the genome. 112
Nur77 target genes in immune cells and neurons actively regulated by Nur77 115
Immune and nervous common Nur77 target genes 118
References 123
Supporting information 126
Supplementary reference 127

Table of figures

Introduction

Figure 1: Location of the four neuroLSD1-exclusive amino acids ….…..…… 23

Chapter I: LSD1 microexon 8a as a sensor of synaptic dopamine and negative regulator of LSD1 expression

Figure 1: AMPH acute administration modulates H3K4 methylation and LSD1-RCOR1 protein levels…… 40
Figure 2: AMPH chronic administration decreases total LSD1 expression in a neuroLSD1-dependent way…… 43
Figure 3: uLSD1/neuroLSD1 ratio is modulated by D2R-mediated signaling…….46
Figure 4: NeuroLSD1 null mice exhibit AMPH-induced locomotor activity similar to WT…… 49
Figure 5: neuroLSD1 null mice exhibit decreased electrically evoked dopamine release in response to AMPH. …… 52
Figure S.1 uLSD1/neuroLSD1 transcripts ratio remains constant in the hippocampus after acute AMPH injection. ……..…….. 59
Figure S.2: AMPH chronic administration modulated total LSD1 and neuroLSD1 expression in the PFC. …….. 59
Figure S.3: neuroLSD1 proportion is increased in the PFC after systemic quinpirole injection. ……...60
Figure S.4: Percentage of exon 2a inclusion in D2R deficient mice is similar to WT. …….. 61

Annex 1: rqf-PCR standardization

Figure1: rqf-PCR, examples of primer design and the PCR generated amplicons... 63
Figure 2: Example of electropherograms ..…… 64
Figure 3: Validation of rqf-PCR, measuring all LSD1 isoforms…… 65

Chapter II: Transactivation of IEGs by neuroLSD1, a mechanism dependent on phosphorylation state of an exclusively neuronal-expressed threonine.

Figure 1: characterization of NR4A1 promoter region. …… 79
Figure 2: uLSD1 and neuroLSD1 induce NR4A1 promoter activity …….. 82
Figure 3: Similar bicuculline-dependent induction of IEGs in cultured hippocampal neurons of wild-type and neuroLSD1 null mice…….....84
Figure S.1: Active chromatin marks in NR4A1 promoter region. ……..…….. 92
Figure S.2: NR4A1-luciferase concentration-effect curve. ……... 93

Discussion

Figure1: neuroLSD1 mediated negative feedback, proposed model……..……..120

Annex 2: A bioinformatics approach reveals Nur77-regulated genes common to the nervous system and immune system

Figure1: Nur77 binds to active promoters and strong enhancers in K562 cells…....104
Figure 2: Nur77 target genes in neurons and immune cells. ……..107
Figure 3: GO analysis of common target genes for Nur77 among the immune and nervous systems. …… 110

Table index

Chapter I: LSD1 microexon 8a as a sensor of synaptic dopamine and negative regulator of LSD1 expression

Table 1: Dopamine content in the striatum of WT, HT and neuroLSD1 null mice…… 63

Annex 2: A bioinformatics approach reveals Nur77-regulated genes common to the nervous system and immune system

Table S.1: Nur77 target genes in the K562 cell line……116
Table S.2: Nur77 target genes in NSC……116
Table S.3: Nur77 target genes in NC……116
Table S.4: Nur77 target genes common to lymphatic and neuronal systems ……117
Table S.5: GO terms enriched in the analysis of Nur77 target genes……117

Resumen

Los genes tempranos inmediatos (IEG, por sus siglas en inglés) son rápida y transitoriamente inducidos luego de la estimulación neuronal y su función está estrechamente relacionada con plasticidad sináptica y regulación de la expresión génica. El IEG, *NR4A1* (Nur77) es un factor de transcripción altamente modulado por la transmisión dopaminérgica y se ha relacionado a enfermedades que se caracterizan por alteraciones en el sistema dopaminérgico como estrés, ansiedad, adicción y esquizofrenia. Sin embargo, los mecanismos que regulan su expresión, así como su función específica en las neuronas, no están del todo comprendidos. Nosotros proponemos a la enzima epigenética, Desmetilasa Específica de Lisina 1 (LSD1 por sus siglas en inglés) como un modulador de la expresión de *NR4A1*. LSD1 tiene una variante neuronal específica, neuroLSD1, que es necesaria para la diferenciación neuronal y participa en procesos como memoria, aprendizaje y respuesta a estrés. Ratones nulos para neuroLSD1 son menos propensos a mostrar un comportamiento ansioso, asociado con una menor inducción de IEGs comparado con ratones nativos. Los datos mencionados anteriormente nos llevan a proponer a LSD1 como un efector de las respuestas moleculares y de comportamiento mediadas por dopamina. Nuestros datos sugieren que la señalización a través de los receptores D2 de dopamina regulan la expresión de LSD1 y neuroLSD1. La administración aguda y crónica de anfetamina provoca cambios transitorios y a largo plazo en los niveles de LSD1, revelando un sistema de regulación negativa ejercido por neuroLSD1 sobre su propio gen. La caracterización neuroquímica y locomotora de ratones nulos para neuroLSD1 mostró una disminución en la liberación de dopamina, pero niveles similares de sensibilización locomotora cuando son tratados con anfetamina, en comparación a ratones

nativos. Nuestros datos también muestran que tanto LSD1 como neuroLSD1 incrementan la actividad del promotor de *NR4A1*. Mediante el tratamiento con bicuculina de cultivos de neuronas hipocampales de ratones nulos para neuroLSD1 descartamos que neuroLSD1 es esencial para inducir la expresión de IEGs. Nuestros datos sugieren que la fosforilación de una treonina específica de neuroLSD1 es un interruptor de la transcripción de los IEGs. En conclusión, mostramos que LSD1 y neuroLSD1 son lectores de los niveles sinápticos de dopamina y modulan la expresión de *NR4A1,* un gen ligado a la neurotransmisión de dopamina. Finalmente, utilizamos las bases de datos disponibles para identificar los genes blanco de NR4A1 en un esfuerzo por revelar su función.

Abstract

Immediate Early genes (IEGs) are fast and transiently induced after neuronal stimulation, and their function is closely related to synaptic plasticity and gene expression regulation. The IEG, *NR4A1* (Nur77) is a transcription factor highly modulated by dopaminergic transmission and is related to diseases characterized by imbalances in dopamine system, such as stress, anxiety, addiction, and schizophrenia. However, mechanisms modulating its expression are not fully described as well as their specific function in neurons. Here we propose the epigenetic enzyme, Lysine-Specific Demethylase 1 (LSD1, KDM1A) as modulator of the *NR4A1* expression. LSD1 has a neuronal specific variant, neuroLSD1, that is necessary for neuronal differentiation and participates in processes such as memory, learning, and stress response. Mice null for neuroLSD1 are less prone to develop anxious behavior, associated with lower induction of IEGs compared to wild type littermates. All the aforementioned data lead us to propose LSD1 as an effector of the molecular and behavioral dopamine-mediated response. Our data suggest that signaling through D2 dopamine receptors regulates LSD1 and neuroLSD1 expression. Acute and repeated administration of amphetamine induce transient and long-term effects on LSD1 levels, revealing a negative feedback regulation exerted by neuroLSD1. Neurochemical and locomotor characterization of neuroLSD1 null mice show decreased dopamine release but similar locomotor sensitization when treated with amphetamine compared to wild-type mice. Our data also show that both LSD1 and neuroLSD1 increase the activity of the *NR4A1* promoter. By bicuculline treatment of cultured hippocampal neurons from neuroLSD1 null mice, we rule out that neuroLSD1 is essential for IEGs expression. Our data suggest that the phosphorylation of a neuroLSD1-specific threonine

conform an on/off switch for IEGs transcription. In conclusion, we show than LSD1 and neuroLSD1 are readers of dopamine synaptic levels and modulate the expression of the dopamine related IEG *NR4A1*. Finally, we use available data bases to identify NR4A1 target genes in an effort to unveil its function.

Introduction

1.- Immediate early genes

Cellular response to stimuli involves several processes occurring at different times. For instance, opening ligand-gated channels happens in milliseconds, the increase of second messengers in the cytoplasm in seconds or minutes, and long-lasting morphological changes can take hours. Gene expression induction also results from cellular stimulation. A group of genes can increase their transcriptional rate in a short time (few minutes from stimuli), and in the absence of protein synthesis, these genes are called immediate-early by analogy to virus genes[1,2] The immediate-early genes (IEGs) are also characterized by their low or undetectable basal expression and short lifetime of their mRNAs[1,3]. Unlike their transcriptional induction, the decay of their mRNA depends on protein synthesis[1].

Many IEGs code for transcription factors enabling the cell to start adequate programs in response to a particular stimulus. But also structural or effector proteins coded by IEGs have been described[4], like ARC (Activity-Regulated Cytoskeleton-associated protein)[5] and HOMER1a (Homer protein homolog 1, isoform A)[6], both involved in the regulation of the postsynaptic structure and function[7]. Concordantly, gene ontology analyses of human IEGs show enrichment in terms of transcriptional regulation and molecular functions[8].

The first genes described as immediate-early in eukaryotic cells were *Fos* and *Myc*, both coding transcription factors. Lau et al. demonstrated in 1985 and 1987 that these genes are fast and transiently induced in the presence of the protein synthesis inhibitor

cycloheximide, during Go/G1 transition and upon platelet-derived growth factor (PDGF) and fibroblast growth factor (FGF) stimulation[1,2].

Further studies showed that the IEGs induction patterns depend on both signaling maintaining and cellular context[9]. While transient stimulation leads to a concordant transient induction of IEGs, as *Fos* and *Erg1*, a sustained stimuli can maintain IEGs overexpression during all the time of cell stimulation[10].

Several intracellular pathways, as ERK MAPK, P38 MAPK, PKC, and RhoA-actin, activates regulatory proteins involved in the modulation of IEGs expression in response to a wide extensive kind of cellular stimuli like mitogens, growth factors, immune and neuronal signaling, cellular stress, etc.[11]. These signaling pathways can also lead to activation of other factors as the serum-response factor (SRF)[9] or induce histone modifications[12,13] both phenomena crucial for IEGs inductions.

1.1 IEGs structural features.

A growing amount of information about IEGs expression regulation is generated from individual experiments in specific conditions. Due to the variability of IEG responses, to establish a defined promoter region structure that rules the definition of IEGs is, until now, an elusive task. However, most of the IEGs share some fundamental properties: 1. A defined and unique transcription start site (TSS), 2. A high affinity TATA box on their core promoter and, 3. A reduced length and number of exons compared to other protein-coding genes[8].

Tullai and coworkers characterized the genetic features of the promoter regions of 49 IEGs from T98G human glioblastoma cells stimulated with PDGF. In their study, binding sites for the transcription factors, SRF, nuclear factor B (NF-κβ), PAX-3, and early growth response (KROX), are enriched on the upstream regions of human IEGs[8]. On the other hand, the binding sites for SRF, NF-κβ, cyclic AMP response element-binding protein

(CREB), and activator protein-1 (AP-1), are not only over-represented on the upstream regions of IEGs they are also highly conserved among species[8].

Pre-loaded RNA Polymerase II (Pol II) is on the IEGs promoters in resting conditions, increasing the amount of attached Pol II after stimulation[8,14]. Even though this is not a particular characteristic of IEGs, the Pol II occupancy after stimuli on the IEGs promoter is significantly higher than that observed on other kinds of genes[8]. *FOS* and *FOSB* are examples of these; they possess the preinitiation complex bound to their promoter on basal conditions but not detectable transcript, suggesting a paused Pol II and a modulatory mechanism at the transcriptional elongation level[15].

CpG islands are found only in a fraction of IEGs. CpG associated gene presents fewer stable nucleosomes, and therefore chromatin remodeling plays a discreet role in their induction[11]. For instance, the IEGs promoter regions are associated with both activation and repression chromatin marks. The active state-related trimethylation of lysine 4 of the histone3 (H3K4me3) abundant across IEGs promoters as well as the repression-related trimethylation of lysine 27 of the histone3 (H3K27me3)[11].

All these features suggest that the kinetics of IEGs expression is regulated by a combinatory of *cis* and *trans* elements. For instance. the differential attachment transcription factors, the presence of a strong TATA box and a paused Pol II. Also, body gene structure is related to fast transcription due to their reduced length and number of exons.

1.2 IEGs expression in neurons

Different IEGs are induced upon neuronal stimulation including, transcription factors, postsynaptic proteins, secretory factors, membrane proteins, and signaling molecules, most of them related to synaptic plasticity[16]. Increase on IEGs levels during a limited and specific time window after neuronal stimulation is necessary for establishment and maintenance of

synaptic long term potentiation (LTP)[17] and consequently, process as memory formation and learning are dependents of IEGs[18,19]

The expression pattern of IEGs in the nervous system is highly specific and differentially modulated by neuronal activity. Due to their reliable temporal and spatial expression pattern, the IEGs have been used to track neuronal activity in brain circuits in response to a specific stimuli[18,20]. These expression patterns will depend on the nature and intensity of the stimuli and the stimulated brain area[3,16,21]. For instance, *Fos* gene transcription increases at a higher stimulation umbral than *Egr-1* and *Arc*[21,22,23]. Therefore, *Fos* expression is mostly used to track neuronal activity after experimentally induced neuronal depolarization or paradigms with a substantial cognitive or emotional burden. In contrast, *Egr-1* or *Arc* expression are used for physiological levels of neuronal responses[16].

The molecular mechanism underlying IEG transcriptional modulation in neurons has been studied principally on how this fast induction could be possible when receptor activation occurs in the synapses, and therefore away from the nucleus. In these regards, calcium signaling is a critical factor in neuronal activity-mediated induction of IEGs[24,25,26]. The increase in cytosolic calcium levels after NMDA receptors activation and opening of voltage-gated ion channels during neuronal membrane depolarization activates the cAMP/PKA and CamKII pathways, resulting in phosphorylation and activation of the transcription factor CREB. Phosphorylated CREB binds the IEGs promoter region through CRE, activating it or increasing its transcriptional rate[27,28,29]. More than one CRE in the proximal promoter region is a common feature of almost all neuronal activity induced IEGs[16,30]. Beyond PKA and CamKII, other stimulus-dependent protein kinases as PI3K, ERK, and p38 MAPK converge on CREB activation in neurons[29], suggesting a wide range of stimuli modulating IEGs expression.

Other transcription factors essential for activity-dependent IEGs transcription in neurons are SRF, cFOS, and MEF2[16,27,31]. Concordantly, IEGs promoter regions are enriched in response elements for each of these transcription factors[32].

2. The immediate-early gene *Nur77*

Nur77 (also known as NGFI-B, TR3, and NR4A1)[33,34] is a ligand-independent transcription factor belonging to the nuclear receptors superfamily[35], and together with Nurr1(NR4A2)[36] and Nor1 (NR4A3)[37], compose the Nur subfamily. An IEG code each of the Nur members and are differentially expressed in the central nervous system[38].

The IEG coding Nur77, called *NR4A1,* is in chromosome twelve in humans and fifteen in mice, according to the genomic navigator assembly tool of the University of California Santa Cruz (UCSC)[39]. The canonical version of *Nr4a1* possesses seven exons in mice, and its mRNA is 2534 bp long (NCBI Reference Sequence: NM_010444.2) coding for a 601 amino-acid (aa) protein (Uniprot identifier: P12813). Two additional isoforms, giving rise shorter proteins, are generated by alternative splicing of the first exons[40]. However, these isoforms remain understudied. In humans, the *NR4A1* gene possesses eight exons, and its mRNA is 2692 bp long (Variant 1, NM_002135.4) coding for a 598 aa protein (P22736-1). Additionally, three mRNA isoforms and two protein variants of 661 and 325 aa are annotated in the NCBI (NM_173157.3, NM_001202233.1, and NM_001202234.1) and the Uniprot databases (P22736-2 and P22736-3) respectively. However, as in mice, these noncanonical isoforms are not studied.

Nur77 was first described in NGF-treated rat pheochromocytoma cells (PC12). It was identified as an IEG by its high and transient induction in the presence of the protein

synthesis inhibitor, cycloheximide[34]. PC12 cells possess an excitable membrane that could be depolarized by neurotransmitters or KCl and differentiate into neurons by treatment with NGF or forskolin[41,42,43]. The induction of Nur77 by the cAMP /PKA signaling pathway is necessary for neurite extension in forskolin-induced differentiation[44]. On the other hand, the increase of Nur77 by membrane depolarization is mediated by the Ca + / Camk pathway[45,46]**.** These two signaling pathways modulating Nur77 expression in PC12 converge in phosphorylation-dependent activation of CREB, Phospho-CREB bind CRE elements in the Nur77 promoter region activating its transcription[47,48].

2.1 Nur77 protein structure and DNA binding

All members of the NR4A transcription factors subfamily (Nur77, Nurr1, and Nor1) share the same protein structure that classical nuclear receptors[49,50]. Unstructured N-Terminal domain containing the transcriptional activation function-1 (AF1) is the less conserved domain among Nur factors with 26 to 28% of amino acid sequence identity. The central DNA binding domain (DBD) possesses two C2-C2 zinc finger motifs and is highly conserved among NR4A factors, with 94 to 95% of amino acid sequence identity. The C-terminal domain, which encloses the ligand-binding domain (LBD) and the ligand-dependent transcriptional activation function 2 (AF-2), is moderately conserved with 58 to 65% of amino acid sequence identity[49,50]. Crystallographic studies demonstrate that the ligand-binding pocket of Nur77 and Nurr1 is filled with bulky hydrophobic amino acids[51,52] and therefore, these transcription factors do not need a ligand to be fully activated. Thus, NR4A factors activity is regulated by interaction with coactivators or corepressors[49], modulation of their mRNA and protein levels[53], and posttranslational modifications[54,55,56].

Different oligomerization states have been described for NR4A subfamily members since all of them can bind DNA either as monomers when recruited to the Nerve-Growth-

Factor Inducible gene B (NGFI-B)-responsive elements (NBRE) (A/TAAAGGTCA)[57,58], or as homodimers or heterodimers to Nur-Responsive Elements (NurRE) (AAATG/AC/TCA)[59,60]. Interestingly, Nur77 and Nurr1 can also form heterodimers with the retinoid x receptor (RXR) when targeting the genome on DR5 elements (GGTTCAnnnnnAGGTCA)[61].

2.2 Nur77 as a reader of dopaminergic transmission

Nur77 is widely expressed in the Central Nervous System (CNS) and is particularly relevant to dopamine neurotransmission[62,63,64,65,66], being expressed in target areas of dopamine neurons including the dorsal striatum (DS), the nucleus accumbens (NAc) and the prefrontal cortex (PFC)[61,62,67]. Remarkably, brain pathologies characterized by imbalances of dopaminergic neurotransmission, such as anxiety, addiction, and schizophrenia, are associated with changes in the expression of Nur77[38,68,69]. Nur77 also seems to play a key role in neurodegenerative disorders. For instance, Nur77 expression is significantly increased at the substantia nigra in animal models of Parkinson's disease. It appears to be involved in the loss of dopaminergic cells, given that the genetic disruption of NR4A1 gene reduced the loss of dopaminergic neurons induced by neurotoxins[70].

The widely used typical antipsychotic, Haloperidol induced a significant increase of Nur77 expression in DS and NAc of brain rodents[65,66,71]. Typical antipsychotics are dopamine D2 receptor D2R antagonists, whose chronic administration often generates extrapyramidal symptoms (motor symptoms), such as catalepsy and tardive dyskinesia[72]. Interestingly, Nur77 deficient mice show resistance to catalepsy induced by antipsychotics[73], even more, Nur77 expression levels were established as a predictive index of a typical (mostly dopaminergic) or atypical (mostly serotoninergic) profile of antipsychotic drugs[66]. On the other hand, the administration of the D2R agonist Quinpirole (QNP) decreases Nur77

transcription in the striatum[62,74]. These data strongly suggest that Nur77 is a readout of D2R activity.

A strong increase of Nur77 expression is observed in NAc and DS, after acute injections of drugs of abuse (i.e., cocaine, methamphetamine)[71,75]. These brain nuclei are composed of 95% of GABAergic medium spiny neurons (MSN) that express either the dopamine D1 receptor (D1R) or D2R[76]. All the drugs of abuse enhance dopamine release from neuronal terminals and therefore stimulates all dopamine receptors (D1-like and D2-like). However, after repeated injections of methamphetamine, Nur77 mRNA levels return to basal, and the initial induction is abolished in chronic administration[75,77]. Interestingly, compulsive running, which is associated with a higher risk of addictive behavior, correlates with decreased Nur77 expression, allowing to propose Nur77 as a protective factor in addiction[78]. Accordingly, Nur77 knockout mice show augmented spontaneous locomotor activity and increased sensitization to high doses of amphetamine[79]. Despite the extensive literature relating Nur77 with dopamine neurotransmission, mechanisms regulating Nur77 expression in the brain remains poorly understood.

Nur77 levels are also regulated by glutamate neurotransmission[80]. In this work, it was proposed that the D2R-dependent increase of Nur77 is generated by the activation of mGluR5 located in D2R MSN, suggesting that D2R blockade in glutamate presynaptic neurons increase glutamate release that should produce the rise of Nur77 expression levels[80]. The signaling pathway that produces the increase of Nur77, after dopamine or glutamate receptors activation in DS or NAc has not been entirely elucidated. However, antecedents from PC12 cells suggest that calcium-mediated signaling could be a key factor in mGluR5 mediated Nur77 increase and, in turn, modulation of adenylate cyclase by dopamine receptors could be contributing to Nur77 expression[81,82,83]. Concordantly, studies

in PC12 have confirmed that Nur77 expression is under CREB transcription factor control[44,48,82].

Alternatively, the Nur77 expression induced by co-activation of D1R and D2R is abolished by blocking ERK/MSK pathway[84], indicating a role for ERK signaling in the control of Nur77 expression.

3. LSD1, an epigenetic modifier

Histone methylation occurs in arginine and lysine residues into the N-terminal histone tail, and transcriptional activity associated depends on their position and methylation state (mono-, di-, or trimethylated). For instance, methylation of the histone 3 lysine 4 (H3K4) is preferentially located on active promoters and enhancers and therefore, associated with active transcription[85]. On the other hand, methylation in H3K9 is preferentially located on silent promoters and heterochromatin and therefore associated with transcriptional repression[86].

The first described histone demethylase was lysine-specific histone demethylase 1A (LSD1, KDM1A), a FAD (flavin adenine dinucleotide)-dependent amine oxidase[87]. LSD1 protein is composed of an N-Terminal unstructured region containing a nuclear localization signal (NLS)[88], a central SWIRM domain thought to mediate protein-protein interaction and binding to histone tail[89,90,91], and a C-Terminal amino-oxidase domain (AOD) which contain the FAD and the active site of the enzyme. The AOD is interrupted by an alpha-helical tower domain that mediates the interaction of LSD1 with the REST corepressor (CoREST, RCOR1)[89,92]. LSD1, together with CoREST[93] and histone deacetylase (HDACs1/2)[94], form a stable core subcomplex recruited by several transcriptional repressor complexes and is responsible for demethylating H3K4me1/me2 in vivo[95]. In contrast, LSD1 forming complexes

with androgen receptors (AR) or estrogen receptors (ER) functions as a transcriptional coactivator by demethylation of H3K9me1/me2[90,96,97].

Kdm1a gene, coding to LSD1, is in chromosome 1 in humans and 4 in mice, and the canonical version possesses nineteen exons. However, two additional exons are incorporated into LSD1 transcript by alternative splicing, generating four splice variants. These exons are termed: E2a (60 bp) coding for 20 amino acids located between the N-terminal and SWIRM domain, and E8a (12 bp) coding four amino-acids, including a phosphorylatable threonine (T369), located next to the tower domain **(Fig. 1)**[92]. Isoforms, including microexon E8a (LSD1 8a and LSD1 2a-8a), express exclusively in neurons and are called neuronal LSD1 (neuroLSD1). The other two variants (LSD1 and LSD1 2a) are widely expressed, even in neurons, and are called ubiquitous LSD1 (uLSD1)[92]. Although neuroLSD1 differs from uLSD1 only in retention of E8a, it seems to have differences in the molecular target and functions[98,99,100]. NeuroLSD1 has been proposed as a dominant-negative of uLSD1, based on its decreased ability to repress transcription[92], further debilitated by E8a-phosphorylation, which blocks the interaction with CoREST and HDAC1/2[98]. Besides, it has been suggested that neuroLSD1 functions as a transcriptional activator that, in complex with CoREST, demethylates H4K20 (me/me2)[100] and in complex with supervilline, demethylates H3K9 (me/me2)[99].

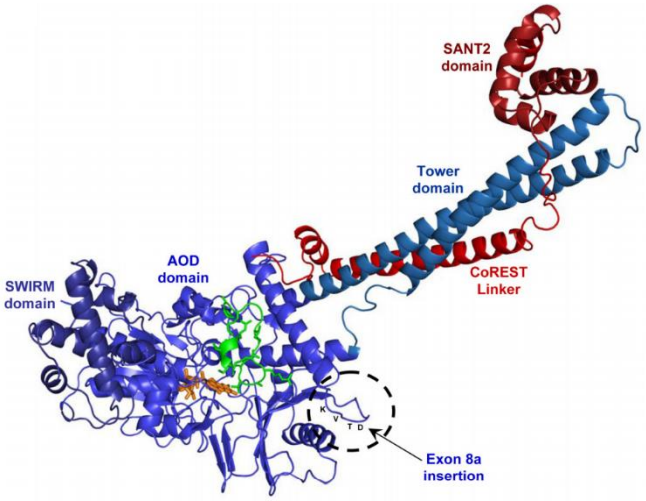

Figure 1: Location of the four neuroLSD1-exclusive amino acids. Overall crystal structure of LSD1-8a– CoREST in complex with a histone peptide. LSD1-8a (residues 171-840) is in light blue, CoREST (residues 308-440) in red, and the histone H3 peptide (residues 1-16) in green. The FAD cofactor is in the orange ball-and-stick representation. The insertion site of E8a (residues Asp369A-Thr369B-Val369C-Lys369D) is highlighted. Modified from Zibetti et. al. 2010[92].

3.1 LSD1 expression and splicing regulation

LSD1 is an epigenetic modulator of gene transcription in different cellular contexts and its overexpression has been reported in several kinds of cancer associated with poor prognosis. Nevertheless, the regulatory mechanisms underlying LSD1 gene transcription, have not yet been elucidated[101]. A recent study suggests that cMyc increases LSD1 expression through binding two non-canonical E-boxes in the *Kdm1a* (gene coding for LSD1) proximal promoter[102].

Three splicing regulators have been identified to modulate the E8a retention into *Kdm1a* transcript, NOVA1, FUBP and SRRM4[103,104]. A reverse complement of exon E8a sequence is located at 3´, this sequence could trap the exon and its donor and acceptor

splicing sites into a double-stranded RNA structure[103]. SRRM4 binds an UGCUGC motif upstream of the splice acceptor site of the exon E8a[102]. It was proposed that interactions of SRRM4 with NOVA1 and FUBP maintain a single-stranded pre-mRNA and therefore eliciting exon E8a inclusion[103,104]. Reduction in NOVA1 expression is observed after pilocarpine administration in mice, correlating with a decrease in E8a retention, suggesting that NOVA1 could be responsible for finely tune exon E8a splicing in response to electrical activity[103].

3.2 LSD1 as a regulator of IEG in brain

LSD1 is largely related to nervous system development and the inclusion of the microexon E8a is required for neuronal maturation[92]. Coincidentally, neuroLSD1 level increases during the perinatal period, whereas uLSD1 proportionally decreases. Later, from postnatal day 15 to adulthood, the uLSD1/neuroLSD1 ratio stabilizes at a value near one in several nuclei of the rat brain[92]. Several lines of research show that neuronal activity transiently modulates uLSD1/neuroLSD1 ratio. For instance, Rusconi et al. (2016) showed that neuroLSD1 mRNA decreases in mice hippocampus seven hours after social stress defeat, recovering normal levels twenty-four hours later[105]. The function of neuroLSD1 has not been fully elucidated. Overexpression of neuroLSD1 in cultured neurons favors morphological maturation[92,98]. However, null mice for neuroLSD1 have a morphologically normal brain discarding an essential role of neuroLSD1 in neuron differentiation and maturation[103]. On the other hand, neuroLSD1 null mice display learning and memory deficiencies[100], show increased threshold for pilocarpine-induced seizures, and low anxiety phenotype[103,105]. Together, these features fit with the role attributed to neuroLSD1 as a regulator of IEG expression. In this regard, Wang et al. (2015) reported impaired induction of IEGs by depolarization with high KCl in cultured neurons from null neuroLSD1 mice[100].It

is noteworthy that the overexpression specifically of the E8a-phosphomimetic neuroLSD1 increases the expression of IEGs in hippocampal neurons in culture, and the opposite effect is observed with uLSD1 and an E8a-phosphodefective neuroLSD1 mutant[98]. Thus, neuroLSD1 has emerged as a pivotal factor regulating the transcription of IEGs. However, if an on/off regulatory unit is formed by neuroLSD1 and uLSD1 or by E8-phosphorylated and E8-unphosphorylated neuroLSD1 is an unaddressed question.

The aforementioned data strongly suggest that the neuronal specific LSD1 variant is essential to IEGs expression in response to neuronal stimuli. neuroLSD1 null mice are less likely to develop stress and anxiety, two behavioral responses modulated by dopaminergic transmission[105]. In this work we evaluated a possible role of LSD1 and neuroLSD1 in dopamine transmission and in the modulation of Nur77, a highly dopamine related IEG. Finally, we made an effort to identify Nur77 target genes by a bioinformatic approach to clarify the function of this transcription factor.

Hypothesis

Dopamine transmission regulates the levels of the ubiquitous and neuronal variants of LSD1, which in turn regulate the expression of Nur77.

General aim

To characterize the effect of dopaminergic transmission on uLSD1 and neuroLSD1 expression, and the role of LSD1 and its splice variants over Nur77 transcription.

Specifics aims

1.- Decipher the relationship between dopamine transmission and uLSD1/neuroLSD1 expression

1.1 Characterize the expression pattern of uLSD1 and neuroLSD1 after acute and chronic amphetamine administration in mice brain.

1.2 Evaluate the role of D1R and D2R over uLSD1 and neuroLSD expression

1.3 Evaluate the role of neuroLSD1 over amphetamine motivated behavior in mice.

1.4 Evaluate the role of neuroLSD1 over dopamine release

2.- Determine the effect of uLSD1 and neuroLSD1 over Nur77 expression.

2.1 Evaluate the effect of uLSD1 and neuroLSD1 over Nur77 promoter activity.

2.2 Evaluate the role of neuroLSD1 over neuronal activity-dependent Nur77 expression

Chapter I

LSD1 microexon E8a as a synaptic dopamine sensor and negative regulator of LSD1 expression

LSD1 microexon E8a as a synaptic dopamine sensor and negative regulator of LSD1 expression

Abbreviated title: Crosstalk between LSD1 and the dopamine system

Montserrat Olivares-Costa[1$], Gianluca Merello[1$], Angélica Escobar, Marcela González[1], Francesco Rusconi[2], Elena Battaglioli[2], and María Estela Andrés[1#]

[1]Department of Cellular and Molecular Biology, Faculty of Biological Sciences, Pontificia Universidad Católica de Chile, Santiago 8330025, Chile. [2]Department of Medical Biotechnology and Translational Medicine, Università Degli Studi di Milano, Via Fratelli Cervi, 93 20090 Segrate MI, Italy.

[#]Correspondence to María Estela Andrés, Department of Cellular and Molecular Biology, Faculty of Biological Sciences, Pontificia Universidad Católica de Chile, Santiago, Chile. mandres@bio.puc.cl.

$: equal contribution

Conflict of interest statement: The authors declare no competing financial interests.

Acknowledgments: This study was funded by Fondecyt grants 1150200 and 1191152.
MO was supported by a Conicyt doctoral fellowship number 21140438. The authors acknowledge the services provided by UC CINBIOT Animal Facility funded by PIA CONICYT* ECM-07 *Program for Associative Research, of the Chilean National Council for Science and Technology.

Abstract

The epigenetic enzyme, Lysine-Specific Demethylase 1 (LSD1, KDM1A) regulates gene expression by demethylating specific lysines at the tails of histones H3 and H4. LSD1 has a splice variant exclusively expressed in neurons (neuroLSD1), which plays a dominant-negative role opposing ubiquitous LSD1 (uLSD1) actions. uLSD1 and neuroLSD1 are regulated by neuronal activity and involved in the modulation of dopamine-related behaviors as stress and anxiety. Here, we studied the crosstalk between LSD1 variants and dopaminergic neurotransmission using acute and repeated amphetamine (AMPH) treatments in wild-type and neuroLSD1 null mice. Acute treatment with AMPH produced a fast and transient decrease in total LSD1 protein without changing uLSD1/neuroLSD1 ratio or LSD1 total mRNA levels. On the other hand, the repeated treatment with AMPH induced a long-term reduction of LSD1 transcript and protein levels. NeuroLSD1 null mice did not show changes in LSD1 expression with repeated AMPH treatment. Fast scan cyclic voltammetry data showed that neuroLSD1 null mice release less dopamine than wild-type littermates in the nucleus accumbens in response to AMPH. Although locomotor activity and behavioral sensitization induced by acute and repeated administration of AMPH, respectively, were similar between both genotypes. In conclusion, our data reveal that neuroLSD1 is necessary for negative homeostatic regulation of LSD1 in prolonged stimuli with psychostimulants, and it is involved in dopamine release regulation.

Significance statement

The epigenetic enzyme LSD1 regulates gene expression by modifying histone methylation. LSD1 has ubiquitous (uLSD1) variants found in all cellular phenotypes and neuron-specific variants (neuroLSD1). The uLSD1/neuroLSD1 ratio in neurons is dynamically modulated by stimuli and determines individuals' stress susceptibility. We studied whether uLSD1/neuroLSD1 ratio varies with dopamine stimulation and the relevance of neuroLSD1 in the responses to amphetamine (AMPH), a potent inductor of dopamine release. Our data show that neuroLSD1 null mice release less dopamine than wild-types in response to AMPH. Acute AMPH stimulation transiently decreases LSD1 protein levels, while repeated AMPH stimulation produce long-term decrease of LSD1 protein and mRNA in a neuroLSD1-dependent process. In conclusion, neuroLSD1 tunes dopamine release and controls the expression of LSD1 through a negative feedback mechanism associated to sustained AMPH stimulation.

Introduction

Lysine Specific Demethylase 1A (LSD1, also termed KDM1A)[1] is an epigenetic modifier that in complex with the transcriptional co-repressor RCOR1 (CoREST1)[2] and the deacetylases HDAC1/2[3] regulates the expression of neuronal genes[4]. LSD1 has four splice variants generated by alternative inclusion of two exons termed E2a (60 bp) and E8a (12 bp). Variants, including microexon E8a (LSD1 8a and LSD1 2a-8a), express exclusively in neurons and are called neuronal LSD1 (neuroLSD1). The other two variants (LSD1 and LSD1 2a) are widely expressed, even in neurons, and are called ubiquitous LSD1 (uLSD1)[5].

NeuroLSD1 and uLSD1 seem to have differences in their molecular targets and functions[5,6,7]. uLSD1 in complex with RCOR1 and HDAC1/2 functions as a transcriptional repressor demethylating mono and dimethylated lysine 4 in histone H3 (H3K4me1/me2)[1]. In contrast, uLSD1 in complexes with androgen and estrogen receptors functions as a transcriptional coactivator[8,9,10]. It has been proposed that neuroLSD1 functions as a dominant-negative of uLSD1, based on its decreased ability to repress transcription[5]. Besides, it has been suggested that neuroLSD1 behaves as a transcriptional coactivator that, in complex with RCOR1, demethylates H4K20 (me/me2)[7] and in complex with supervilline, demethylates H3K9 (me/me2)[6].

The inclusion of the microexon E8a increases during the perinatal period, whereas uLSD1 proportionally decreases. Later, from postnatal day 15 to adulthood, the uLSD1/neuroLSD1 ratio stabilizes at a value near one in several nuclei of the rat brain[5]. uLSD1/neuroLSD1 ratio is transiently modulated by neuronal activity. For instance, Rusconi et al. (2016) showed that neuroLSD1 mRNA decreases in mice hippocampus seven hours after social stress defeat (SDS), recovering normal levels twenty-four hours later[11].

NeuroLSD1 null mice display learning and memory deficiencies[7], an increased threshold for pilocarpine-induced seizures, and a low anxiety phenotype[11,12].

Because the expression of LSD1 and neuroLSD1 are regulated by neuronal activity and are involved in the modulation of dopamine-related behaviors such as stress and anxiety, we propose LSD1 as an effector of the molecular and behavioral dopamine-mediated response. Our data suggest that signaling through D2 dopamine receptors (D2R) regulates LSD1 expression and uLSD1/neuroLSD1 ratio. Acute and repeated administration of AMPH induce transient and long-term effects on LSD1 levels, revealing a negative feedback regulation exerted by neuroLSD1. Neurochemical and locomotor characterization of neuroLSD1 null mice show decreased AMPH-induced dopamine release but similar AMPH induced sensitization in neuroLSD1 null compared to wild-type mice.

Materials and Methods

Animals

Adult male and female neuroLSD1null mice[12] were used in this study (Animal Care Facility of the Faculty of Biological Sciences, Pontificia Universidad Católica de Chile). neuroLSD1 null mice were crossed on a C57BL/6 background. After weaning, siblings were group-housed (four mice/cage) and maintained at the animal facility, under a 12/12 h light/dark cycle (lights off at 7:00 pm), constant temperature (24°C), with food and water available ad libitum. Mice were genotyped using the following primers Fw: 5' – ACGCGTCGACTCTTCAGTGCTTTCTCACTCCCA – 3'; Rv: 5' – ATAGTTTAGCGGCCGCCCTCTATTTTCTGAGCAGCC – 3'. The Bioethical Committee of the Pontificia Universidad Católica de Chile approved all experimental procedures that included animals (protocols ID: 161014004, 160527009, 180808005). All procedures were conducted to reduce the number of animals when possible and reduce their level of pain and discomfort as much as possible.

Drug treatments

Haloperidol (0.5 mg/kg, Sigma–Aldrich) was dissolved in saline containing 5% (vol/vol) acetic acid and pH adjusted to 6.0 with 1 M NaOH. Quinpirole (1 mg/kg, Sigma–Aldrich), SKF 38393 (0.6 mg/kg, ABCAM), and SC5H 23390 (0.2 mg/kg, Sigma-Aldrich) were dissolved in saline solution (NaCl 0.9%). Mice were injected intraperitoneally (ip) with the drugs or the corresponding volume of the vehicle in their home cages. Two hours after the injection, mice were anesthetized with isoflurane and decapitated. Brains were rapidly

extracted, and specific nuclei samples were collected for total RNA extraction by Trizol method (Thermo Fisher).

For AMPH acute or repeated treatments, mice were injected ip with 3 or 6 mg/kg of DL-Amphetamine sulfate (Laboratorios Chile, Santiago, Chile) or an equivalent volume of saline. Repeated treatment with AMPH was carried out every-other-day until completing four injections. Twenty-four hours after the last injection, mice were anesthetized with isoflurane and sacrificed by decapitation. Brain samples were homogenized and maintained in RIPA or Trizol buffer for protein or mRNA analysis, respectively.

Exon Inclusion Frequency by Relative Quantity Fluorescent-PCR (rqf-PCR) and q-PCR.

rqf-PCR was performed as previously described[5]. Briefly, a 6FAM-conjugated fluorescent forward primer (Thermo Fisher) and an unmodified reverse one were used to amplify uLSD1 and neuroLSD1 in the same PCR reaction (detailed explanation and rqf-PCR standardization is in annex1). Amplified products were separated by capillary electrophoresis under denaturing conditions in the sequencing and omics technologies facility of the Pontificia Universidad Católica de Chile. Each amplified product was measured as relative fluorescence unit levels using the software Peak scanner v1.0. The following primers were used to amplify the E8a exon region:

6FAM_Ex8_FW: 6-Fam-5'TCCCATGGCTGTCGTCAGCA3' and Ex11_Rv: 5'CTACCATTTCATCTTTTTCTTTTGG3'.

Primers for q-PCR were: Total LSD1 Fw: 5'AAGCCAGGGATCGAGTAGGT3' and Rv: 5'CTGACGACAGCCATGGGATT3'. GAPDH Fw: 5´GTGTTCCTACCCCCAATGTGT3´ Rv: 5´ATTGTCATACCAGGAAATGAGCTT3´.

SDS-PAGE immunoblot

Brain tissues were homogenized in RIPA lysis buffer (Merck) supplemented with protease inhibitors by ultrasonication. After centrifugation, the supernatant was recovered and quantified using the Micro BCA protein assay kit (Thermo Fisher). LSD1 and RCOR1 Western Blotting was performed on 8% SDS-PAGE and histone modifications was performed on a 12 % SDS-PAGE. Proteins were transferred to 0.45 or 0.2 um PVDF membranes (Millipore). Blocking solution consisted of 5% nonfat dried milk diluted in 0.1% TBS-Tween. Membranes were incubated overnight at 4°C with the following primary antibodies diluted in 0.1% TBS-Tween. Anti-LSD1 rabbit polyclonal (ab17721, Abcam) 1/1000, anti-RCOR1 mouse monoclonal (NeuroMab, 75-039) 1/1000, anti-Lamin B1 rabbit polyclonal (ab16048, Abcam) 1/2000, anti-Fosb rabbit monoclonal (5G4, Cell Signaling Technology) 1/1000, anti-H3K4me2 rabbit polyclonal (ab7766, Abcam) 1/1500. Peroxidase-conjugated secondary antibodies (Jackson Immuno-Research Laboratories, West Grove, PA, USA) were diluted in blocking solution, incubated for 1 hour at room temperature and revealed with SuperSignal West Pico Chemiluminescent Substrate (ThermoFisher Scientific, USA). Optical density of specific bands was normalized to laminB1 using ImageJ software.

Fast Scan cyclic voltammetry

FSCV experiments were performed on isoflurane-anesthetized mice and were carried out as described in[13]. A thermostatically controlled heating pad was used to sustain 37°C core body temperature. Mice were subjected to a craniotomy, and a glassy-carbon microelectrode (working electrode) was placed in the NAc by using the following coordinates AP: +1.3 mm; ML: 1.3 mm; DV: 3 mm, according to the Mouse Brain Atlas of Franklin and Paxinos (1997)[14]. A bipolar stimulating electrode (Plastics One) was placed in the VTA with

the following coordinates AP: -3 mm; ML: 0.8 mm; DV: 3.5 mm. An Ag/AgCl reference electrode was placed contralaterally to the working electrode. A triangle waveform potential was ramped from 0.4 V to +1.2 V (400 V/s every 100 ms). Phasic electrically evoked dopamine release was achieved with the following parameters: monophasic +, 60 pulses, 60 Hz, 300 uA (current stimulus isolator NL800A; Digitimer, Ltd, UK). Data analysis was done using Demon Voltammetry analysis software[14]. Data collection began once electrical stimulation induced a clear dopamine peak with a cyclic voltammogram showing the oxidation of dopamine at 0.6 V. Stimulation was carried out every 5 minutes for 6 baseline measurements. After that, 6 mg/kg ip AMPH was administered, and 24 recordings were performed for 2 hours.

Locomotor sensitization

Mice were injected two consecutive days with saline to obtain the basal locomotor activity. On the third day, mice were injected with either a low (3 mg/kg, ip) or a high (6 mg/kg, ip) dose of AMPH, and locomotor activity quantified during 60 min. In a separate group of animals, the development of locomotor sensitization was assessed by administering either a low (3 mg/kg, ip) or a high (6 mg/kg, ip) dose of AMPH daily until completing six injections. Then, after 10 days of withdrawal, the expression of locomotor sensitization was tested with a challenging injection of AMPH at the same dose applied previously. Locomotor activity was quantified immediately after each injection by transferring the animals to test cages equipped with two infrared lights. Crossovers in the test cage were monitored every minute for 60 min, using a counting device programmed to count only when both infrared light beams were interrupted consecutively.

Statistical analyses

Statistical differences were analyzed using unpaired Student's t-test or one-way ANOVA with Dunnett´s or Turkey Multiple Comparison Test (Prism 9.0). Other statistical parameters (i.e., the n numbers and p values) can be found in figure legends.

Results

Transient modulation of LSD1-RCOR1 protein levels and of H3K4me2 after acute administration of AMPH

To evaluate the hypothesis that LSD1 expression and uLSD1/neuroLSD1 ratio are responsive to dopaminergic transmission, wild-type mice were acutely injected with AMPH, a dopamine secretagogue that indirectly stimulates all dopamine receptors. Total LSD1 mRNA was measured by q-PCR and the proportion of LSD1 splice variants was evaluated by rqf-PCR in dopaminoceptive brain nuclei, two hours after AMPH administration. Total LSD1 and RCOR1 protein levels, along with the substrate H3K4me2, were measured by SDS-PAGE immunoblot at different time points after an acute AMPH injection **(Fig. 1A)**.

Two hours after an acute AMPH (6 mg/kg, i.p.) injection, H3K4me2 levels remained similar to controls **(Fig. 1B)**, while LSD1 and RCOR1 protein levels decreased in the striatum (Fig. 1C, D). At this time point, the total LSD1 mRNA and uLSD1/neuroLSD1 transcripts ratio remained similar to controls in the striatum, PFC **(Fig. 1E, F)**, and hippocampus **(Fig S.1)**.

Eight hours after AMPH injection, H3K4me2, LSD1, and RCOR1 increased significantly in the striatum compared to saline-injected control mice **(Fig. 1B, C, D)**. At 48 hours after AMPH injection, normal values were observed for LSD1, RCOR1, and the substrate H3K4m2 **(Fig. 1B, C, D)**. To test the efficacy of the acute AMPH treatment, ΔFosb protein levels, an immediate-early gene whose expression is induced with drugs of abuse[15], was assessed in the striatum. As shown in figure 1G and H, striatal ΔFosb protein levels increased at two and eight hours after AMPH injection.

These results suggest that LSD1 is modulated by acute AMPH, through some dopamine-induced post-translational mechanism that regulate the stability and/or the translation of the LSD1 and RCOR1 proteins.

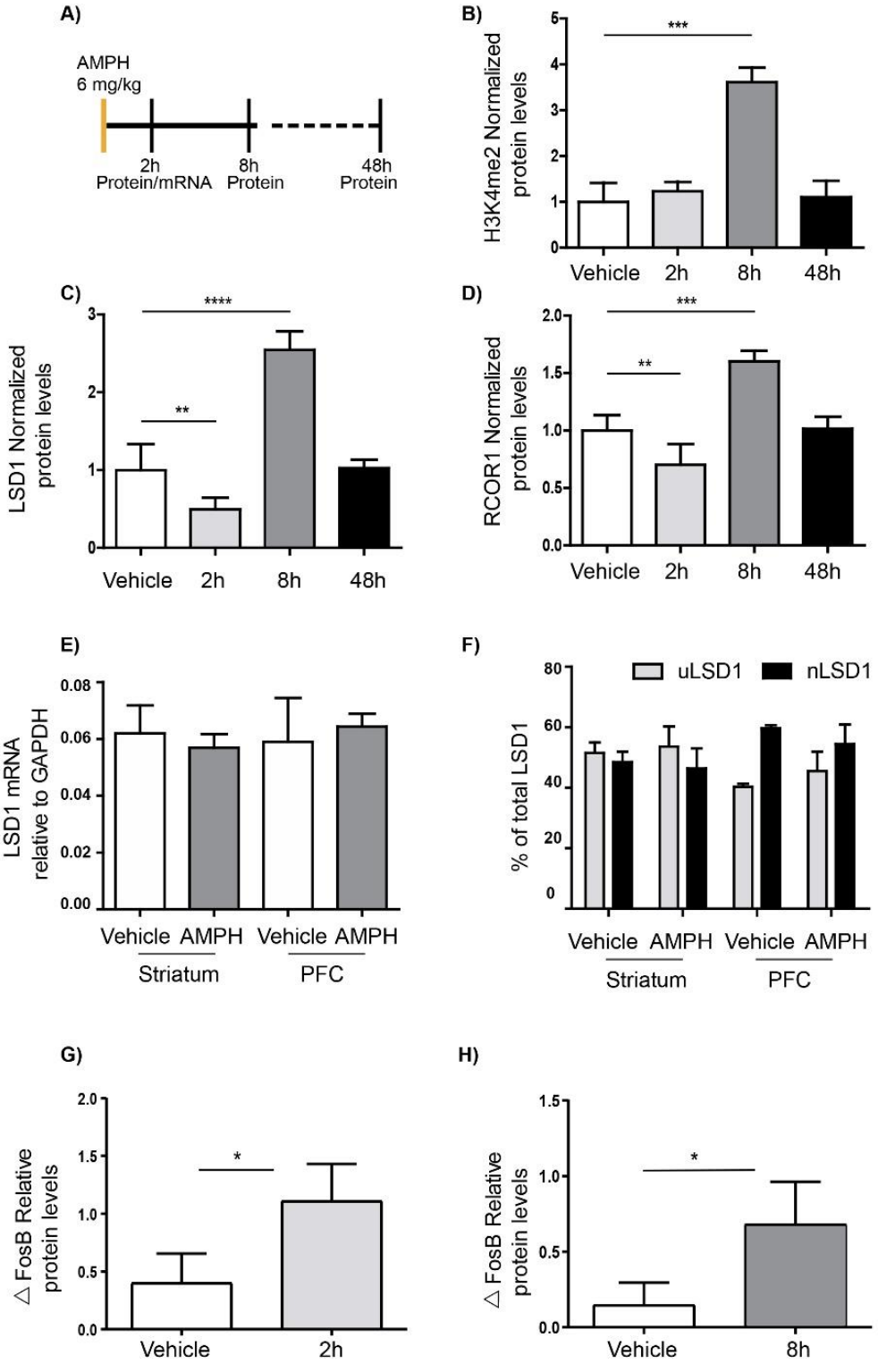
A)
AMPH
6 mg/kg
2h
Protein/mRNA
8h
Protein
48h
Protein
B)
H3K4me2 Normalized protein levels
***
Vehicle
2h
8h
48h
C)
LSD1 Normalized protein levels
****
**
Vehicle
2h
8h
48h
D)
RCOR1 Normalized protein levels
***
**
Vehicle
2h
8h
48h
E)
LSD1 mRNA relative to GAPDH
Vehicle
AMPH
Vehicle
AMPH
Striatum
PFC
F)
uLSD1
nLSD1
% of total LSD1
Vehicle
AMPH
Vehicle
AMPH
Striatum
PFC
G)
△ FosB Relative protein levels
*
Vehicle
2h
H)
△ FosB Relative protein levels
*
Vehicle
8h

Figure 1: AMPH acute administration modulates H3K4 methylation and LSD1-RCOR1 protein levels. A) Scheme of the experimental procedure. **B-D)** Quantification of H3K4me2 (B), LSD1 (C) and RCOR1 (D) protein levels in the striatum of mice injected with vehicle or after 2, 8, and 48 hours of acute AMPH injection, assessed by SDS-PAGE immunoblot. Differences were analyzed by one-way ANOVA, followed by Dunnett's multiple comparison test. **E)** Total amount of LSD1 mRNA relative to GAPDH measured by qPCR from the striatum and the PFC of mice, two hour after an acute AMPH or vehicle injection. **F)** Relative uLSD1 and neuroLSD1 mRNA expression assessed by rqf-PCR from the striatum and the PFC of mice, two hours after an acute AMPH or vehicle injection. **G, H)** Quantification of ΔFosb protein levels relative to Lamin_B1, in the striatum of WT mice injected with vehicle or after 2 (G), or 8 (H) hours of acute AMPH injection assessed by SDS-PAGE immunoblot. Differences were analyzed by unpaired t test. All data correspond to the mean ± SD of at least 3 independent experiments. **P<0.01; ***P<0.001; ****P<0.0001.

Repeated administration of AMPH decreases LSD1 in mice brain by a neuroLSD1-dependent negative feedback.

Repeated administration of AMPH produces long-lasting changes in gene expression in the brain[17,18]. Our previous data showed that LSD1 protein levels modulated by acute AMPH administration, suggesting a role of LSD1 as a sensor of dopaminergic stimulation. To further inquire about this idea, we tested the effect of repeated AMPH administration in wild-type and neuroLSD1 null mice. A 6 mg/kg dose was injected once every two days until for a total of four injections; mRNA and proteins were extracted twenty-four hours after the last injection **(Fig. 2A)**. Total LSD1 transcript, neuroLSD1 transcript proportion, and the levels of LSD1 and H3K4me2 protein were measured in the hippocampus, the striatum, and the PFC.

Twenty-four hours after the last AMPH injection, a sharp decrease in total LSD1 mRNA and protein levels was observed in the hippocampus, the striatum **(Fig. 2B to E)**, and the PFC **(Fig S.2A)** of wild-type mice. Associated with these changes, a significant increase in the neuroLSD1 transcript proportion was observed in all tested nuclei **(Fig. 2H,**

I and S.2B). The epigenetic mark H3K4me2 did not show changes in the hippocampus, but a significant decrease was observed in the striatum of wild-type mice, twenty-four hours after the last AMPH injection **(Fig. 2F, G)**. Altogether the data indicate that LSD1 expression is subjected to negative regulation by repeated dopaminergic stimuli.

In stark contrast to the wild-type mouse, the neuroLSD1 null mice showed no change of total LSD1 mRNA in the hippocampus, the striatum, nor PFC twenty-four hours after the last injection of AMPH **(Fig. 2B,C and S.2A)**. Similarly, LSD1 protein levels were unchanged twenty-four hours after the last AMPH injection, in the hippocampus and striatum of AMPH repeatedly treated neuroLSD1 null mouse **(Fig.2D, E)**. These data indicate that repeated stimulation of the dopamine system leads to a decrease in total LSD1 levels through a neuroLSD1-mediated self-regulatory system. Although LSD1 levels were not modified in brain nuclei of neuroLSD1 null mice, H3K4me2 levels decreased significantly in the hippocampus and the striatum twenty-four hours after the last injection of AMPH **(Fig. 2F)**.

To further look for evidence for LSD1 controlling its own transcription, we analyzed publicly available databases from ChIP-Seq for LSD1 in mice cortical neurons unstimulated or stimulated with KCL[7]. Concordantly with our data, the ChIP-seq analysis shows that LSD1 is tagged to its promoter in stimulated condition **(Fig. S.2C)**, reinforcing the idea of a self-regulatory system.

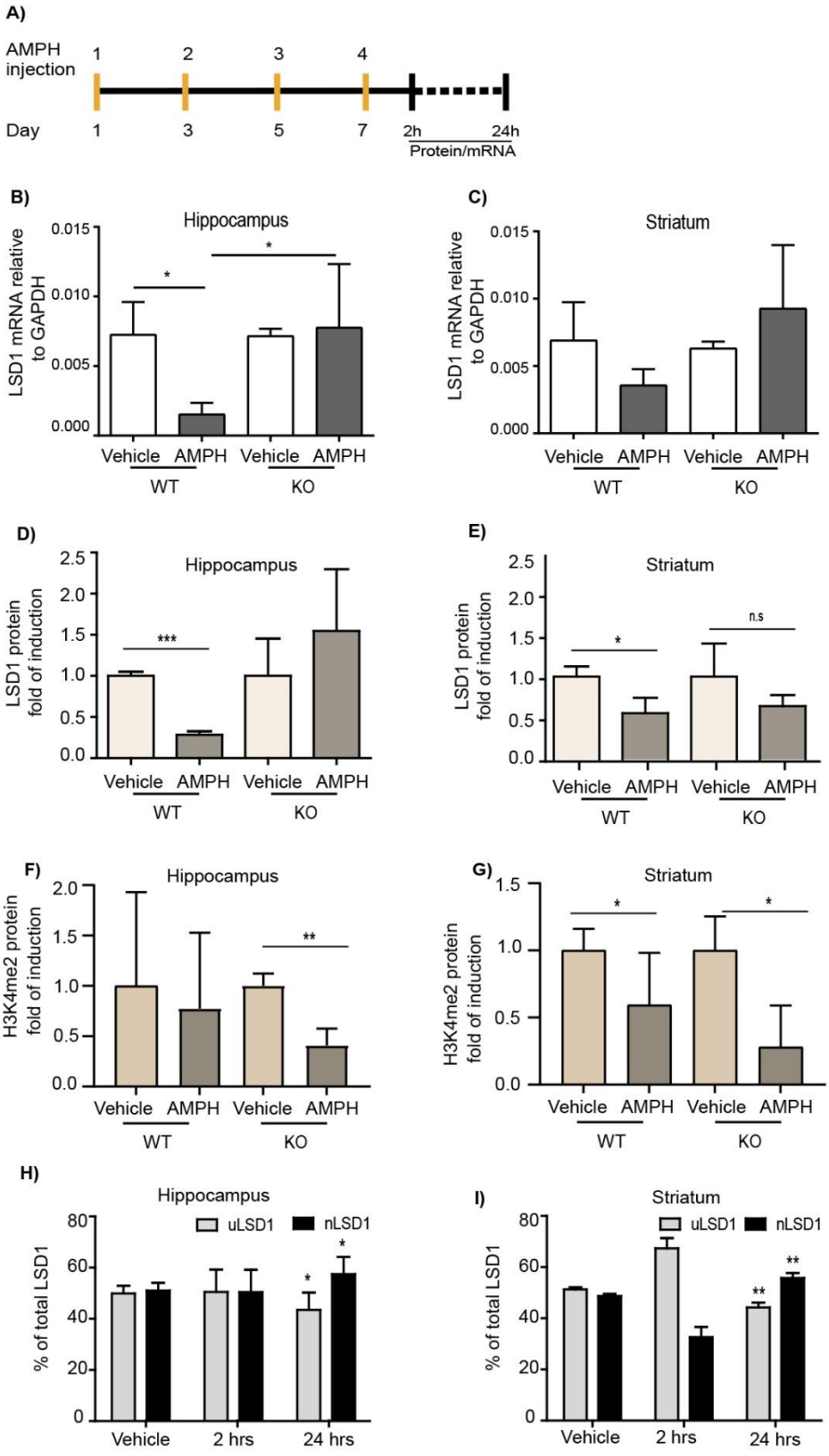
A)
AMPH injection
1
2
3
4
Day
1
3
5
7
2h
24h
Protein/mRNA
B)
Hippocampus
LSD1 mRNA relative to GAPDH
0.015
0.010
0.005
0.000
*
*
Vehicle
AMPH
Vehicle
AMPH
WT
KO
C)
Striatum
LSD1 mRNA relative to GAPDH
0.015
0.010
0.005
0.000
Vehicle
AMPH
Vehicle
AMPH
WT
KO
D)
Hippocampus
LSD1 protein fold of induction
2.5
2.0
1.5
1.0
0.5
0.0
***
Vehicle
AMPH
Vehicle
AMPH
WT
KO
E)
Striatum
LSD1 protein fold of induction
2.5
2.0
1.5
1.0
0.5
0.0
*
n.s
Vehicle
AMPH
Vehicle
AMPH
WT
KO
F)
Hippocampus
H3K4me2 protein fold of induction
2.0
1.5
1.0
0.5
0.0
**
Vehicle
AMPH
Vehicle
AMPH
WT
KO
G)
Striatum
H3K4me2 protein fold of induction
1.5
1.0
0.5
0.0
*
*
Vehicle
AMPH
Vehicle
AMPH
WT
KO
H)
Hippocampus
uLSD1
nLSD1
% of total LSD1
80
60
40
20
0
*
*
Vehicle
2 hrs
24 hrs
I)
Striatum
uLSD1
nLSD1
% of total LSD1
80
60
40
20
0
**
**
Vehicle
2 hrs
24 hrs

Figure 2: AMPH repeated administration decreases total LSD1 expression in a neuroLSD1-dependent way. A) scheme of the experimental procedure. **B, C)** Total amount of LSD1 mRNA relative to GAPDH measured by qPCR in the hippocampus (B) and the striatum (C) of mice injected repeatedly with AMPH or vehicle. Total RNA was extracted 24 hours after the last injection.*P<0.05 by One-way ANOVA followed by Turkey Multiple Comparison Test. **D,E)** Fold of induction of LSD1 protein from the hippocampus (D) and the striatum (E) of mice injected repeatedly with AMPH or vehicle, assessed by SDS-PAGE immunoblot. **F,G)** Fold of induction of H3K4me2 protein from the hippocampus (F) and the striatum (D) of mice injected repeatedly with AMPH or vehicle, assessed by SDS-PAGE immunoblot. Proteins extracts were obtained 24 hours after the last injection. *P<0.05, **P<0.01, ***P<0.001 by Student's unpaired t-test. **H, I)** Relative mRNA expression of uLSD1 and neuroLSD1 assessed by rqf-PCR in the striatum and hippocampus of mice injected repeatedly with AMPH or vehicle. *P<0.05, **P<0.01 (compared to vehicle) Student's unpaired t-test. All data are presented as mean ± SD of at least three independent experiments.

Selective D2 receptor modulation alters LSD1 alternative splicing in the striatum.

The above data indicate that LSD1 expression and retention of the microexon E8a are regulated by dopaminergic neurotransmission. To determine what type of dopamine receptor is involved in this regulation, we analyzed LSD1 expression and neuroLSD1 proportion in the striatum, and PFC after acute stimulation or blockade of D1R or D2R using agonists and antagonists. In the striatum, the proportion of uLSD1 (average 56.5%) exceeds that of neuroLSD1 (average 43.5%), remaining unchanged two hours after the acute injection of either agonists or antagonists of D1R (SKF 38393 and SCH 23390 respectively) **(Fig. 3A)**. Strikingly, the proportion of neuroLSD1 increased significantly with an acute injection of quinpirole (QNP) and haloperidol (HAL) **(Fig. 3A)**, D2R agonist and antagonist, respectively. This result may be due to the fact that low doses of QNP can preferentially stimulate the presynaptic D2Rs, thus decreasing the extracellular levels of dopamine. In the PFC, the proportion of neuroLSD1 (average 52.4%) is higher than uLSD1 (average 47.6%) and increases further with QNP acute injection **(Fig S.3A)**. Total levels of LSD1 transcript

remained constant in all conditions **(Fig S.3B, C)**, suggesting that D2R-mediated neurotransmission selectively regulates E8a inclussion into the LSD1 transcript.

To further analyze the role of D2R regulating E8a retention into LSD1 transcript, we studied uLSD1 and neuroLSD1 proportion in the D2R deficient mice[19]. We found similar proportions of uLSD1 and neuroLSD1 expressed in the striatum of functional D2R deficient mice (51.2% and 48.8%, respectively), suggesting that basal dopamine neurotransmission through D2R maintains a lower retention of E8a **(Fig. 3B)**. This genotype-associated difference was only observed when we assessed E8a inclusion. rqf-PCR experiments designed to evaluate E2a transcripts ratio showed no differences between wild-type and D2R deficient mice **(Fig S.4)**, indicating an E8a selective regulatory mechanism.

D2Rs are differentially expressed in different nuclei of the mammalian brain. The highest expression is observed in the striatum, substantia nigra, and olfactory bulb of the rat brain. On the other hand, cortical regions show lower D2R immunoreactivity than the striatum[20]. To test whether these D2R differential expression profiles could be correlated with differences in the relative abundances of transcripts of the LSD1 variants, we also compared the percentage of neuroLSD1 in two brain nuclei with different D2R levels, the striatum, and the PFC. Interestingly, the percentage of neuroLSD1 was significantly higher in the PFC (53.0%) compared to the striatum (43.5%) **(Fig. 3C)**. These findings reinforce the idea that D2R-mediated dopaminergic neurotransmission decreases E8a inclusion.

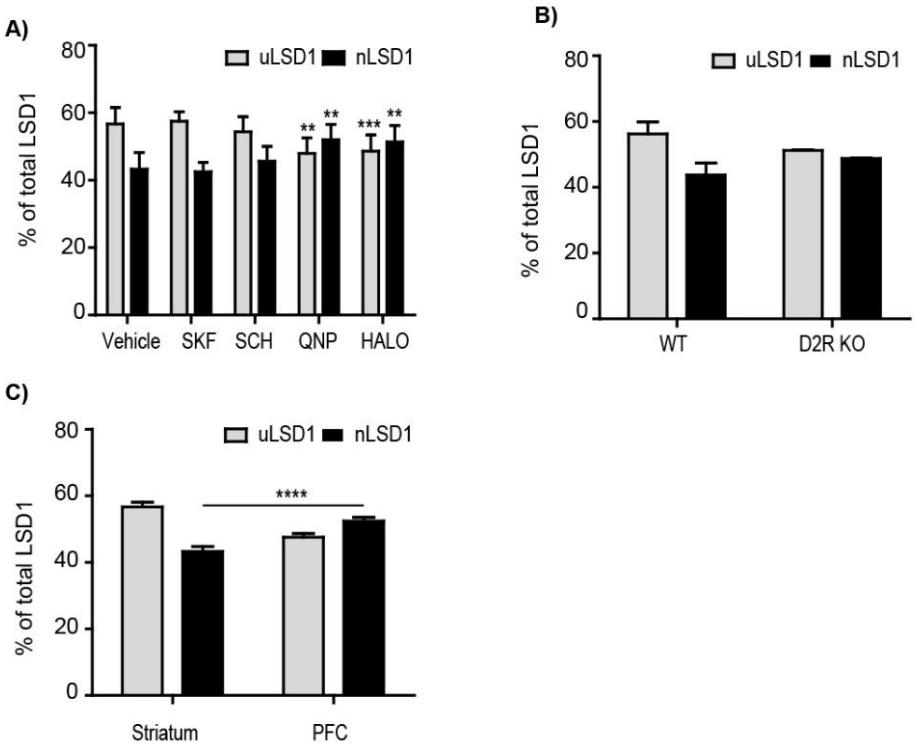

Figure 3: uLSD1/neuroLSD1 ratio is modulated by D2R-mediated signaling. A) Relative mRNA expression of uLSD1 and neuroLSD1 (nLSD1) assessed by rqf-PCR from the striatum of mice 2 h after injected acutely with haloperidol (HALO), quinpirole (QNP), SKF 38393 (SKF), SCH 23390 (SCH) or vehicle. Data correspond to the mean ± SD of at least six independent experiments, ** P <0.01, *** P <0.001 (compared to vehicle) by One-way ANOVA Dunnett's Multiple Comparison Test. **B)** Relative mRNA expression of uLSD1 and neuroLSD1 (nLSD1) assessed by rqf-PCR from the striatum of WT and D2R deficient mice (D2R KO). Data correspond to the mean ± SD of at least two independent experiments. **C)** Relative mRNA expression of uLSD1 and neuroLSD1 (nLSD1) assessed by rqf-PCR from mice striatum and pre-frontal cortex (PFC). Data correspond to the average ± SD of ten independent experiments. ****P<0.0001 One-way ANOVA followed by Turkey Multiple Comparison.

Wild-type and neuroLSD1 null mice display similar locomotor response to AMPH administration.

Given that neuronal activity regulates the uLSD1/neuroLSD1 ratio and that LSD1 modulates dopamine-related behaviors such as stress and anxiety[11], we tested the hypothesis that neuroLSD1 regulates dopamine release and associated behaviors. To address this idea, we compared locomotor activity and locomotor sensitization after acute and repeated administration of AMPH, in wild-type and mice null for neuroLSD1.

Two saline injections were administered before AMPH to rule out the stress-induced behavioral alteration. The locomotor activity of wild-type and neuroLSD1 null mice in response to saline injections was indistinguishable **(Fig. 4A, B)**. A similar significant increase in AMPH-induced locomotor activity was observed in both genotypes at a 6 mg/kg AMPH dose **(Fig. 4A)**. To rule out possible ceiling effects due to the dose administered, the locomotor activity was also evaluated at 3 mg/kg AMPH in a new group of animals. A significant increase in AMPH-induced locomotor activity was also observed in wild-type and neuroLSD1 null mice **(Fig. 4B)**. However, the neuroLSD1 null group presented a significantly higher variance than the WT group at a dose of 6mg/kg AMPH **(Fig. 4A)**. These results indicate that the locomotor response of neuroLSD1-deficient mice to acute AMPH administration is similar to wild-type mice. However, the increased variability of neuroLSD1 null mice locomotor response suggests a role for neuroLSD1 in AMPH sensitivity

Next, we asked whether neuroLSD1 null mice develop AMPH-induced locomotor sensitization. To this end, wild-type and neuroLSD1 null mice were injected daily with low (3 mg/kg) or high (6 mg/kg) doses of AMPH for six consecutive days, followed by a 10 days withdrawal period. After abstinence, a challenge dose of AMPH was administered to evaluate locomotor sensitization.

Wild-type and neuroLSD1 null mice injected with 6 mg/kg AMPH increased their locomotor activity to a similar level and maintained it during the six days of the test, indicating a ceiling response devoid of gradual increments **(Fig. 4C, D)**. Interestingly, the locomotor activity of wild-type but not that of neuroLSD1 null mice increased in response to a challenge AMPH injection, indicating that the expression of sensitization at this high dose of AMPH is suppressed in the absence of neuroLSD1 **(Fig. 4C, D)**. Conversely, the lower 3 mg/kg of AMPH induced a gradual increment of locomotor activity and locomotor sensitization expression in both genotypes with minor differences in behavioral dynamics between them **(Fig. 4D, E)**. These results suggest that neuroLSD1 is not required for AMPH-induced sensitized behaviors.

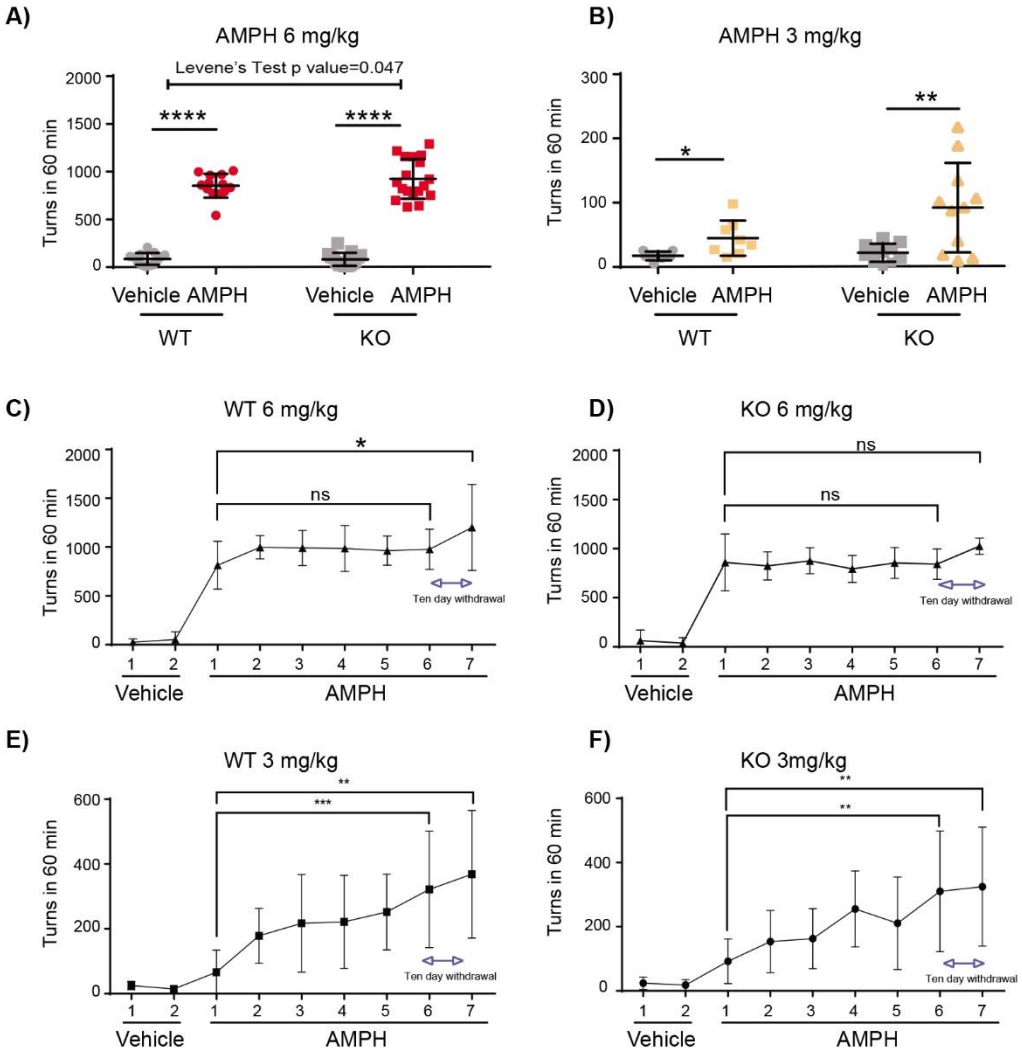

Figure 4: NeuroLSD1 null mice exhibit AMPH-induced locomotor activity and sensitization similar to wild-types. A, B) Horizontal locomotor activity (turns per hour) induced by a single dose of AMPH 6 mg/Kg (A) or 3 mg/kg (B). Control conditions (vehicle) correspond to the average of locomotor activity registered after vehicle administration in two consecutive days. (n= 8 to 15 per genotype). Levene's test to compare two variances was conducted between AMPH groups. Differences between saline and AMPH-induced locomotor activity was analyzed by paired t-test. **C to F)** Horizontal locomotor activity (turns per hour) measured immediately after the administration of AMPH 6 mg/kg (C, D) or 3 mg/kg (E, F) in WT (C, E) or neuroLSD1 KO mice (D, F). Paired t-test or One-way ANOVA (KO 3 mg/kg) with Tukey's multiple comparison test. Data are presented as mean ± SD; *P < 0.05, **P < 0.01, ***P < 0.001, ****P < 0.0001.

neuroLSD1 null mice exhibit reduced release and faster reuptake of dopamine in response to AMPH

To further inquire into the neurochemical features of neuroLSD1 null mice, we studied phasic dopamine release and its modulation by AMPH in the nucleus accumbens (NAc) of wild-type, heterozygous (HT), and neuroLSD1 null mice. Fast Scan Cyclic Voltammetry (FSCV) was performed to determine electrically evoked dopamine release in the NAc. A bipolar stimulating electrode was placed in dopaminergic VTA cell bodies and a carbon recording electrode in the NAc of anesthetized mice. Six baseline measurements were collected before a 6 mg/kg AMPH injection, then recorded every 5 minutes for a total of 24 measurements for 2 hours. A representative example of basal and AMPH-induced phasic dopamine release in wild-type and neuroLSD1 null mice is shown in figures 5A and B. No differences were observed in electrically evoked dopamine release between genotypes **(Fig. 5A to C)**. As expected, wild-type mice showed an AMPH-induced increase in electrically evoked phasic dopamine release compared to pre-drug baseline levels. The heterozygous mice showed a lower amount of released dopamine (measured by dopamine-release peak height) compared to wild-type animals, while neuroLSD1 null showed the lowest increase of extracellular dopamine after AMPH administration **(Fig. 5D)**. The quantification of the area under the curve (AUC) of peak height measurements made during the 2-hour analysis showed a significant difference between heterozygous and null mice and a tendency between wild-types and neuroLSD1 null mice (p value = 0.0522) **(Fig. 5E)**. Quantification of tau, a measurement of dopamine reuptake, resulted in a significant difference between wild-type and heterozygous mice **(Fig. 5F, G)**.

The AUC of each peak of dopamine release can be taken as a measure of both, release and reuptake of dopamine. As shown in figure 5H and I, wild-type are significantly

different to neuroLSD1 null mice in this parameter, reinforcing differences observed in peak height (dopamine release) and tau (dopamine reuptake) separately **(Fig. 5H, I)**.

We rule out that lower dopamine release induced by AMPH in neuroLSD1 null mice is due to decreased presynaptic dopamine availability since dopamine content in the tissue does not differ between genotypes **(Table 1)**. These results indicate that neuroLSD1 does not appear to play a preponderant role in physiological dopaminergic neurotransmission. However, it appears to have a dose-dependent role in supraphysiological dopamine release and reuptake, such as that induced by AMPH.

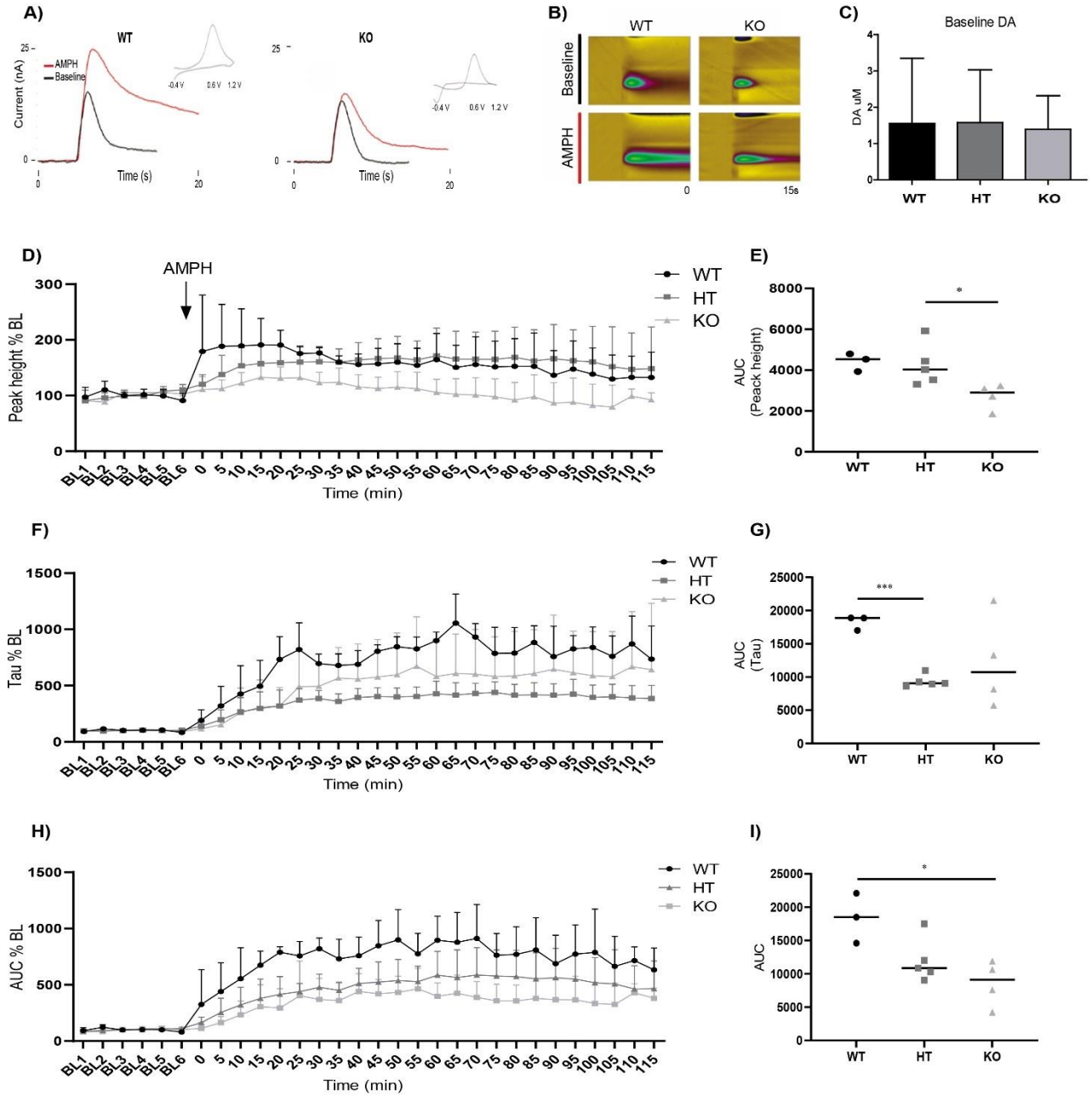

Figure 5: neuroLSD1 null mice exhibit decreased electrically evoked dopamine release in response to AMPH. (A) Examples of dopamine release dynamics. Top panels show current vs time in wild-type (WT) and neuroLSD1 null mice (KO). Black trace (representative trace) shows electrically evoked current generated under basal conditions. Red trace (representative trace) shows electrically evoked current generated 25 minutes after AMPH 6 mg/kg. Cyclic voltammograms (top right corner) in response to the applied potential. The oxidation of dopamine occurs at 0.6 V. **B)** Representation of the current generated, depicted in color, in response to the applied potential and the time of registration. **C)** Average extracellular dopamine (DA) concentration after electrical stimulation under basal conditions per genotype. **D)** Average maximum peak height normalized with respect

to baseline conditions at different time points after AMPH 6 mg/kg administration in WT, HT, and neuroLSD1 null mice (KO). A recording was performed every five minutes for two hours. **D)** AUC quantification of the graph in (C). **E)** Average of tau normalized with respect to baseline conditions at different time points after AMPH 6 mg/kg administration in WT, HT, and neuroLSD1 null mice (KO). A recording was performed every five minutes for two hours. **F)** AUC quantification of the graph in (E). **G)** Average of AUC for dopamine-release peak, normalized with respect to baseline conditions at different time points after AMPH 6 mg/kg administration in wild-type (WT), heterozygous (HT), and neuroLSD1 null mice (KO). A recording was performed every five minutes for two hours. **H)** AUC quantification of the graph in (E). Differences were analyzed by one-way ANOVA or Welch's ANOVA Test with Tukey's or Dunnet's multiple comparison test, (n = 3 – 5 per genotype). Data are presented as mean ± SD; *P < 0.05, ***P < 0.001.

Genotype	DA, ng/mg protein
WT, n=4	277.3 ± 165.3
HT, n=2	286.2 ± 59.8
KO, n=3	396.4 ± 273.5

Table 1: Dopamine content in the striatum of WT, HT and neuroLSD1 null mice.
Tissue dopamine content was quantified by HPLC-EC as described in Fuentealba et al (2006)[21].

Discussion

Dopamine is the principal regulator of motivated behaviors and a common target for drugs of abuse[22,23]. Understanding the adaptation mechanisms of the dopaminergic system is critical to reveal the etiology and find possible treatments for diseases such as Parkinson, schizophrenia, and addiction.

This work provides evidence suggesting that the uLSD1/neuroLSD1 transcript ratio is a sensor for dopamine neurotransmission that responds differently to acute or repeated stimuli of this system. Our data show that acute AMPH stimulation transiently decreases LSD1 protein levels. In contrast, repeated AMPH stimulation produces a long-term decrease of LSD1 protein and mRNA in a neuroLSD1-dependent process, suggesting that a self-regulatory negative feedback mechanism controls the expression of LSD1.

The uLSD1/neuroLSD1 transcript ratio remains around one in neurons under basal conditions. This ratio changes due to various acute stimuli that transiently decrease E8a inclusion. For example, it was shown that neuroLSD1 transcript decreases in the hippocampus seven hours after pilocarpine administration, returning to normal levels at twenty-four hours[12]. Social defeat stress (SDS) also produces a transient decrease in neuroLSD1 transcript in the same time window. This effect is accompanied by an increase in the total amount of LSD1 protein observed seven hours after SDS[11]. Our data show that acute AMPH administration induced an initial decrease (2 hours) and then an increase (8 hours) in LSD1 total protein levels at eight hours, similar to that observed in the hippocampus with SDS. This data allows suggesting that neuronal stimulation induces a transient decrease in LSD1 protein stability. Remarkably, the posterior increase in LSD1 protein levels coincides with the decrease in neuroLSD1 transcripts[11,12]. These data allow proposing that neuroLSD1 exerts an inhibitory mechanism on LSD1 transcription so that the decrease in neuroLSD1 suppresses a brake on gene transcription.

Contrary to what was observed with acute stimulation, repeated AMPH administration induced a long-lasting decrease in total levels of LSD1 protein and mRNA. Twenty-four hours after the acute AMPH stimulus, LSD1 protein levels and the uLSD1/neuroLSD1 ratio have returned to normal values. Conversely, twenty-four hours after repeated stimuli, LSD1 protein levels, and uLSD1/neuroLSD1 ratio are significantly lower than normal levels. This data suggests that uLSD1/neuroLSD1 ratio functions as a dopamine sensor whose value is modified according to whether the stimulus is repeated. In addition, the data show that neuroLSD1 proportion change in an opposite way than total LSD1, reinforcing the idea of a negative regulatory loop.

Concordantly, neuroLSD1 null mice are blind to the effects of repeated AMPH, maintaining the same levels of total LSD1 mRNA and protein as non-treated animals. These results point out that neuroLSD1 is necessary for the AMPH-mediated LSD1 decreased levels. We suggest that this is due to a transcriptionally regulatory loop of neuroLSD1 on its promoter, further supported by the ChIP seq data showing that LSD1 is bound to its own promoter. The elucidation of the specific mechanism involved deserves further work.

Our data suggest that dopamine through D2R negatively regulates E8a inclusion. We observed that the expression of D2R inversely correlates with the expression of neuroLSD1. Brain nuclei that express low levels of D2R such as the PFC[20,24] show higher levels of neuroLSD1, compared to the striatum that has higher levels of D2R and lower levels of neuroLSD1. This idea was corroborated in the striatum of D2R null mice, where the abundance of neuroLSD1 is higher than controls. Accordingly, the acute administration of the D2R antagonist haloperidol induce an increase of neuroLSD1 proportion in the striatum.

AMPH administration increases locomotor activity by increasing dopamine extracellular levels in the striatum[25]. An intriguing observation was that neuroLSD1 null mice

show a locomotor response to AMPH similar to native mice, but a greatly diminished neurochemical response. We do not have an explanation for this finding. We believe that the maintenance of the locomotor response to AMPH is due to a postsynaptic compensatory effect, probably related to increased dopamine receptors. Future studies of dopamine transporter and dopamine receptors functionality in neuroLSD1 null mice is necessary to unveil the origin of the altered response to AMPH.

In conclusion, our data show the involvement of neuroLSD1 in sensing dopamine transmission. Finally, our data reveal a neuroLSD1-dependent self-regulatory loop that was evident after repeated AMPH administration, pointing to a role for neuroLSD1 in the fine-tuning of neuronal transcriptional responses after repeated drug administration

References

1. Shi Y, Lan F, Matson C, Mulligan P, Whetstine JR, Cole PA, Casero RA, Shi Y. Histone demethylation mediated by the nuclear amine oxidase homolog LSD1. Cell (2004)
2. Andres, M. E. et al. CoREST: A functional corepressor required for regulation of neural- specific gene expression. Proc. Natl. Acad. Sci. U. S. A. (1999).
3. Humphrey, G. W. et al. Stable Histone Deacetylase Complexes Distinguished by the Presence of SANT Domain Proteins CoREST/kiaa0071 and Mta-L1. J. Biol. Chem. (2001) .
4. Ballas, N., Grunseich, C., Lu, D. D., Speh, J. C. & Mandel, G. REST and its corepressors mediate plasticity of neuronal gene chromatin throughout neurogenesis. Cell (2005).
5. Zibetti C, Adamo A, Binda C, Forneris F, Toffolo E, Verpelli C, Ginelli E, Mattevi A, Sala C, Battaglioli E.. Alternative splicing of the histone demethylase LSD1/KDM1 contributes to the modulation of neurite morphogenesis in the mammalian nervous system. J. Neurosci. (2010)
6. Laurent B, Ruitu L, Murn J, Hempel K, Ferrao R, Xiang Y, Liu S, Garcia BA, Wu H, Wu F, Steen H, Shi Y. A Specific LSD1/KDM1A Isoform Regulates Neuronal Differentiation through H3K9 Demethylation. Mol. Cell (2015)
7. Wang J, Telese F, Tan Y, Li W, Jin C, He X, Basnet H, Ma Q, Merkurjev D, Zhu X, Liu Z, Zhang J, Ohgi K, Taylor H, White RR, Tazearslan C, Suh Y, Macfarlan TS, Pfaff SL, Rosenfeld MG. LSD1n is an H4K20 demethylase regulating memory formation via transcriptional elongation control. Nat. Neurosci. (2015)
8. Metzger E, Wissmann M, Yin N, Müller JM, Schneider R, Peters AH, Günther T, Buettner R, Schüle R.LSD1 demethylates repressive histone marks to promote androgen-receptor-dependent transcription. Nature (2005)
9. Garcia-Bassets I, Kwon YS, Telese F, Prefontaine GG, Hutt KR, Cheng CS, Ju BG, Ohgi KA, Wang J, Escoubet-Lozach L, Rose DW, Glass CK, Fu XD, Rosenfeld MG. Histone Methylation-Dependent Mechanisms Impose Ligand Dependency for Gene Activation by Nuclear Receptors. Cell (2007).
10. Cai C, He HH, Gao S, Chen S, Yu Z, Gao Y, Chen S, Chen MW, Zhang J, Ahmed M, Wang Y, Metzger E, Schüle R, Liu XS, Brown M, Balk SP. Lysine-Specific Demethylase 1 Has Dual Functions as a Major Regulator of Androgen Receptor Transcriptional Activity. Cell Rep. (2014).
11. Rusconi F, Grillo B, Ponzoni L, Bassani S, Toffolo E, Paganini L, Mallei A, Braida D, Passafaro M, Popoli M, Sala M, Battaglioli E. LSD1 modulates stress-evoked transcription of immediate early genes and emotional behavior. Proc. Natl. Acad. Sci. U. S. A. (2016).
12. Rusconi F, Paganini L, Braida D, Ponzoni L, Toffolo E, Maroli A, Landsberger N, Bedogni F, Turco E, Pattini L, Altruda F, De Biasi S, Sala M, Battaglioli E. LSD1 neurospecific alternative splicing controls neuronal excitability in mouse models of epilepsy. Cereb. Cortex (2015).
13. Escobar AP, Cornejo FA, Olivares-Costa M, González M, Fuentealba JA, Gysling K, España RA, Andrés ME. Reduced dopamine and glutamate neurotransmission in the nucleus accumbens of quinpirole-sensitized rats hints at inhibitory D2 autoreceptor function. J. Neurochem. (2015).
14. Franklin, K. B. J., and G. Paxinos. A stereotaxic atlas of the mouse brain. *San Diego: Academic* (1997).
15. Yorgason, J. T., España, R. A. & Jones, S. R. Demon Voltammetry and Analysis software: Analysis of cocaine-induced alterations in dopamine signaling using multiple kinetic measures. J. Neurosci. Methods (2011).

16. Nestler, E. J., Barrot, M. & Self, D. W. ΔFosB: A sustained molecular switch for addiction. Proc. Natl. Acad. Sci. U. S. A. (2001).
17. Kodama M, Akiyama K, Ujike H, Shimizu Y, Tanaka Y, Kuroda S. A robust increase in expression of arc gene, an effector immediate early gene, in the rat brain after acute and chronic methamphetamine administration. Brain Res. (1998).
18. Takaki M, Ujike H, Kodama M, Takehisa Y, Yamamoto A, Kuroda S Increased expression of synaptophysin and stathmin mRNAs after methamphetamine administration in rat brain. Neuroreport. (2001).
19. Kelly MA, Rubinstein M, Asa SL, Zhang G, Saez C, Bunzow JR, Allen RG, Hnasko R, Ben-Jonathan N, Grandy DK, Low MJ. Pituitary lactotroph hyperplasia and chronic hyperprolactinemia in dopamine D2 receptor-deficient mice. Neuron (1997).
20. Levey AI, Hersch SM, Rye DB, Sunahara RK, Niznik HB, Kitt CA, Price DL, Maggio R, Brann MR, Ciliax BJ. Localization of D1 and D2 dopamine receptors in brain with subtype-specific antibodies. Proc. Natl. Acad. Sci. USA (1993).
21. Fuentealba JA, Gysling K, Magendzo K, Andrés ME. Repeated administration of the selective kappa-opioid receptor agonist U-69593 increases stimulated dopamine extracellular levels in the rat nucleus accumbens. J Neurosci Res. 2006
22. Palmiter, R. D. Dopamine signaling in the dorsal striatum is essential for motivated behaviors: Lessons from dopamine-deficient mice. in Annals of the New York Academy of Sciences (2008).
23. Volkow, N. D., Wise, R. A. & Baler, R. The dopamine motive system: Implications for drug and food addiction. Nature Reviews Neuroscience (2017).
24. Weiner DM, Levey AI, Sunahara RK, Niznik HB, O'Dowd BF, Seeman P, Brann MR. D1 and D2 dopamine receptor mRNA in rat. Proc. Natl. Acad. Sci. USA (1991).
25. Hyman, S. E., Malenka, R. C. & Nestler, E. J. Neural mechanisms of addiction: The role of reward-related learning and memory. Annual Review of Neuroscience (2006).

Supplementary data

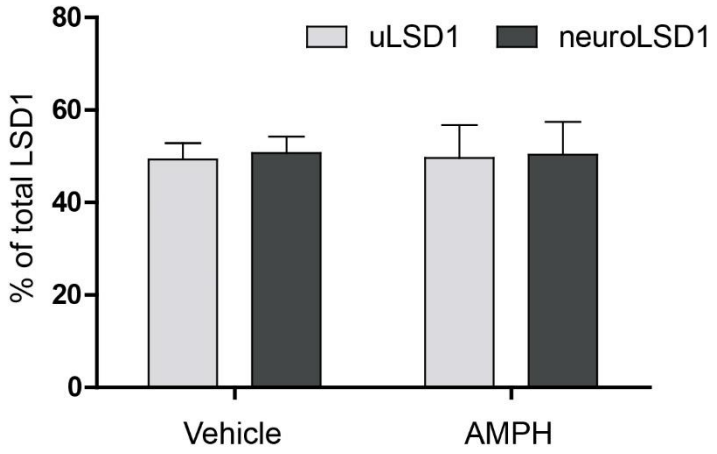

Figure S.1 uLSD1/neuroLSD1 transcripts ratio remains constant in the hippocampus after acute AMPH injection. Relative uLSD1 and neuroLSD1 mRNA expression assessed by rqf-PCR from the hippocampus of mice, two hours after an acute AMPH (6 mg/kg) or vehicle injection. At least three independent experiments are graphed by condition. Data are presented as mean ± SD.

.

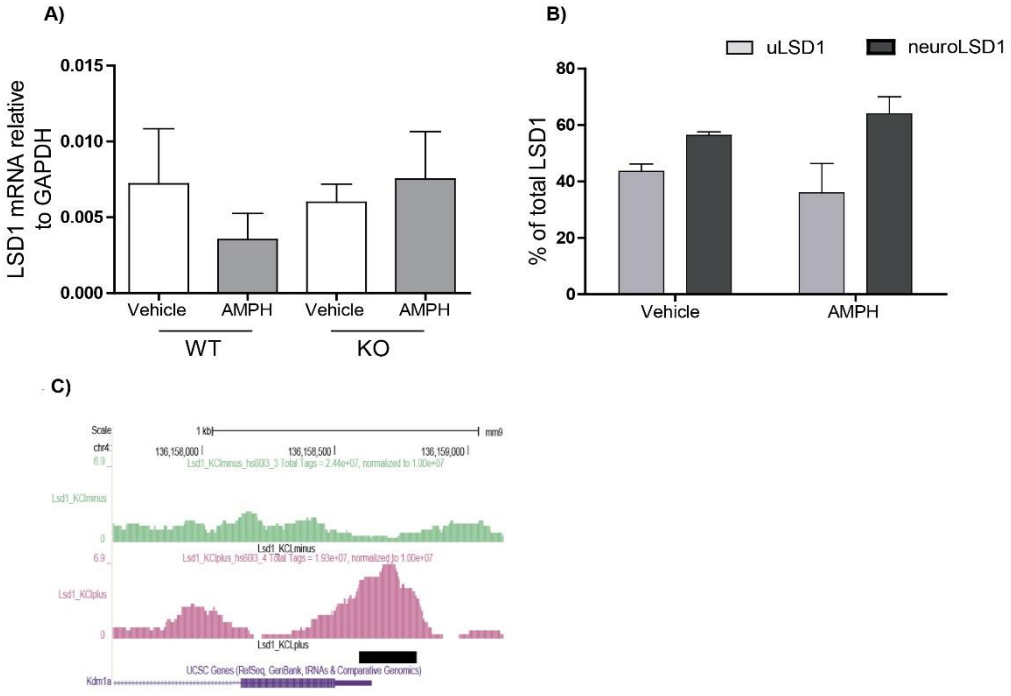

Figure S.2: AMPH repeated administration modulates total LSD1 and neuroLSD1 expression in the PFC. Total RNA was extracted 24 hours after the last injection, from PFC of mice injected repeatedly with AMPH or vehicle. **A)** Total amount of LSD1 mRNA relative to GAPDH measured by qPCR. Data correspond to the mean ± SD of at least three independent experiments. **B)** Relative mRNA expression of uLSD1 and neuroLSD1 assessed by rqf-PCR. Data are presented as the mean ± SD of the percentage of each isoform of at least three independent experiments. **C)** LSD1 binding, black boxes, in the mouse *Kdm1a* promoter region of control neurons (KCl_minus) and K+-stimulated neurons (KCl_plus), according to data published by Wang et al. in 2015. Scheme modified from the genome browser tool of the UCSC.,

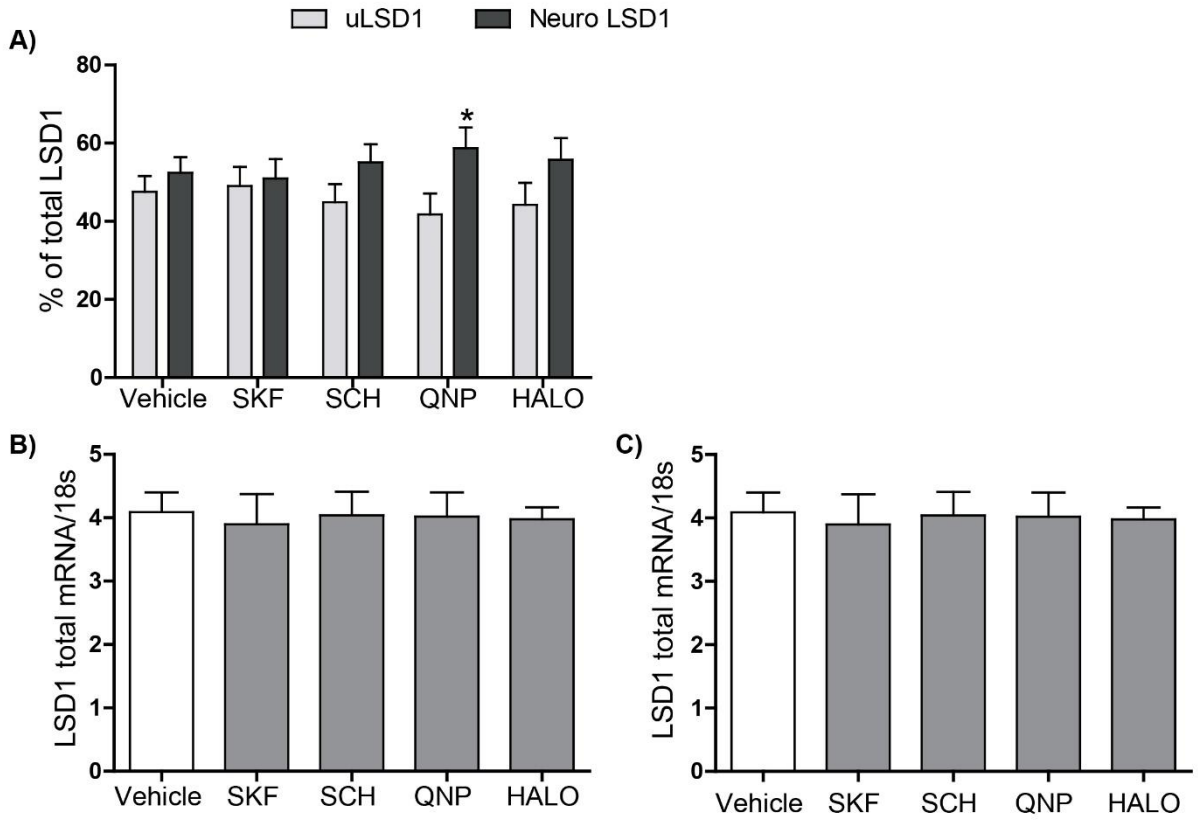

Figure S.3: neuroLSD1 proportion is increased in the PFC after systemic quinpirole injection. Total mRNA was extracted from the PFC of mice, two hours after acute haloperidol (HALO), quinpirole (QNP), SKF 38393 (SKF), SCH 23390 (SCH) or vehicle injection **A)** Relative expression of uLSD1 and neuroLSD1 (nLSD1) assessed by rqf-PCR. At least six independent experiments are graphed by condition, ** P <0.01 (compared to vehicle) by One-way ANOVA Dunnett's Multiple Comparison Test. **B, C)** Total LSD1 mRNA relative to 18s measured by qPCR from the B) the PFC and C) the striatum. Three independent experiments are graphed by condition. Data are presented as mean ± SD.

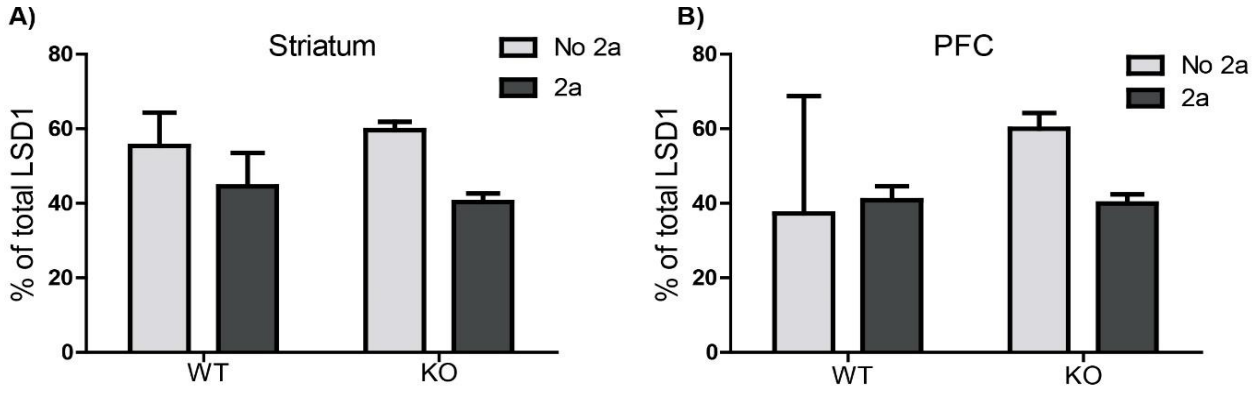

Figure S.4: Percentage of exon 2a inclusion in D2R deficient mice is similar to WT. Relative mRNA expression of uLSD1 and neuroLSD1 (nLSD1) assessed by rqf-PCR (see annex1) from **A)** the striatum and **B)** the PFC of WT and D2R deficient mice (KO). Three independent experiments are graphed by condition. Data are presented as mean ± SD.

Annex 1

rqf-PCR standardization

Exon Inclusion Frequency by Relative Quantity Fluorescent-PCR (rqf-PCR) is a technique designed to quantify the proportion of short sequences retained into a specific mRNA[1]. In this case, we used it to quantify alternative splicing of the *Kdm1a* gene (coding for LSD1). Two set of primers were designed to amplify all LSD1 splicing variants, or exclusively the region of E8a insertion (used to distinguish uLSD1 from neuroLSD1) **(Fig. 1 A and C)**. This mean the amplification of four or two different-size fragments, in a single PRC reaction. Differences in PCR products size is due to presence or absence of the alternative exons E2a and E8a (E2a= 60pb, E8a=12 pb) **(Fig1 B and D)**.

One of the primers used in the PCR reaction must be conjugated with a fluorochrome, to our experiments we used a 6-FAM-conjugated forward primer (Thermo Fisher). A fluorescent primer in the PCR reaction means that all the generated amplicons will be fluorescent labeled.

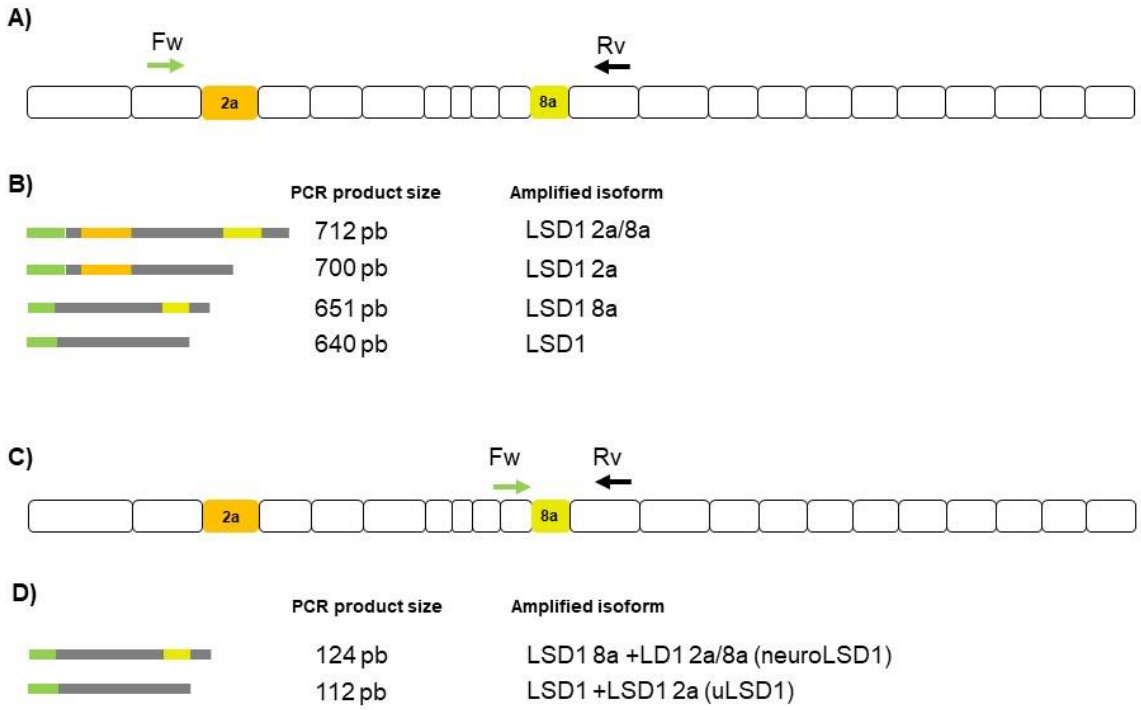

Figure1: rqf-PCR, examples of primer design and the PCR generated amplicons. **A and C)** Scheme of LSD1 mRNA, each box represents an exon. Alternative included exons, E2a and E8a are colored in orange and yellow, respectively. Rows indicate primers sequence location. The green row represents the fluorochrome-conjugated primer. A) Location of primers designed to amplify all LSD1 splicing variants. C) Location of primers designed to amplify the region of E8a insertion. **B and D)** Schematic view of each of the PCR generated amplicons. Green boxes represent a fluorescent region. Generated amplicons differ in length due to the presence of E2a and/or E8a, colored in orange and yellow, respectively. Length of each amplicon and represented LSD1 isoforms are specified. B) PCR generated amplicons using primers graphed in A. D) PCR generated amplicons using primers graphed in C.

The fluorescent-labeled PCR products were then separated by capillary electrophoresis coupled to fluorescent detection in the sequencing and omics technologies facility of the Pontificia Universidad Católica de Chile. As result of this procedure, we obtain a peak of detected fluorescence for each size of our PCR products **(Fig2**). Each amplified product was measured as relative fluorescence unit (RFU), considering the height of the peak. The

analysis was performed using the free available software, form Thermo Fisher, Peak scanner v1.0. (https://www.thermofisher.com/order/catalog/product/4381867#/4381867). For each sample, the heights of all specific peaks are summed, and the result is considering 100%. Then, the percentage corresponding to each fragment-size is calculated according to its peak-height. The size standard used were GS1200liz (for amplicons of all LSD1 isoforms) and GS500liz (Thermo Fisher) (form amplicons from E8a insertion region)

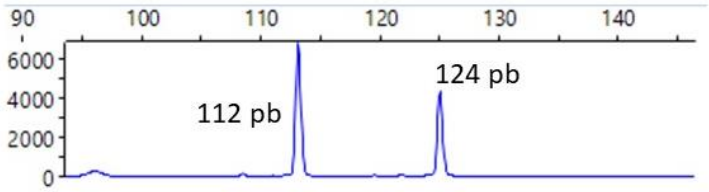

Figure 2: Example of electropherograms derived from the amplification of cDNA from mice brain. The higher peak corresponds to amplification of uLSD1 and the smaller to neuroLSD1.

Retention of neurospecific E8a in LSD1 transcripts is increased during neuronal development, whereas uLSD1 proportionally decreases. On the other hand, the inclusion of E2a is a steady event on neuronal development[1]. We use this model to corroborate that the proportion of each fragment size is proportional to the retention of E2a and or E8a. Rat cortical neurons were cultured by until 6 DIV and LSD1 isoforms were measured at different times. As expected, retention of E8a was continuously increased from DIV0 to DIV6, while no changes were observed in E2a retention **(Fig. 3A to C)**. Rqf-PCR designed to amplify region of E8a insertion **(Fig. 1C, D)** was validate comparing the amplification efficiency of two plasmid templates, pCGN-HA LSD1 and pCGN-HA LSD1-8a. The correspondence between variability in the molar ratio of the templates and the relative percentage of each

amplicon is illustrated in figure 3D of this section. We also use brain tissue from neuroLSD1 null mice to validate the specificity of the rqf-PCR **(Fig. 3D)**.

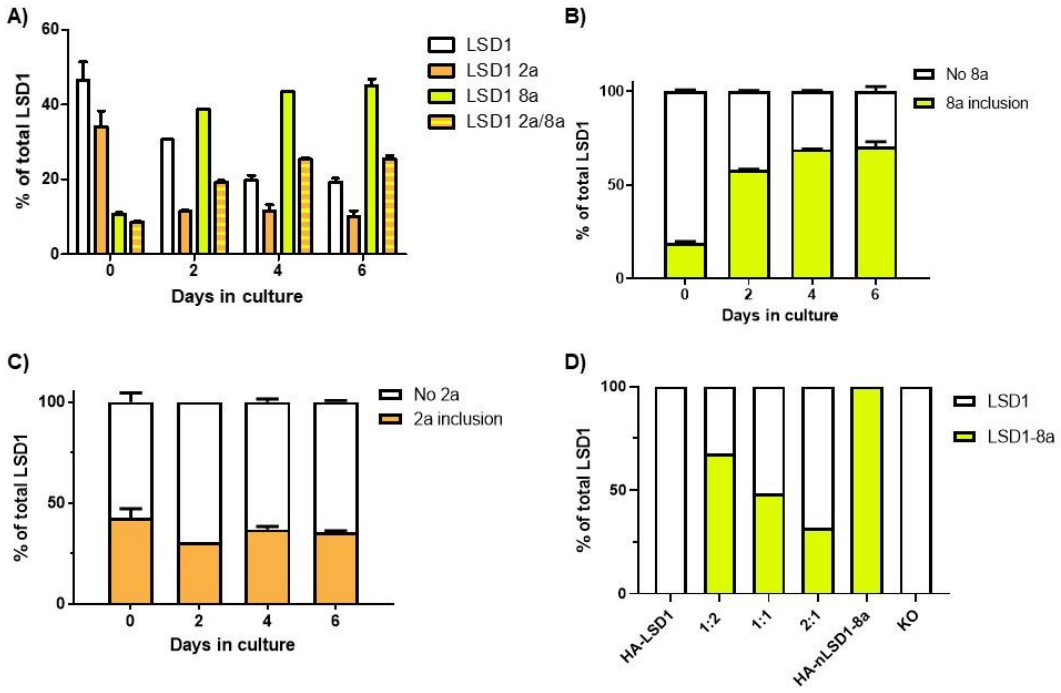

Figure 3: Validation of rqf-PCR, measuring all LSD1 isoforms. A) Percentage of each of the LSD1 isoforms in rat cortical neurons cultured for different time periods. **B)** percentage of isoforms that retain exon 8a (LSD1 8a + LSD1 2a / 8a), in yellow, and isoforms that do not retain exon 8a (LSD1 + LSD 2a) in white. **C)** percentage of isoforms that retain exon 2a (LSD1 2a + LSD1 2a / 8a), in orange, and isoforms that do not retain exon 2a (LSD1 + LSD 8a) in white. the data are shown as a percentage of each isoform concerning the total LSD1, averaging a total of two separate experiments. Data are presented as mean ± SD. **D)** Percentage of transcripts retaining or not the E8a. Different molar ratio of pCGN-HA LSD1: pCGN-HA LSD1-8a, or cDNA from neuroLSD1 null mice (KO) were used as template.

1. Zibetti et. al. Alternative splicing of the histone demethylase LSD1/KDM1 contributes to the modulation of neurite morphogenesis in the mammalian nervous system. J. Neurosci. (2010)

Chapter II

Transactivation of IEGs by neuroLSD1, a mechanism dependent on phosphorylation state of an exclusively neuronal-expressed threonine.

Activation of the IEGs *NR4A1* by neuroLSD1, a mechanism dependent on phosphorylation state of an exclusively neuronal-expressed threonine.

Abbreviated title: uLSD1 and neuroLSD1 transactivate IEGs

Montserrat Olivares-Costa[1], Marcela González[1], Francesco Rusconi[2], Elena Battaglioli[2,] and María Estela Andrés[1#]

[1]Department of Cellular and Molecular Biology, Faculty of Biological Sciences, Pontificia Universidad Católica de Chile, Santiago 8330025, Chile. [2]Department of Medical Biotechnology and Translational Medicine, Università Degli Studi di Milano, Via Fratelli Cervi, 93 20090 Segrate MI, Italy.

[#]Correspondence to María Estela Andrés, Department of Cellular and Molecular Biology, Faculty of Biological Sciences, Pontificia Universidad Católica de Chile, Santiago, Chile. mandres@bio.puc.cl.

Conflict of interest statement: The authors declare no competing financial interests.

Acknowledgments: This study was funded by Fondecyt grants 1150200 and 1191152. MO was supported by a Conicyt doctoral fellowship number 21140438. The authors acknowledge the services provided by UC CINBIOT Animal Facility funded by PIA CONICYT* ECM-07 *Program for Associative Research, of the Chilean National Council for Science and Technology.

Abstract

Lysine-Specific Demethylase 1 (LSD1, KDM1A) is an epigenetic enzyme that regulates gene expression forming complexes with the co-repressor RCOR1 and the histone desacetylases HDAC1/2. LSD1 has splicing variants that express only in neurons, collectively called neuroLSD1. neuroLSD1 differs from ubiquitous LSD1 (uLSD1) in the inclusion of a microexon codifying four amino acids, among them a phosphorylatable threonine. Mice null for neuroLSD1 are less responsive to stressful stimuli and present altered memory and learning. The functional role of neuroLSD1 has not been fully elucidated. NeuroLSD1 has been proposed to be essential for the induction of immediate early genes (IEG) by playing a dominant negative role against uLSD1. However, direct demonstration of these functions is lacking. Here we studied uLSD1 and neuroLSD1 role modulating the expression of *NR4A1*, an IEG induced in neurons by several stimuli as drugs of abuse, antipsychotics, and stress. Reporter assays showed that both uLSD1 and neuroLSD1 similarly induced the expression of the luciferase reporter driven by the human *NR4A1* promoter. The phosphodefective mutant of threonine in the neuroLSD1 microexon also increases *NR4A1* promoter activity, whereas the phosphomimetic mutant was silent. To further test neuroLSD1 role in IEGs expression, we used the null mouse for this variant. Bicuculline treatment of cultured hippocampal neurons showed that IEGs *NR4A1*, *FOS*, and *ARC* are similarly induced in the neuroLSD1 null as in the wild-type mice. Our data rule out that neuroLSD1 is essential for IEGs expression and instead suggests that the phosphorylated and unphosphorylated forms of neuroLSD1 conform an on/off switch for IEGs transcription.

Significance statement

Neuronal stimulation is followed by a molecular response that leads to the maintenance of internal homeostasis through, among other regulations, the transcription of immediate early genes (IEG). *NR4A1* is an IEG transiently expressed in the brain after stress, drugs of abuse intake, and antipsychotics administration. Here we show that the epigenetic enzyme LSD1 and its neuronal-exclusive variant neuroLSD1 are capable of inducing *NR4A1* in neurons. neuroLSD1 has a phosphorylatable threonine. Mutants of neuroLSD1 that cannot be phosphorylated also induce *NR4A1*, whereas mutants of neuroLSD1 that mimic phosphorylation are transcriptionally silent. We propose that LSD1 and neuroLSD1 play the same role in activating IEGs and that specific phosphorylation of neuroLSD1 is an on/off switch for modulating IEGs expression.

Introduction

Cellular response to stimuli involves processes occurring at different times. A group of genes can increase their transcriptional rate in short time (few minutes from stimuli), and in the absence of protein synthesis, these genes are called immediate-early by analogy to virus genes[1,2]. The immediate-early genes (IEGs) are also characterized by their low or undetectable basal expression and short lifetime of their mRNAs[1,3]. Many IEGs code for transcription factors enabling the cell to start adequate programs in response to stimuli. To this group of IEGs belong NR4A1 (also known as NGFI-B, TR3, and Nur77), a ligand-independent nuclear receptor[4,5]. NR4A1 was first described in NGF-treated rat pheochromocytoma cells (PC12), where its high and transient induction resisted protein synthesis inhibitor, cycloheximide[6]. NR4A1 is widely expressed in the Central Nervous System (CNS) and has been linked to processes involving neuronal plasticity[7], maintenance of dopamine-receptive neurons[8], and modulation of mitochondrial function in neurons during chronic stress[9]. The expression of NR4A1 is regulated by dopaminergic transmission[10]. Drugs that directly or indirectly stimulate dopamine receptors as drugs of abuse and typical antipsychotics, strongly induce NR4A1 expression[11,12,13]. Moreover, altered NR4A1 expression has been observed in multiple disorders associated with the dopaminergic system as addiction, Parkinson's disease, schizophrenia, and stress, among others[10,14,15].

Recent evidence points to a relevant role for the epigenetic enzyme Lysine Specific Demethylase 1A (LSD1, also termed KDM1A)[16] as a regulator of IEGs expression. LSD1 regulates gene expression by forming complexes with RCOR1 (CoREST1)[17] corepressor and histone deacetylases HDAC1/2[18]. LSD1 has four splice variants generated by alternative inclusion of two exons termed E2a (60 bp) and E8a (12 bp). Variants, including

the microexon E8a (LSD1 8a and LSD1 2a-8a) express exclusively in neurons and are called neuronal LSD1 (neuroLSD1). The other two variants (LSD1 and LSD1 2a) are widely expressed, even in neurons, and are called ubiquitous LSD1 (uLSD1)[19]. NeuroLSD1 differs from uLSD1 in a stretch of 4 amino acids codified in the microexon E8a[19]. Among these four amino acids, the phosphorylatable threonine (T369b) regulates the interaction of neuroLSD1 with the corepressors RCOR1 and HDAC1/2[20], enabling a fast modification of the binding and transcriptional regulatory capacities of neuroLSD1.

One of the functional roles attributed to neuroLSD1 is the regulation of the expression of IEGs. In this regard, Wang et al. (2015) reported impaired induction of IEGs by depolarization with high KCl in cultured neurons from null neuroLSD1 mice[21]. It is noteworthy that the overexpression specifically of the E8a-phosphomimetic neuroLSD1 increases the expression of IEGs in cultured hippocampal neurons, and the opposite effect is observed with uLSD1 and with the E8a-phosphodefective neuroLSD1 mutant[20]. Thus, neuroLSD1 has emerged as a pivotal factor regulating the transcription of IEGs. However, a direct proof of this function is lacking as well as whether phosphorylation of threonine encoded in the E8a exon plays a regulatory role.

To better understand the role of neuroLSD1 as an effector of neuronal activity-induced IEGs expression, neurons cultured from native and neuroLSD1 null mice were stimuli-synchronized with bicuculline, and temporal expression pattern of IEGs and LSD1 variants were measured. Furthermore, we studied the role of LSD1 variants in the NR4A1 promoter region. Our data rule out the hypothesis that neuroLSD1 is essential to induce IEGs but show that E8a-threonine phosphorylation regulates neuroLSD1 function in IEG transcription.

Materials and Methods

Animals

Adult male and female C57BL/6 mice, pregnant adult Sprague–Dawley rats and pregnant adult transgenic mice were used for the study (Animal Care Facility of the Faculty of Biological Sciences, Pontificia Universidad Católica de Chile). Group-housed animals (four mice/cage; three rat/cage) were maintained in the animal facility, under a 12/12 h light/dark cycle (lights off at 19 hrs. pm), constant temperature (24°C), with food and water available ad libitum. Transgenic mice for nLSD1[22] were crossed on a C57BL/6 background.

All experimental procedures that included animals were approved by the Bioethical Committee of the Faculty of Biological Sciences of the Pontificia Universidad Católica de Chile (protocols ID: 161014004, 160527009, 180808005). All procedures were conducted in order to reduce the number of animals when possible and to reduce their level of pain and discomfort as much as possible.

qPCR and rqf-PCR

rqf-PCR was performed as previously described[19]. Briefly, a 6FAM-conjugated fluorescent forward primer (Thermo Fisher) and a reverse unmodified one were used to amplify uLSD1 and neuroLSD1 in the same PCR reaction. Amplified products were separated by capillary electrophoresis under denaturing conditions, in the sequencing and omics technologies facility of the Pontificia Universidad Católica de Chile. The amount of each amplified product was measured as relative fluorescence unit levels using the software Peak scanner v1.0.

The following primers were used to amplify exon E8a containing region: Ex8_FW: 6-Fam-5´TCCCATGGCTGTCGTCAGCA3´; Ex11_Rv: 5´CTACCATTTCATCTTTTTCTTTTGG3´. Primers for qPCR were: NR4A1 Fw: 5´CACCCACCTCTCCGAACCGT3´ Rv: 5´GGGACTTGGTGGAGGTCACGGGT3´; cFOS Fw: 5´AATGGTGAAGACCGTGTCAG3´ Rv: 5´GCTTGGAGTGTATCTGTCAGC3´; ARC Fw: 5´GTCTTCTACCGTCTGGAG3´ Rv: 5´ATCAGCTTCCTGGCAGTAG3´; GAPDH Fw: 5´GTGTTCCTACCCCCAATGTGT3´ Rv: 5´ATTGTCATACCAGGAAATGAGCTT3´; total LSD1 Fw: 5´AAGCCAGGGATCGAGTAGGT3´ Rv: 5´CTGACGACAGCCATGGGATT3´.

In silico characterization of the *NR4A1* promoter region

NR4A1 genomic sequences were obtained from the human (GRch37 / hg19), mouse (NCBI37/mm9), and rat (RGSC 6.0/rn6) genomes. Sequence analysis to define the percentage of identity between human, mouse and rat promoter region was performed using the Clustal Omega tool[23] from the European Bioinformatics Institute (EMBL-EBI). Location of CpG island, ChIP-Seq binding sites, transcription start site (TSS), and active chromatin marks into the human genome were defined using the genome browser tool of the University of California Santa Cruz (UCSC)[24]. The strongest TSS gene was defined according to the eukaryotic promoter database[25]. Active chromatin regions were defined by the chromatin state segmentation by HMM from ENCODE / Broad[26]. Transcription factors binding sites were obtained from ChIP-Seq databases from the ENCODE project repository[27,28]. Cis-element Cluster Finder (Cister)[29] analysis was performed on the human *NR4A1* promoter using default parameters. Analysis of databases (GEO accession: GSE63271) from Wang et al., 2015[21] was performed adding custom tracks to the genome browser tool of the UCSC.

Cell lines culture conditions

Human embryonic kidney 293T cells (HEK293T) cells were cultured in Dulbecco's modified Eagle's medium supplemented with 10% fetal bovine serum (FBS). Rat pheochromocytoma cell line (PC12) was cultured in Dulbecco's modified Eagle's medium supplemented with 10% horse serum and 5% FBS. Both cell lines were supplemented with 1% penicillin/streptomycin and maintained at 37°C and 5% CO2.

Transient transfection and reporter gene assays

Transient transfection and reporter gene assays were performed in HEK293T and PC12 cell lines. pGL3 plasmid coding firefly luciferase under the control of the human *NR4A1* promoter was used as reporter (100ng) (Reporter plasmid was kindly provided by Dr. Xiao-kun Zhang). Different amounts of pCGN encoding LSD1, LSD1-8a, LSD1-8a T369bA, LSD1-8a T369bD or LSD1-8a/K661A or the empty vector, were co-transfected along with **β**-galactosidase reporter (25 ng), as transfection efficiency control vector, and p-Bluescript to equate the amount of transfected DNA. Protein extracts were obtained 48 h after transfection and luciferase activity measured in Turner Biosystems TD-20e luminometer. Each value of luciferase activity was normalized by protein absorbance and **β**-galactosidase activity.

Chromatin immunoprecipitation (ChIP) assays

ChIP assays were performed from HEK293T co-transfected with the pGL3-*NR4A1*-Luc and pCGN-LSD1. Cells from 100mm dish (~80% confluent) were fixed with 1% formaldehyde for 10 minutes at room temperature and then collected in a lysis buffer containing 5 mM HEPES (pH 8.0), 85 mM KCl, 0.5% Triton X-100, and protease inhibitors. Nuclear pellets were resuspended in a nuclear lysis buffer containing 50 mM Tris-HCl (pH

8.0), 10 mM EDTA, and 1% SDS plus protease inhibitors, then sonicated to reduce DNA length to between 200 and 800 bp. Nuclear extracts were precleared overnight at 4°C using protein A/G agarose beads (Santa Cruz, Inc.). The chromatin suspension (100 µl) was diluted 10-fold in ChIP dilution buffer containing 16.7mM Tris-HCL (pH 8.0), 167mM NaCl, 1.2mM EDTA, 1.1% Triton X-100, 0.01% SDS and 1mM PMSF and incubated with 2µg of anti-LSD1 antibody (ABCAM, AB17721), or rabbit IgG overnight at 4°C. Immunocomplexes were collected on protein A/G-agarose beads pre-adsorbed with 2% BSA and salmon sperm DNA (Thermo Fisher) for 2 h at 4ºC. A/G-agarose beads attached to immunocomplexes were washed consecutively with ChIP dilution buffer; dialysis buffer (50 mM Tris-HCL (pH 8.0), 2mM EDTA, 0.2% Sarkosyl); TSE-500 Buffer (20 mM Tris-HCL (pH 8.0), 500 mM NaCl, 2 mM EDTA, 1% Triton X-100, 0.1% SDS); LiCl Buffer (100mM Tris-HCL (pH 8.0), 500 mM LiCl, 1% Triton X-100, 1% deoxycholic acid), and Tris-EDTA buffer (10 mM Tris-HCL (pH 8.0), 1 mM EDTA). Then, immunocomplexes were eluted with 50 mM NaHCO3, 1% SDS, and cross-links were reversed by heating at 65°C overnight. DNA was treated with proteinase K, extracted with phenol-chloroform, precipitated, and resuspended in 30 µl of Tris-EDTA buffer. *NR4A1* promoter was amplified by PCR from immunoprecipitated DNA using the following primers, Forward: 5'GCGGGCGAGAGGAAAACTA3'; Reverse: 5'GCGAGCTTTGGCCATACAAG 3'.

Primary culture and bicuculline treatment

E18 embryos from adult Sprague–Dawley rats or neuroLSD1 null and WT mice were used for the primary culture studies. Pregnant mice and rats were decapitated, and embryos obtained by cesarean section. Embryos were decapitated and the hippocampus dissected out. Neurons were prepared as described in[30]. Pyramidal neurons were maintained for 14 days (DIV 14) in neurobasal medium (Gibco) supplemented with B27 supplement (Gibco),

1% penicillin/streptomycin and 0.05 mM glutamine. Bicuculline (50 uM) was added to DIV 14 neurons for 30 minutes, and then washed away by changing the medium three times. Cultures were put back into the incubator and total RNA was extracted at different times. WT and neuroLSD1 null neuronal cultures were obtained by crossing heterozygous mice, in those cases, neurons from each embryo were cultured separately, and embryos were genotyped.

Immunofluorescence

Immunofluorescent detection of cFOS was performed as previously described in Pereira et al (2017)[30] with minor modifications. Briefly, cells were fixed with 4% paraformaldehyde by 15 minutes, permeabilized with 0.25% Triton X-100 and blocked with 3% BSA by 1 h. Cells were incubated with rabbit polyclonal anti-cFOS (Santa Cruz, Inc., diluted 1:100) and with a fluorescent anti-rabbit Alexa 594. Finally, cells were incubated with 1:10000 Hoechst and mounted over DAKO. Coverslips were rinsed three times with PBS between each step. Immunofluorescence images were acquired with the 40× objective in an Olympus DS-Fi2 epifluorescence microscope equipped with a Nikon DS-fi2 camera operated with the standard QC capture software (Q-Imaging).

Statistical analyses

Statistical differences were analyzed using unpaired Student’s t-test or one-way ANOVA with Dunnett´s Multiple Comparison Test (Prism 9.0). Other statistical parameters (i.e. the n numbers and p values) can be found in figure legends.

Results

Structure and characterization of *NR4A1* promoter region

Several lines of evidence suggest that neuroLSD1 is necessary to neuronal activity-dependent increase of IEGs[20,21,31]. With this in mind, we studied if LSD1 and neuroLSD1 regulate the expression of the IEG *NR4A1*, a transcription factor highly related to dopamine transmission[10]. To this end, we first characterized the promoter of *NR4A1* and then compared the effect of LSD1 and neuroLSD1 in reporter assays.

The *NR4A1* gene is located on chromosome twelve in humans and fifteen in mice. According to the genomic navigator assembly tool of the University of California Santa Cruz (UCSC)[24], four variants of the *NR4A1* gene are generated by alternative splicing of the first exons in humans. We selected the most expressed variants 1 and 2 that share the first exon and give rise to the same 598 amino acid protein. The *NR4A1* promoter region was defined as the 2 kb sequence upstream of the strongest transcription start site (TSS, **Fig. 1A)**. Sequence analysis shows that human *NR4A1* gene promoter is about 60% identical to its mouse and rat counterparts **(Fig. 1C)**. Cis-element Cluster Finder (Cister)[29] showed several characteristics of cis-regulatory elements of IEG proximal promoters[32,33], such as a strong TATA-Box (not shown), several SP1 binding sites and CRE elements, confirmed by the human-mice-rat (HMR) Conserved Transcription Factor Binding Sites data from the UCSC genome browser **(Fig. 1A)**, and concordant with the characterization of the rat promoter[34].Classification of this genomic regions as active promoter in many different cell lines, according to chromatin state segmentation by Ernst et al. 2011[26], **(Fig. S1)**, **(Fig. 1A)**[33] further confirms that a canonical IEG promoter drives the expression of *NR4A1*. The

presence of a CpG island, an infrequent feature of IEG promoters, was also observed in the *NR4A1* proximal promoter region.

Bioinformatics analyses showed binding of the LSD1 partners, REST transcription factor, RCOR1 (CoREST1), and HDAC1/2 in the *NR4A1* promoter region **(Fig. 1A)**. To test if LSD1 is also tagged to *NR4A1* promoter, we analyzed the data obtained by Wang et al (2015) from ChIP-Seqs for LSD1 in unstimulated or KCl-stimulated mice cortical neurons[21]. We found that LSD1 is attached to the *NR4A1* proximal promoter in both conditions **(Fig. 1B)**, further supporting that LSD1 is part of a pre-assembled complex at the *NR4A1* promoter.

A)

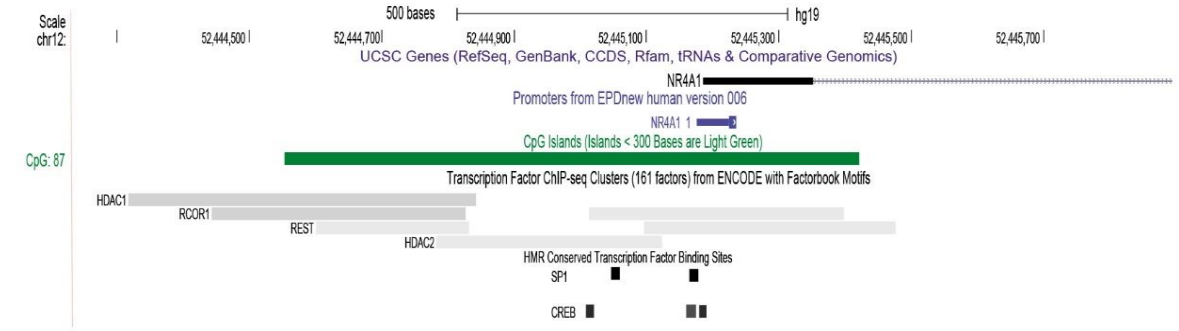

B)

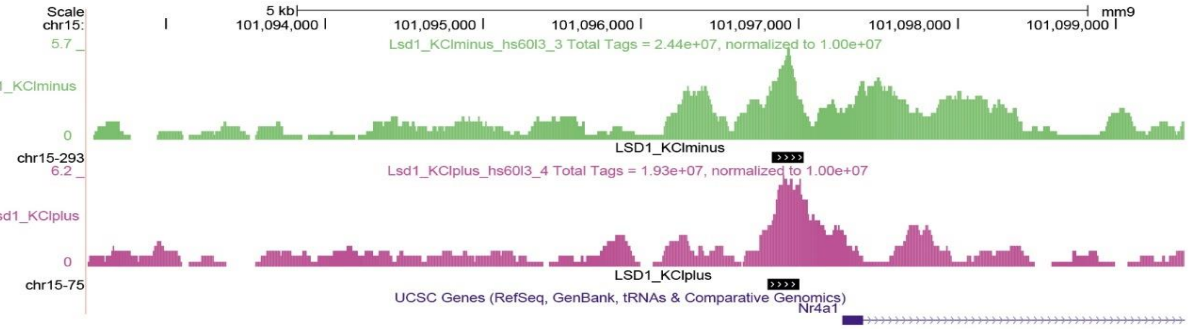

C)

	Percent Identity		
Especies	Human	Mouse	Rat
Human	100.00	59.91	61.01
Mouse	59.91	100.00	86.64
Rat	61.01	86.64	100.00

Figure 1: characterization of *NR4A1* promoter region A) IEG-like features of the human *NR4A1* promoter, adapted from the genome browser tool of the University of California Santa Cruz. **B)** LSD1 binding, black boxes, in the mouse *Nr4a1* promoter region of control neurons (KClminus) and K+-stimulated neurons (KClplus), according to data published by Wang et al. in 2015[21]. Scheme modified from the genome browser tool of the UCSC. **C)** Matrix of identity between human, mouse, and rat *NR4A1* promoter region (-2kb from TSS).

LSD1 and neuroLSD1 but not the phosphomimetic neuroLSD1 mutant increase *NR4A1* promoter activity

Previous data showing binding of LSD1 in *NR4A1* promoter prompted us to test the action of LSD1 and neuroLSD1 variant on *NR4A1* transcription. To this end, we carried out reporter assays using the human *NR4A1* promoter described above fused to the luciferase reporter.

Reporter gene assays were performed with a fixed amount (100 ng) of the *NR4A1*-luciferase reporter selected from a DNA concentration-effect curve carried out in HEK293T cells **(Fig. S2)**. Equivalent molar amounts of pCGN plasmids encoding uLSD1 (sequence without exons 2a and 8a), neuroLSD1 (LSD1 containing the exon 8a), or the empty vector were co-transfected along with the *NR4A1*-luciferase reporter in HEK293-T cells. Unexpectedly, both uLSD1 and neuroLSD1 increase the luciferase activity compared to the empty vector in HEK293T cells **(Fig. 2A)**. These data were replicated in PC12 cells **(Fig. 2B)**. To further test the ability of LSD1 to regulate the transcription of *NR4A1*, we studied LSD1 binding to the *NR4A1* promoter. Our ChIP-PCR assays showed that endogenous LSD1 is attached to the *NR4A1* proximal promoter in the reporter plasmid and overexpression of uLSD1 increases the binding **(Fig. 2C)**, thus correlating with the increased induction of luciferase activity.

As mentioned E8a microexon of neuroLSD1 encodes 4 amino acids stretch including a phosphorylatable threonine (T369b)[20]. Therefore, we wondered whether T369b phosphorylation of neuroLSD1 plays a regulatory role in IEGs expression. To this end, we tested the ability of the phosphomimetic T369bD (T/D) and phosphodefective T369bA (T/A) mutants of neuroLSD1[20] to regulate *NR4A1* promoter activity. Reporter assays showed that phosphodefective neuroLSD1 T/A mutant exhibited a similar ability to increase luciferase activity as wild type neuroLSD1 and uLSD1. In contrast, phosphomimetic neuroLSD1 T/D

did not modify *NR4A1*-luciferase reporter activity compared to the control **(Fig. 2A)**. These effects were not related to changes in protein levels of LSD1 variants or mutants as observed in western blot assays **(Fig. 2D)**. These data indicate that uLSD1, as well as the dephosphorylated form of neuroLSD1, activates *NR4A1* promoter, and phosphorylation of T369b of neuroLSD1 would limit this capacity.

LSD1 regulates the transcriptional response of its target genes in different ways[35]. One way is participating in transcriptional complexes that post-translationally modify the histone tails. In these complexes, LSD1 demethylates the tail of histone H3[16,36]. A second way is through forming structural complexes with proteins harboring SNAG domains[37], similar to like the tail of histone H3, in which LSD1 is hooked[38]. A third way is through modifying interacting proteins stability[39]. Taking this information into account, we wondered whether the catalytic enzymatic activity of LSD1 is required to increase the *NR4A1* promoter activity by using the mutant LSD1K661ΔA (K/A), which is unable to demethylate the lysine 4 in histone H3[20]. As shown in the **figure 2E**, the catalytically inert mutant LSD1 K/A was as efficient as uLSD1 and neuroLSD1 inducing NR4A1-luciferase reporter activity. To further support this evidence, cells were incubated from transfection to harvest time with tranylcypromine (0.5 mM), an inhibitor of the enzymatic activity of LSD1[40]. Supporting previous data, tranylcypromine did not modify the activating effect of uLSD1 and neuroLSD1 over the *NR4A1* promoter **(Fig. 2F)**. Altogether, these data suggest that uLSD1 and neuroLSD1 induce *NR4A1* expression by a catalytically independent mechanism.

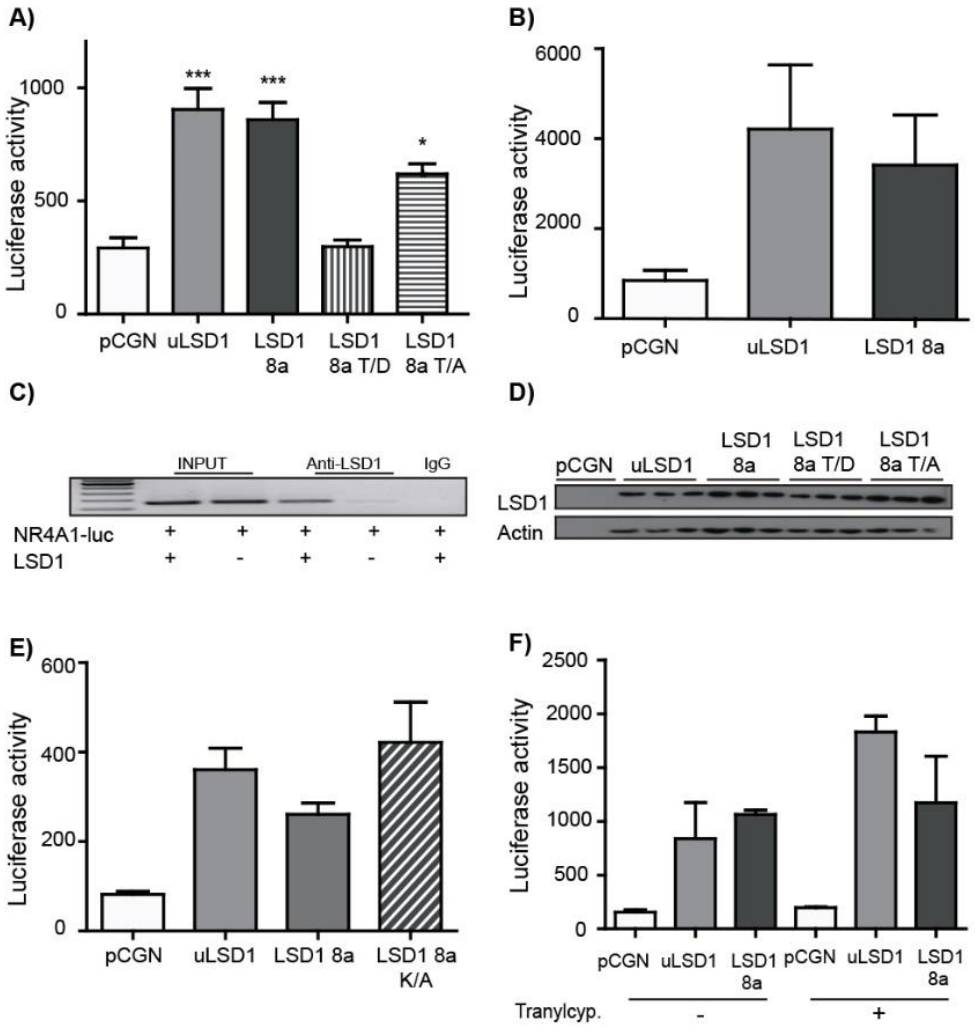

Figure 2: uLSD1 and neuroLSD1 induce *NR4A1* promoter activity. A) Luciferase activity in extracts of PC-12 cells transfected with *NR4A1*-Luciferase reporter and pCGN (empty vector), uLSD1, or neuroLSD1 (LSD1 8a). Data are presented as means ± SEM of two independent experiments performed by triplicate. **B)** Luciferase activity measured in extracts of HEK283T cells transfected with *NR4A1*-Luciferase reporter and pCGN, uLSD1, neuroLSD1 (LSD1 8a), neuroLSD1 phosphomimetic mutant (LSD1 8a T/D) or neuroLSD1 8a phosphodefective mutant (LSD1 8a T/A). Data are presented as mean ± SEM of at least three independent experiments performed by triplicate. *P<0.05, ***P<0.001 by Kruskal-Wallis test followed by Dunn's Multiple Comparison Test. **C)** ChIP-PCR from HEK293T cells transfected with *NR4A1*-Luciferase reporter and uLSD1 (+) or controls (-). PCR of the immunoprecipitated DNA was performed using primers to amplify the proximal *NR4A1* promoter region. N=1.**D)** Western blot of whole extracts of HEK293T, graphed in B, showing similar protein levels of LSD1 variants. **E)** Luciferase activity in extracts of HEK293T cells transfected with NR4A1-Luciferase reporter and pCGN, LSD1, LSD1 8a, or the LSD1 catalytic-mutant (uLSD1 K/A). Data are presented as mean ± SD of a single experiment performed by triplicate. **F)** Luciferase activity in extracts of HEK293T cells transfected with NR4A1-Luc reporter and pCGN, LSD1, or LSD1 8a plasmids, treated with 0.5 mM of tranylcypromine (+) or vehicle (-). Data are presented as mean ± SD of a single experiment performed by triplicate.

Similar induction of *NR4A1* and cFOS in wild-type and neuroLSD1 null mice cultured neurons.

To better understand how neuroLSD1 is involved in the regulation of IEGs expression, we carried out a temporal course study of neuroLSD1 and uLSD1 expression, along with IEGs. To this end, rat hippocampal neurons at DIV14 were incubated for 30 minutes with bicuculline, a GABA receptors antagonist that induces a synchronized synaptic activation of neurons[41]. After 30 minutes of bicuculline incubation, the culture medium was replaced to remove bicuculline, and neurons were harvested at different time points **(Fig. 3A)**. rqf-PCR showed that the proportion of uLSD1/neuroLSD1 did not vary during 60 minutes after bicuculline. However, a progressive decrease of neuroLSD1 was observed between 90 and 150 minutes after bicuculline treatment **(Fig. 3B)**. cFos immunosignal and *NR4A1* mRNA levels showed a progressive induction during the 70 minutes after bicuculline treatment **(Fig. 3C and D)**. Then, NR4A1 mRNA levels started to decrease from 90 minutes after bicuculline treatment, correlating with the diminished neuroLSD1 proportion at the same time **(Fig. 3B and D)**. These data suggest that the induction of IEGs is not related to changes in uLSD1/neuroLSD1 proportion, but IEGs turning to basal corelates with a decrease in the relative amount of neuroLSD1.

Previous studies suggest that neuroLSD1 is necessary for the induction of IEGs expression by neuronal stimuli and that uLSD1 would have an opposite role, repressing them[31]. Since our reporter gene assays showed that both uLSD1 and neuroLSD1 have the same activating effect on *NR4A1* promoter, we studied whether IEGs induction is impaired in neuroLSD1 null mice. Using the bicuculline treatment in cultured hippocampal neurons from WT and neuroLSD1 null mice, we assessed the induction of the IEGs c*Fos*, *Arc* and *Nr4a1* by qPCR. In line with reporter assays, the expression of *Nr4a1*, *Fos*, and *Arc*, increased similarly in WT and neuroLSD1 null neurons 70 minutes after bicuculline

treatment **(Fig. 3E and F)**, demonstrating that neuroLSD1 is not necessary to induce IEGs expression by neuronal stimuli. Altogether, these data indicate that neuroLSD1 is not essential to IEGs induction but suggest that the ratio between phosphorylated and unphosphorylated forms of neuroLSD1 could be important to regulate the transcriptional rate of IEGs.

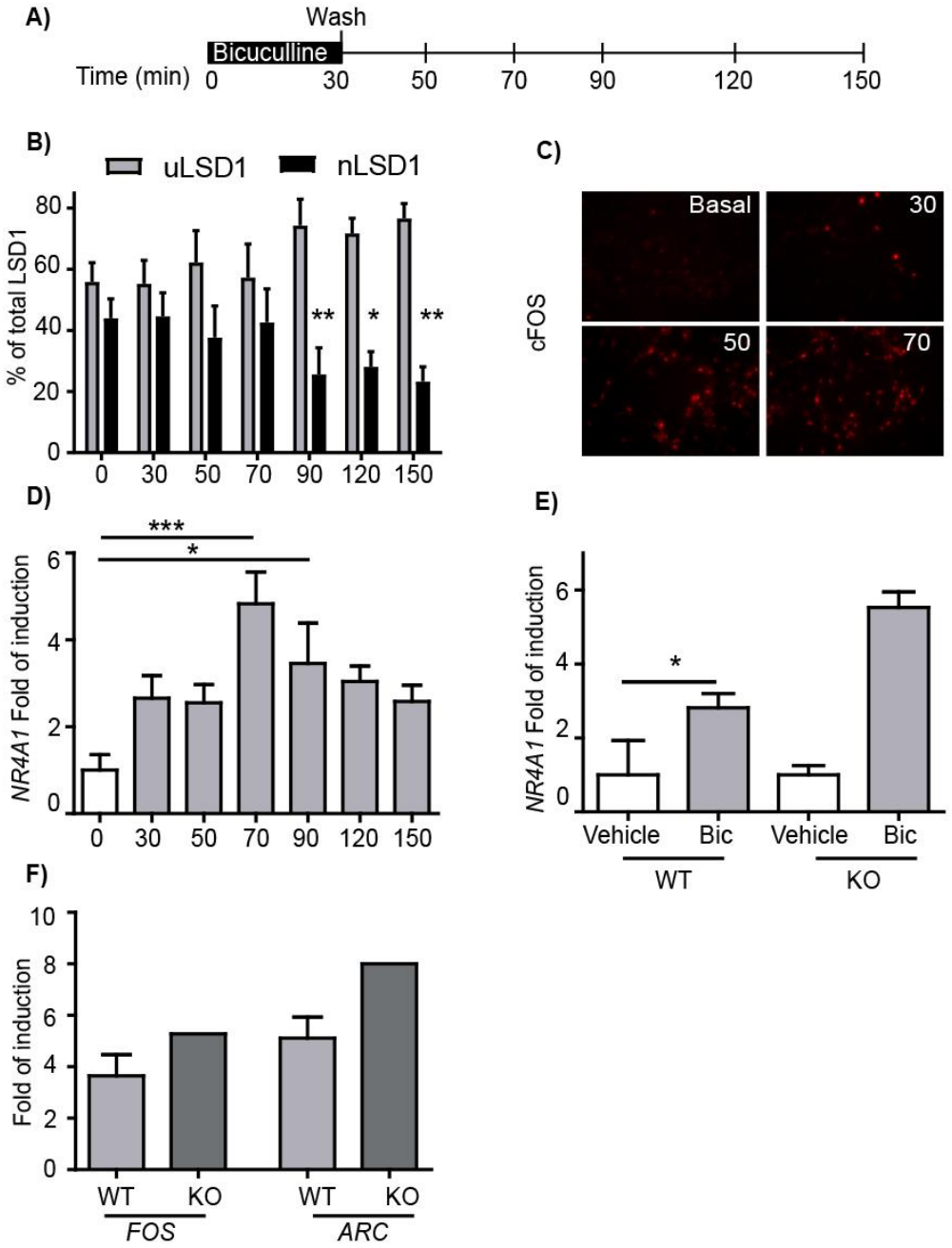

Figure 3: Similar bicuculline-dependent induction of IEGs in cultured hippocampal neurons of wild-type and neuroLSD1 null mice. A) Bicuculline treatment pipeline. 14DIV neurons were treated with 50 uM bicuculline for 30 minutes and mRNA was extracted at indicated times. **B)** Relative mRNA expression of uLSD1 and neuroLSD1 (nLSD1) assessed by rqf-PCR in primary cultures of rat hippocampal neurons treated with bicuculline. Data are presented as mean ± SD of at least three independent experiments for each time points. *P<0.05, **P<0.01 by one-way ANOVA, followed by Dunnett's multiple comparison test. Compared to basal condition **C)** Immunofluorescence detection of cFOS in primary cultures of rat hippocampal neurons treated with bicuculline. Basal corresponds to untreated neurons and numbers indicate time from initiation of bicuculline treatment. **D)** Fold of induction of *Nr4a1*measured by q-PCR in primary cultures of rat hippocampal neurons treated with bicuculline. The X-axis indicates the time (min) from bicuculline treatment. Data are presented as mean ± SEM of at least five independent experiments performed by duplicate. *P<0.05, ***P<0.001 by One-way ANOVA followed by Dunnett´s Multiple Comparison Test. **E, F)** Fold of induction of *Nr4a1*(E), *Fos* and *Arc* (F) assessed by qPCR in primary cultures of WT and neuroLSD1 null mice hippocampal neurons after 70 minutes from bicuculline treatment. Data are presented as mean ± SEM of one to three independent experiments performed by duplicate. *P<0.05 by Student's unpaired t-test.

Discussion

Transient induction of IEGs expression in the CNS is crucial to initiate gene programs for plasticity[42]. It has been proposed that neuroLSD1 is necessary to properly induce stimuli regulated IEGs, while uLSD1 would act as a repressor[21,31]. This work provides evidence that neuroLSD1 is not essential to induce IEGs. Here is shown that uLSD1 and neuroLSD1 plays a similar role, increasing the activity of the *NR4A1* promoter. We propose that uLSD1/neuroLSD1 ratio is related to transcriptional modulation and phosphorylation of the specific E8a-encoded threonine is a switch to transcriptional activity.

Our data from bicuculline-induced synchronized stimulation show a robust induction of the IEGs, *Fos*, *Arc*, and *Nr4a1* in hippocampal neurons of the neuroLSD1 null mice, discarding that neuroLSD1 is essential for IEGs induction. Reporter assays showing that uLSD1 activates the *NR4A1* gene promoter, similarly as neuroLSD1 suggest that uLSD1 may replace neuroLSD1 in the neuroLSD1 null mice. Our data does not necessarily conflict with the finding of impaired IEGs induction in neuroLSD1 heterozygous mice seven hours after acute social stress defeat (SDS) reported by Rusconi et al. (2016)[31] nor with the finding of decreased IEGs induction in cortical neurons of neuroLSD1 null mice four hours after KCl treatment reported by Wang et al. (2015)[21]. We hypothesize that these differences are due to the time after stimuli in which IEGs were measured. Induction of IEGs is quick and transient, and we specifically wondered about the role of neuroLSD1 in the initial induction of IEGs. Our observations do not rule out a possible role for neuroLSD1 in the descendant part of the expression kinetics of IEGs. However, our data do not support an essential role for neuroLSD1 in the induction of IEGs. Instead, our data support a homeostatic role for neuroLSD1 regulating IEGs expression. On the one hand, the temporal study of the

uLSD1/neuroLSD1 ratio in bicuculline-stimulated neurons shows that initially, the proportion of neuroLSD1 remains constant, indicating that a change in the ratio of LSD1 isoforms would not be necessary for the induction of IEGs. Then, neuroLSD1 decreases progressively, correlating with the gradual return of NR4A1 to basal levels, suggesting that modifications in the uLSD1/neuroLSD1 ratio could be related to a long-term adaptive response, however more studies are required to test this idea.

Our bioinformatics analysis and ChIP assays indicate that LSD1 is bound to the *NR4A1* promoter before and after neuronal stimulation. In line with these data, previous work showed that both uLSD1 and neuroLSD1, together with RCOR1 and HDAC2 co-repressors, are bound to IEG promoters, forming complexes with the serum response factor, SRF[31].

Interestingly, reporter gene assays showed that the phosphomimetic neuroLSD1 mutant is silent on the *NR4A1* promoter, while the phosphodefective behaves as the wild type neuroLSD1, inducing the transcription of the reporter driven by the NR4A1 promoter. These data suggest that the phosphorylation/dephosphorylation of T369b in neuroLSD1 could be the molecular switch regulating LSD1-mediated IEGs activation, in a neuronal-specific mechanism. The phosphorylation in T369b disrupts the interaction of neuroLSD1 with the co-repressors RCOR1 and HDACs[20], providing a mechanism that allows the alternation for this variant to interact with other proteins.

Furthermore, our data show that the catalytic function of LSD1 is not required to induce the activity of the *NR4A1* promoter. Reporter assays showed that the catalytically inert neuroLSD1K661A efficiently induced the *NR4A1*-Luciferase reporter, and the LSD1 inhibitor, tranylcypromine, was unable to reduce the induction of *NR4A1*-Luciferase reporter by either uLSD1 or neuroLSD1. These data raise the possibility that both uLSD1 and

neuroLSD1 play a co-activator role on *NR4A1* promoter, independent of their canonical catalytic function.

The uLSD1/neuroLSD1 ratio remains around one in neurons under basal conditions. However, this ratio changes due to various stimuli that transiently decrease E8a inclusion. For example, neuroLSD1 mRNA decreases in the hippocampus seven hours after pilocarpine administration, returning to normal levels at twenty-four hours[22]. SDS also produces a transient decrease in neuroLSD1 at the same time window[31].

We propose that this uLSD1/neuroLSD1 adaptive system could be a causative mechanism to desensitize IEG expression after repeated stimuli. Since the phosphomimetic and phosphodefective forms of neuroLSD1 have opposite effects on the *NR4A1* promoter, proteomic analysis of each variant is needed to understand the role of this post-translational modification in vivo.

In conclusion, our data show that LSD1 and neuroLSD1 increase *NR4A1* promoter activity. We rule out that neuroLSD1 it is necessary to IEGs induction and propose the phosphorylation of T369b as a molecular switch that determines transcriptional output of IEGs.

References

1. Lau, L. F. & Nathans, D. Identification of a set of genes expressed during the G0/G1 transition of cultured mouse cells. EMBO J. (1985).
2. Lau, L. F. & Nathans, D. Expression of a set of growth-related immediate early genes in BALB/c 3T3 cells: Coordinate regulation with c-fos or c-myc. Proc. Natl. Acad. Sci. U. S. A. (1987)
3. Sheng, M. & Greenberg, M. E. The regulation and function of c-fos and other immediate early genes in the nervous system. Neuron (1990).
4. Mangelsdorf DJ, Thummel C, Beato M, Herrlich P, Schütz G, Umesono K, Blumberg B, Kastner P, Mark M, Chambon P, Evans RM. The nuclear receptor superfamily: The second decade. Cell (1995).
5. Maruyama K, Tsukada T, Ohkura N, Bandoh S, Hosono T, Yamaguchi K. The NGFI-B subfamily of the nuclear receptor superfamily. International Journal of Oncology (1998).
6. Milbrandt, J. Nerve growth factor induces a gene homologous to the glucocorticoid receptor gene. Neuron (1988).
7. Chen Y, Wang Y, Ertürk A, Kallop D, Jiang Z, Weimer RM, Kaminker J, Sheng M. Activity-induced Nr4a1 regulates spine density and distribution pattern of excitatory synapses in pyramidal neurons. Neuron (2014).
8. Rouillard, C. et al. Genetic disruption of the nuclear receptor Nur77 (Nr4a1) in rat reduces dopamine cell loss and L-Dopa-induced dyskinesia in experimental Parkinson's disease. Exp. Neurol. (2018).
9. Jeanneteau F, Barrère C, Vos M, De Vries CJM, Rouillard C, Levesque D, Dromard Y, Moisan MP, Duric V, Franklin TC, Duman RS, Lewis DA, Ginsberg SD, Arango-Lievano M. The stress-induced transcription factor NR4a1 adjusts mitochondrial function and synapse number in prefrontal cortex. J. Neurosci. (2018)..
10. Campos-Melo, D., Galleguillos, D., Sánchez, N., Gysling, K. & Andrés, M. E. Nur transcription factors in stress and addiction. Frontiers in Molecular Neuroscience (2013).
11. Beaudry, G., Langlois, M.-C., Weppe, I., Rouillard, C. & Lévesque, D. Contrasting Patterns and Cellular Specificity of Transcriptional Regulation of the Nuclear Receptor Nerve Growth Factor-Inducible B by Haloperidol and Clozapine in the Rat Forebrain. J. Neurochem. (2002)
12. Maheux, J., Éthier, I., Rouillard, C. & Lévesque, D. Induction patterns of transcription factors of the Nur family (Nurr1, Nur77, and Nor-1) by typical and atypical antipsychotics in the mouse brain: Implication for their mechanism of action. J. Pharmacol. Exp. Ther. (2005).
13. Sánchez N, Coura R, Engmann O, Marion-Poll L, Longueville S, Hervé D, Andrés ME, Girault JA. Haloperidol-induced Nur77 expression in striatopallidal neurons is under the control of protein phosphatase 1 regulation by DARPP-32. Neuropharmacology (2014).
14. Xing, G., Zhang, L., Russell, S. & Post, R. Reduction of dopamine-related transcription factors Nurr1 and NGFI-B in the prefrontal cortex in schizophrenia and bipolar disorders. Schizophr. Res. (2006).
15. Lévesque, D. & Rouillard, C. Nur77 and retinoid X receptors: crucial factors in dopamine-related neuroadaptation. Trends in Neurosciences (2007).
16. Shi Y, Lan F, Matson C, Mulligan P, Whetstine JR, Cole PA, Casero RA, Shi Y. Histone demethylation mediated by the nuclear amine oxidase homolog LSD1. Cell (2004)

17. Andrés ME, Burger C, Peral-Rubio MJ, Battaglioli E, Anderson ME, Grimes J, Dallman J, Ballas N, Mandel G. CoREST: A functional corepressor required for regulation of neural-specific gene expression. Proc. Natl. Acad. Sci. U. S. A. (1999).

18. Humphrey GW, Wang Y, Russanova VR, Hirai T, Qin J, Nakatani Y, Howard BH. Stable Histone Deacetylase Complexes Distinguished by the Presence of SANT Domain Proteins CoREST/kiaa0071 and Mta-L1. J. Biol. Chem. (2001).

19. Zibetti C, Adamo A, Binda C, Forneris F, Toffolo E, Verpelli C, Ginelli E, Mattevi A, Sala C, Battaglioli E. Alternative splicing of the histone demethylase LSD1/KDM1 contributes to the modulation of neurite morphogenesis in the mammalian nervous system. J. Neurosci. (2010).

20. Toffolo E, Rusconi F, Paganini L, Tortorici M, Pilotto S, Heise C, Verpelli C, Tedeschi G, Maffioli E, Sala C, Mattevi A, Battaglioli E. Phosphorylation of neuronal Lysine-Specific Demethylase 1LSD1/KDM1A impairs transcriptional repression by regulating interaction with CoREST and histone deacetylases HDAC1/2. J. Neurochem. (2014).

21. Wang J, Telese F, Tan Y, Li W, Jin C, He X, Basnet H, Ma Q, Merkurjev D, Zhu X, Liu Z, Zhang J, Ohgi K, Taylor H, White RR, Tazearslan C, Suh Y, Macfarlan TS, Pfaff SL, Rosenfeld MG. LSD1n is an H4K20 demethylase regulating memory formation via transcriptional elongation control. Nat. Neurosci. (2015).

22. Rusconi F, Paganini L, Braida D, Ponzoni L, Toffolo E, Maroli A, Landsberger N, Bedogni F, Turco E, Pattini L, Altruda F, De Biasi S, Sala M, Battaglioli E. LSD1 neurospecific alternative splicing controls neuronal excitability in mouse models of epilepsy. Cereb. Cortex (2015).

23. Madeira F, Park YM, Lee J, Buso N, Gur T, Madhusoodanan N, Basutkar P, Tivey ARN, Potter SC, Finn RD, Lopez R. The EMBL-EBI search and sequence analysis tools APIs in 2019. Nucleic Acids Res. (2019).

24. Kent WJ, Sugnet CW, Furey TS, Roskin KM, Pringle TH, Zahler AM, Haussler D. The Human Genome Browser at UCSC. Genome Res. (2002).

25. Dreos, R., Ambrosini, G., Périer, R. C. & Bucher, P. The Eukaryotic Promoter Database: expansion of EPDnew and new promoter analysis tools. Nucleic Acids Res. (2014).

26. Ernst J, Kheradpour P, Mikkelsen TS, Shoresh N, Ward LD, Epstein CB, Zhang X, Wang L, Issner R, Coyne M, Ku M, Durham T, Kellis M, Bernstein BE. Mapping and analysis of chromatin state dynamics in nine human cell types. Nature (2011)

27. Dunham, I. et al. An integrated encyclopedia of DNA elements in the human genome. Nature (2012).

28. Wang, J. et al. Sequence features and chromatin structure around the genomic regions bound by 119 human transcription factors. Genome Res. (2012).

29. Frith, M. C., Hansen, U. & Weng, Z. Detection of cis-element clusters in higher eukaryotic DNA. Bioinformatics (2001).

30. Pereira, L. A., Munita, R., González, M. P. & Andrés, M. E. Long 3'UTR of Nurr1 mRNAs is targeted by miRNAs in mesencephalic dopamine neurons. PLoS One (2017).

31. Rusconi F, Grillo B, Ponzoni L, Bassani S, Toffolo E, Paganini L, Mallei A, Braida D, Passafaro M, Popoli M, Sala M, Battaglioli E. LSD1 modulates stress-evoked transcription of immediate early genes and emotional behavior. Proc. Natl. Acad. Sci. U. S. A. (2016).

32. Sheng, M. & Greenberg, M. E. The regulation and function of c-fos and other immediate early genes in the nervous system. Neuron (1990).

33. Bahrami, S. & Drabløs, F. Gene regulation in the immediate-early response process. Advances in Biological Regulation (2016).

34. Watson, M. A. & Milbrandt, J. The NGFI-B gene, a transcriptionally inducible member of the steroid receptor gene superfamily: genomic structure and expression in rat brain after seizure induction. Mol. Cell. Biol. (1989)

35. Gu F, Lin Y, Wang Z, Wu X, Ye Z, Wang Y, Lan H. Biological roles of LSD1 beyond its demethylase activity. Cellular and Molecular Life Sciences (2020).

36. Metzger E, Wissmann M, Yin N, Müller JM, Schneider R, Peters AH, Günther T, Buettner R, Schüle R. LSD1 demethylates repressive histone marks to promote androgen-receptor-dependent transcription. Nature (2005).

37. Welcker JE, Hernandez-Miranda LR, Paul FE, Jia S, Ivanov A, Selbach M, Birchmeier C. Insm1 controls development of pituitary endocrine cells and requires a SNAG domain for function and for recruitment of histone-modifying factors. Dev. (2013).

38. Lin Y, Wu Y, Li J, Dong C, Ye X, Chi YI, Evers BM, Zhou BP. The SNAG domain of Snail1 functions as a molecular hook for recruiting lysine-specific demethylase 1. EMBO J. (2010).

39. Lan H, Tan M, Zhang Q, Yang F, Wang S, Li H, Xiong X, Sun Y. LSD1 destabilizes FBXW7 and abrogates FBXW7 functions independent of its demethylase activity. Proc. Natl. Acad. Sci. U. S. A. (2019).

40. Schmidt, D. M. Z. & Mccafferty, D. G. trans-2-Phenylcyclopropylamine Is a Mechanism-Based Inactivator of the Histone Demethylase LSD1. Biochemistry (2007)

41. Arnold FJ, Hofmann F, Bengtson CP, Wittmann M, Vanhoutte P, Bading H. Microelectrode array recordings of cultured hippocampal networks reveal a simple model for transcription and protein synthesis-dependent plasticity. J. Physiol. (2005).

42. Kim, S., Kim, H. & Um, J. W. Synapse development organized by neuronal activity-regulated immediate-early genes. Experimental and Molecular Medicine (2018)

Supplementary data

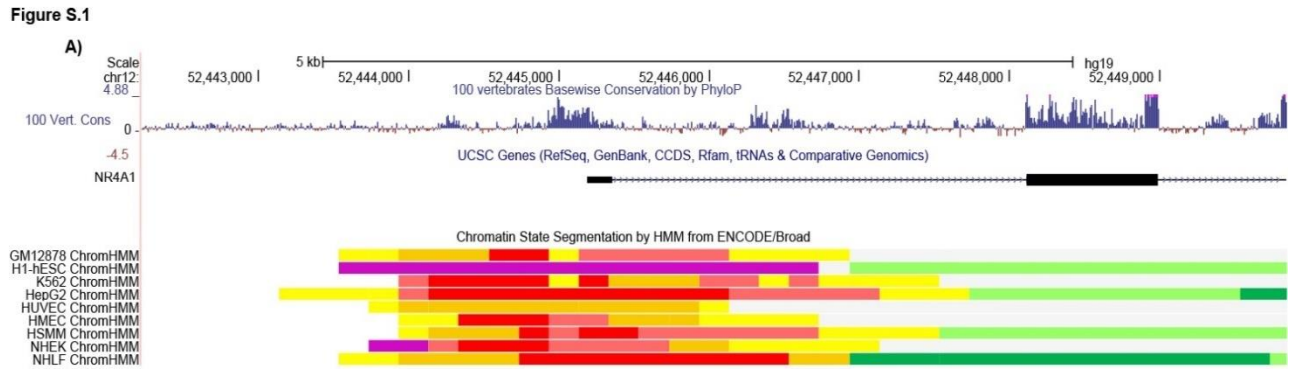

Figure S.1: Active chromatin marks in *NR4A1* promoter region. Scheme of the *NR4A1* proximal promoter region. First and second exons are represented as black boxes. Segment of chromatin classified as active promoter according to chromatin state segmentation by Ernst et al. 2011, are shown in red, pink represent weak promoter and purple poised or inactive promoter. Orange and yellow represent strong or weak enhancer, respectively. Different tone of green represents transcribed regions. Cell line represented on each line of chromatin segmentation are indicated at left. Scale bar, chromosome position and conservation among vertebrates are also showed on top. Scheme modified from the genome browser tool of the UCSC.

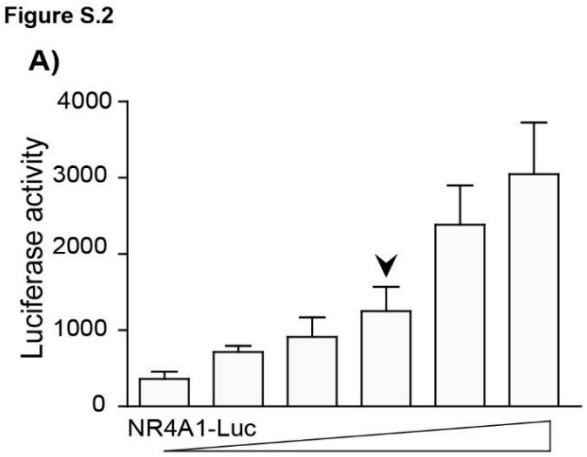

Figure S.2: *NR4A1*-luciferase concentration-effect curve. Luciferase activity measured in extracts of HEK283T cells transfected with growing amount of the NR4A1-Luciferase reporter (25, 50, 75, 100, 150 and 200 ng). Row head indicate transfection of 100ng of NR4A1-Luciferase reporter, this amount is used in all reporter gene assays on this article.

Discussion

In the present work, we provide novel insights into the molecular changes induced by dopamine signaling. This is the first study linking LSD1 and neuroLSD1 with dopaminergic transmission and discarding an essential role for neuroLSD1 in stimuli-induced IEGs transcription. According to our data, LSD1 and its neuronal variant participate in pre- and post-synaptic events, and modulate homeostatic response to chronic AMPH treatment, revealing a negative transcriptional feedback system mediated by neuroLSD1. We demonstrate an inductive role of LSD1 and neuroLSD1 over Nur77 expression, one of the IEG most important to dopamine response, and propose the phosphorylation state of the neuroLSD1-exclusive threonine as responsible for the fast induction of IEGs.

A fraction of IEGs, including Nur77, possess CpG island on their promoters. CpG associated genes have fewer stable nucleosomes, and therefore chromatin remodeling plays a discreet role in their induction[11,106]. This is consistent with our data that LSD1 demethylase activity is not required to activate the Nur77 promoter. For many IEGs, it has been described that the preinitiation complex is bound to their promoter under basal conditions, associated with Pol II in paused[8,14,15]. It has been proposed that neuroLSD1 promotes gene transcription by demethylation of H4K20 and allow the release of Pol II and transcriptional elongation[100]. We and others have show that LSD1 and neuroLSD1 bind IEGs promoters[100,105] leading to propose that both isoforms could be components of a pre-assembled complex in the proximal promoter of Nu77. From our reporter gene assays, we suggest that phosphorylation of T369b in neuroLSD1 maintains basal levels of Nur77

transcription, and dephosphorylation emerges as a quick mechanism for Nur77 induction. If this is due to changes in the neuroLSD1 protein interaction or due to paused Pol II release is an interesting question that requires further studies. For a dephosphorylation-dependent induction of Nur77, an activity dependent phosphatase must be involved. This and the circumstances on which phosphorylation and dephosphorylation of neuroLSD1 occur are topics of considerable interest that constitute the next step in this investigation field.

Impaired IEGs induction has been reported in neuroLSD1 null mice[100,105]. However, our data demonstrate that neuroLSD1 is not essential for IEGs induction and suggest that the ratio between phosphorylated and unphosphorylated neuroLSD1 tun the transcription of IEGs in response to repeated neuronal stimuli.

The fact that LSD1 and the uLSD1/neuroLSD1 ratio respond differently in acute versus chronic AMPH administration indicates that an adaptive response is occurring to repeated presentation of a stimulus. This adaptive response operates as an analog mode of regulation (i.e., the initial response differs from the response after repeated stimuli). We propose that this adaptative uLSD1/neuroLSD1 system could be a causative mechanism to desensitize IEGs expression after repeated stimuli[75,107]. These findings are relevant because the prolonged Nur77 transcription during chronic stress is detrimental to mitochondrial energetic competence and diminishes dendritic spines number[108].

NeuroLSD1 null mice cannot down-regulate total LSD1 after repeated AMPH administration, unveiling a negative regulatory feedback over LSD1 transcription, confirming that the role of neuroLSD1 could be to set the neuronal response after repeated stimuli (Fig. 1). The elucidation of the specific mechanism involved deserves further work.

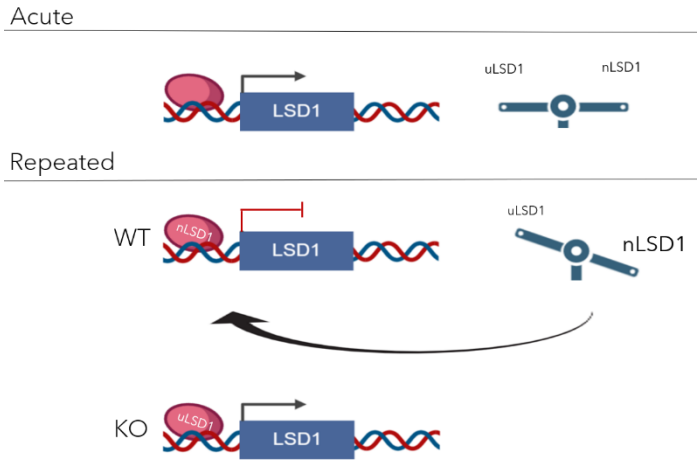

Figure1: neuroLSD1 mediated negative feedback, proposed model.
Acute AMPH administration do not produce changes in LSD1 transcriptional rate or isoforms proportions. However repeated AMP administration decreases total LSD1 transcription while increases neuroLSD1 proportion. These molecular effects of repeated AMPH administration are absents in neuroLSD1 null mice. We propose that LSD1 is tagged to their own promoter after stimuli, due to neuroLSD1 proportion is increased in repeated treatment it is more probably to find this isoform in the promoter.

A greatly diminished AMPH-induced dopamine release is observed in neuroLSD1 null mice compared to wild types littermates. This data demonstrates that neuroLSD1 is also involved in dopaminergic neurons activity. Interestingly, AMPH-induced locomotor activity in neuroLSD1 null mice is similar to wild types. We believe that the maintenance of the locomotor response to AMPH is due to a postsynaptic compensatory effect, probably related to increased dopamine receptors. Understanding neuroLSD1 pre-synaptic effect and proposed post-synaptic compensatory mechanism requires further studies.

Here we show that LSD1 and neuroLSD1 regulate Nur77 transcription, and in turn, LSD1 splicing is selectively modulated by D2R mediated signaling. As Nur77 expression is a readout of D2R activity[66,74], we propose LSD1 as a link between D2R signaling and Nur77 expression. This is a previously undescribed pathway connecting D2R signaling and Nur77-mediated transcriptional changes. Due to the role of Nur77 in neurons remains poorly

understood, we made an effort to identify Nur77 target genes and to clarify the function of this transcription factor. We use available databases to identify Nur77 target genes and their possible role through gene ontology analyses. We identify several Nur77 target genes mainly related to cellular adhesion and anchoring. Furthermore, we were able to find genes that link Nur77 role in immune and neuronal systems (annex 2).

In conclusion, the work presented here constitutes an overturn of what was known about neuroLSD1, we rule out that it is essential to IEGs induction and position it as a regulator of neuronal adaptive responses to chronic stimuli. We also propose that control of the phosphorylation state in T369b of neuroLSD1 is the mechanism underlying LSD1 mediated IEGs transcriptional regulation.

References

1. Lau, L. F. & Nathans, D. Expression of a set of growth-related immediate early genes in BALB/c 3T3 cells: Coordinate regulation with c-fos or c-myc. Proc. Natl. Acad. Sci. U. S. A. (1987).
2. Lau, L. F. & Nathans, D. Identification of a set of genes expressed during the G0/G1 transition of cultured mouse cells. EMBO J. (1985)
3. Sheng, M. & Greenberg, M. E. The regulation and function of c-fos and other immediate early genes in the nervous system. Neuron (1990).
4. Leslie, J. H. & Nedivi, E. Activity-regulated genes as mediators of neural circuit plasticity. Progress in Neurobiology vol. 94 223–237 (2011).
5. Lyford GL, Yamagata K, Kaufmann WE, Barnes CA, Sanders LK, Copeland NG, Gilbert DJ, Jenkins NA, Lanahan AA, Worley PF. Arc, a growth factor and activity-regulated gene, encodes a novel cytoskeleton-associated protein that is enriched in neuronal dendrites. Neuron (1995).
6. Brakeman PR, Lanahan AA, O'Brien R, Roche K, Barnes CA, Huganir RL, Worley PF. Homer: A protein that selectively binds metabotropic glutamate receptors. Nature (1997)
7. Kim, S., Kim, H. & Um, J. W. Synapse development organized by neuronal activity-regulated immediate-early genes. Experimental and Molecular Medicine (2018).
8. Tullai JW, Schaffer ME, Mullenbrock S, Sholder G, Kasif S, Cooper GM. Immediate-early and delayed primary response genes are distinct in function and genomic architecture. J. Biol. Chem. 282, 23981–23995 (2007).
9. Fowler, T., Sen, R. & Roy, A. L. Regulation of primary response genes. Molecular Cell vol. 44 348–360 (2011).
10. Glauser, D. A. & Schlegel, W. Mechanisms of transcriptional regulation underlying temporal integration of signals.
11. Bahrami, S. & Drabløs, F. Gene regulation in the immediate-early response process. Advances in Biological Regulation (2016).
12. Flouriot G, Huet G, Demay F, Pakdel F, Boujrad N, Michel D. The actin/MKL1 signalling pathway influences cell growth and gene expression through large-scale chromatin reorganization and histone post-translational modifications. Biochem. J. (2014).
13. Ciccarelli, A. & Giustetto, M. Role of ERK signaling in activity-dependent modifications of histone proteins. Neuropharmacology (2014).
14. Levine, M. Paused RNA polymerase II as a developmental checkpoint. Cell. (2011).
15. Kim, T. H. et al. A high-resolution map of active promoters in the human genome. Nature. (2005).
16. Okuno, H. Regulation and function of immediate-early genes in the brain: Beyond neuronal activity markers. Neuroscience Research. (2011).
17. Abraham, W. C., Dragunow, M. & Tate, W. P. The role of immediate early genes in the stabilization of long-term potentiation. Mol. Neurobiol. (1991).
18. Bisagno, V. & Cadet, J. L. Expression of immediate early genes in brain reward circuitries: Differential regulation by psychostimulant and opioid drugs. Neurochemistry International. (2019).
19. Minatohara, K., Akiyoshi, M. & Okuno, H. Role of immediate-early genes in synaptic plasticity and neuronal ensembles underlying the memory trace. Front. Mol. Neurosci. 8, (2016).
20. Kubik, S., Miyashita, T. & Guzowski, J. F. Using immediate-early genes to map hippocampal subregional functions. Learning and Memory. (2007).

21. Wisden W, Errington ML, Williams S, Dunnett SB, Waters C, Hitchcock D, Evan G, Bliss TV, Hunt SP. Differential expression of immediate early genes in the hippocampus and spinal cord. Neuron. (1990).

22. Waltereit R, Dammermann B, Wulff P, Scafidi J, Staubli U, Kauselmann G, Bundman M, Kuhl D. Arg3.1/Arc mRNA induction by Ca2+ and cAMP requires protein kinase a and mitogen-activated protein kinase/extracellular regulated kinase activation. J. Neurosci. (2001).

23. Worley PF, Bhat RV, Baraban JM, Erickson CA, McNaughton BL, Barnes CA. Thresholds for synaptic activation of transcription factors in hippocampus: Correlation with long-term enhancement. J. Neurosci. (1993).

24. Konradi, C., Leveque, J. C. & Hyman, S. E. Amphetamine and dopamine-induced immediate early gene expression in striatal neurons depends on postsynaptic NMDA receptors and calcium. J. Neurosci. (1996).

25. Greenberg, M. E., Thompson, M. A. & Sheng, M. Calcium regulation of immediate early gene transcription. J. Physiol. Paris (1992).

26. Cole, A. J., Saffen, D. W., Baraban, J. M. & Worley, P. F. Rapid increase of an immediate early gene messenger RNA in hippocampal neurons by synaptic NMDA receptor activation. Nature (1989).

27. Kandel, E. R. The molecular biology of memory: CAMP, PKA, CRE, CREB-1, CREB-2, and CPEB. Molecular Brain. (2012).

28. Sheng, M. & Greenberg, M. E. The regulation and function of c-fos and other immediate early genes in the nervous system. Neuron (1990).

29. Lonze, B. E. & Ginty, D. D. Function and regulation of CREB family transcription factors in the nervous system. Neuron. (2002).

30. Changelian, P. S., Feng, P., King, T. C. & Milbrandt, J. Structure of the NGFI-A gene and detection of upstream sequences responsible for its transcriptional induction by nerve growth factor. Proc. Natl. Acad. Sci. U. S. A. (1989).

31. Ramanan N, Shen Y, Sarsfield S, Lemberger T, Schütz G, Linden DJ, Ginty DD. SRF mediates activity-induced gene expression and synaptic plasticity but not neuronal viability. Nat. Neurosci. (2005).

32. Rodríguez-Tornos, F. M., San Aniceto, I., Cubelos, B. & Nieto, M. Enrichment of Conserved Synaptic Activity-Responsive Element in Neuronal Genes Predicts a Coordinated Response of MEF2, CREB and SRF. PLoS One (2013).

33. Hazel, T. G., Nathans, D. & Lau, L. F. A gene inducible by serum growth factors encodes a member of the steroid and thyroid hormone receptor superfamily. Proc. Natl. Acad. Sci. U. S. A. (1988)

34. Milbrandt, J. Nerve growth factor induces a gene homologous to the glucocorticoid receptor gene. Neuron (1988).

35. Mangelsdorf DJ, Thummel C, Beato M, Herrlich P, Schütz G, Umesono K, Blumberg B, Kastner P, Mark M, Chambon P, Evans RM. The nuclear receptor superfamily: The second decade. Cell (1995).

36. Law, S. W., Conneely, O. M., DeMayo, F. J. & O'Malley, B. W. Identification of a new brain-specific transcription factor, nurr1. Mol. Endocrinol. (1992).

37. Ohkura N, Ito M, Tsukada T, Sasaki K, Yamaguchi K, Miki K. Structure, mapping and expression of a human NOR-1 gene, the third member of the Nur77/NGFI-B family. Biochim. Biophys. Acta - Gene Struct. Expr. (1996).

38. Campos-Melo, D., Galleguillos, D., Sánchez, N., Gysling, K. & Andrés, M. E. Nur transcription factors in stress and addiction. Frontiers in Molecular Neuroscience (2013).

39. Kent WJ, Sugnet CW, Furey TS, Roskin KM, Pringle TH, Zahler AM, Haussler D.. The Human Genome Browser at UCSC. Genome Res. (2002).

40. Rehman, S. ur, Sarwar, T., Husain, M. A., Ishqi, H. M. & Tabish, M. Identification of two novel isoforms of mouse NUR77 lacking N-terminal domains. IUBMB Life(2017).

41. Boonstra, J., Moolenaar, W. H. & Harrison, P. H. Ionic responses and growth stimulation induced by nerve growth factor and epidermal growth factor in rat pheochromocytoma (PC12) cells. J. Cell Biol. (1983).

42. Greene, L. A. & Tischler, A. S. PC12 Pheochromocytoma Cultures in Neurobiological Research. Elsevier. (1982).

43. Bouron, A., Becker, C. & Porzig, H. Functional expression of voltage-gated Na+ and Ca2+ channels during neuronal differentiation of PC12 cells with nerve growth factor or forskolin. Naunyn. Schmiedebergs. Arch. Pharmacol. (1999).

44. Maruoka H, Yamazoe R, Takahashi R, Yatsuo K, Ido D, Fuchigami Y, Hoshikawa F, Shimoke K. Molecular mechanism of nur77 gene expression and downstream target genes in the early stage of forskolin-induced differentiation in PC12 cells. Sci. Rep. (2020).

45. Jeong Kyo Yoon & Lau, L. F. Transcriptional activation of the inducible nuclear receptor gene nur77 by nerve growth factor and membrane depolarization in PC12 cells. J. Biol. Chem. (1993).

46. Yoon, J. K. & Lau, L. F. Involvement of JunD in transcriptional activation of the orphan receptor gene nur77 by nerve growth factor and membrane depolarization in PC12 cells. Mol. Cell. Biol. (1994).

47. Watson, M. A. & Milbrandt, J. The NGFI-B gene, a transcriptionally inducible member of the steroid receptor gene superfamily: genomic structure and expression in rat brain after seizure induction. Mol. Cell. Biol. (1989)

48. Fass, D. M., Butler, J. E. F. & Goodman, R. H. Deacetylase Activity Is Required for cAMP Activation of a Subset of CREB Target Genes. J. Biol. Chem. (2003).

49. Kurakula, K., Koenis, D. S., van Tiel, C. M. & de Vries, C. J. M. NR4A nuclear receptors are orphans but not lonesome. Biochimica et Biophysica Acta - Molecular Cell Research. (2014).

50. Giguère, V. Orphan Nuclear Receptors: From Gene to Function*. Endocr. Rev. (1999).

51. Wang Z, Benoit G, Liu J, Prasad S, Aarnisalo P, Liu X, Xu H, Walker NP, Perlmann T. Structure and function of Nurr1 identifies a class of ligand-independent nuclear receptors. Nature (2003).

52. Flaig, R., Greschik, H., Peluso-Iltis, C. & Moras, D. Structural basis for the cell-specific activities of the NGFI-B and the Nurr1 ligand-binding domain. J. Biol. Chem. (2005).

53. Ojeda, V., Fuentealba, J. A., Galleguillos, D. & Andrés, M. E. Rapid increase of Nurr1 expression in the substantia nigra after 6-hydroxydopamine lesion in the striatum of the rat. J. Neurosci. Res. (2003).

54. Galleguillos D, Vecchiola A, Fuentealba JA, Ojeda V, Alvarez K, Gómez A, Andrés ME. PIASy Represses the Transcriptional Activation Induced by the Nuclear Receptor Nurr1. J. Biol. Chem. (2004).

55. Arredondo C, Orellana M, Vecchiola A, Pereira LA, Galdames L, Andrés ME.. PIASy Enhanced SUMO-2 Modification of Nurr1 Activation-Function-1 Domain Limits Nurr1 Transcriptional Synergy. PLoS One, (2013).

56. Hazel, T. G., Misra, R., Davis, I. J., Greenberg, M. E. & Lau, L. F. Nur77 is differentially modified in PC12 cells upon membrane depolarization and growth factor treatment. Mol. Cell. Biol. (1991).

57. Wilson, T. E., Fahrner, T. J., Johnston, M. & Milbrandt, J. Identification of the DNA binding site for NGFI-B by genetic selection in yeast. Science. (1991).

58. Wilson, T. E., Fahrner, T. J. & Milbrandt, J. The orphan receptors NGFI-B and steroidogenic factor 1 establish monomer binding as a third paradigm of nuclear receptor-DNA interaction. Mol. Cell. Biol. (1993)

59. Philips A, Lesage S, Gingras R, Maira MH, Gauthier Y, Hugo P, Drouin J. Novel dimeric Nur77 signaling mechanism in endocrine and lymphoid cells. Mol. Cell. Biol. (1997).

60. Maira, M., Martens, C., Philips, A. & Drouin, J. Heterodimerization between Members of the Nur Subfamily of Orphan Nuclear Receptors as a Novel Mechanism for Gene Activation. Mol. Cell. Biol. (1999).

61. Zetterström, R. H., Solomin, L., Mitsiadis, T., Olson, L. & Perlmann, T. Retinoid X receptor heterodimerization and developmental expression distinguish the orphan nuclear receptors NGFI-B, Nurr1, and Nor1. Mol. Endocrinol. (1996).

62. Gervais, J., Soghomonian, J. J., Richard, D. & Rouillard, C. Dopamine and serotonin interactions in the modulation of the expression of the immediate-early transcription factor, nerve growth factor-inducible B, in the striatum. Neuroscience. (1999).

63. Beaudry, G., Langlois, M.-C., Weppe, I., Rouillard, C. & Lévesque, D. Contrasting Patterns and Cellular Specificity of Transcriptional Regulation of the Nuclear Receptor Nerve Growth Factor-Inducible B by Haloperidol and Clozapine in the Rat Forebrain. J. Neurochem. (2002).

64. Werme, M., Olson, L. & Brené, S. NGFI-B and Nor1 mRNAs are upregulated in brain reward pathways by drugs of abuse: different effects in Fischer and Lewis rats. Mol. Brain Res. (2000).

65. Langlois, M. C., Beaudry, G., Zekki, H., Rouillard, C. & Lévesque, D. Impact of antipsychotic drug administration on the expression of nuclear receptors in the neocortex and striatum of the rat brain. Neuroscience. (2001).

66. Maheux, J., Éthier, I., Rouillard, C. & Lévesque, D. Induction patterns of transcription factors of the Nur family (Nurr1, Nur77, and Nor-1) by typical and atypical antipsychotics in the mouse brain: Implication for their mechanism of action. J. Pharmacol. Exp. Ther. (2005).

67. Xiao, Q., Castillo, S. O. & Nikodem, V. M. Distribution of messenger RNAs for the orphan nuclear receptors NURR1 and NUR77 (NGFI-B) in adult rat brain using in situ hybridization. Neuroscience (1996).

68. Xing, G., Zhang, L., Russell, S. & Post, R. Reduction of dopamine-related transcription factors Nurr1 and NGFI-B in the prefrontal cortex in schizophrenia and bipolar disorders. Schizophr. Res. (2006).

69. Lévesque, D. & Rouillard, C. Nur77 and retinoid X receptors: crucial factors in dopamine-related neuroadaptation. Trends in Neurosciences (2007).

70. Rouillard C, Baillargeon J, Paquet B, St-Hilaire M, Maheux J, Lévesque C, Darlix N, Majeur S, Lévesque D. Genetic disruption of the nuclear receptor Nur77 (Nr4a1) in rat reduces dopamine cell loss and L-Dopa-induced dyskinesia in experimental Parkinson's disease. Exp. Neurol. (2018).

71. Werme, M., Ringholm, A., Olson, L. & Brené, S. Differential patterns of induction of NGFI-B, Nor1 and c-fos mRNAs in striatal subregions by haloperidol and clozapine. Brain Res. (2000).

72. Casey, D. E. Neuroleptic drug-induced extrapyramidal syndromes and tardive dyskinesia. Schizophr. Res. (1991).

73. Ethier I, Beaudry G, St-Hilaire M, Milbrandt J, Rouillard C, Lévesque D. The Transcription Factor NGFI-B (Nur77) and Retinoids Play a Critical Role in Acute Neuroleptic-Induced Extrapyramidal Effect and Striatal Neuropeptide Gene Expression. Neuropsychopharmacology. (2004).

74. St-Hilaire, M., Landry, É., Lévesque, D. & Rouillard, C. Denervation and repeated L-DOPA induce a coordinate expression of the transcription factor NGFI-B in striatal projection pathways in hemi-parkinsonian rats. Neurobiol. Dis. (2003).

75. St-Hilaire, M., Tremblay, P. O., Lévesque, D., Barden, N. & Rouillard, C. Effects of cocaine on c-Fos and NGFI-B mRNA expression in transgenic mice underexpressing glucocorticoid receptors. Neuropsychopharmacology. (2003).

76. Gerfen, C. R. & Surmeier, D. J. Modulation of striatal projection systems by dopamine. Annu. Rev. Neurosci. (2011).

77. Mccoy, M. T. et al. Chronic methamphetamine exposure suppresses the striatal expression of members of multiple families of immediate early genes (IEGs) in the rat: normalization by an acute methamphetamine injection. (2011).

78. Werme, M., Thorén, P., Olson, L. & Brené, S. Addiction-prone Lewis but not Fischer rats develop compulsive running that coincides with downregulation of nerve growth factor inducible-B and neuron-derived orphan receptor 1. J. Neurosci. (1999).

79. Bourhis E, Maheux J, Paquet B, Kagechika H, Shudo K, Rompré PP, Rouillard C, Lévesque D. The transcription factors Nur77 and retinoid X receptors participate in amphetamine-induced locomotor activities. Psychopharmacology (Berl). (2009).

80. Maheux J, St-Hilaire M, Voyer D, Tirotta E, Borrelli E, Rouillard C, Rompré PP, Lévesque D. Dopamine D2 Antagonist-Induced Striatal Nur77 Expression Requires Activation of mGlu5 Receptors by Cortical Afferents. Front. Pharmacol. (2012).

81. Kovalovsky D, Refojo D, Liberman AC, Hochbaum D, Pereda MP, Coso OA, Stalla GK, Holsboer F, Arzt E. Activation and induction of Nur77/Nurr1 in corticotrophs by CRH/cAMP: Involvement of calcium, protein kinase a, and MAPK pathways. Mol. Endocrinol. (2002).

82. Lam BY, Zhang W, Ng DC, Maruthappu M, Roderick HL, Chawla S. CREB-dependent Nur77 induction following depolarization in PC12 cells and neurons is modulated by MEF2 transcription factors. J. Neurochem. (2010).

83. Klopotowska D, Matuszyk J, Rapak A, Gidzinska B, Cebrat M, Ziolo E, Strzadala L. Transactivation activity of Nur77 discriminates between Ca2+ and cAMP signals. Neurochem. Int. (2005).

84. Bourhis, E., Maheux, J., Rouillard, C. & Lévesque, D. Extracellular signal-regulated kinases (ERK) and protein kinase C (PKC) activities are involved in the modulation of Nur77 and Nor-1 expression by dopaminergic drugs. J. Neurochem. (2008).

85. Collins, B. E., Greer, C. B., Coleman, B. C. & Sweatt, J. D. Histone H3 lysine K4 methylation and its role in learning and memory. Epigenetics and Chromatin (2019).

86. Barski A, Cuddapah S, Cui K, Roh TY, Schones DE, Wang Z, Wei G, Chepelev I, Zhao K. High-Resolution Profiling of Histone Methylations in the Human Genome. Cell (2007).

87. Shi Y, Lan F, Matson C, Mulligan P, Whetstine JR, Cole PA, Casero RA, Shi Y. Histone demethylation mediated by the nuclear amine oxidase homolog LSD1. Cell (2004)

88. Jin Y, Kim TY, Kim MS, Kim MA, Park SH, Jang YK. Nuclear import of human histone lysine-specific demethylase LSD1. Nuclear import of human histone lysine-specific demethylase LSD1. J. Biochem. (2014).

89. Yang M, Gocke CB, Luo X, Borek D, Tomchick DR, Machius M, Otwinowski Z, Yu H. Structural Basis for CoREST-Dependent Demethylation of Nucleosomes by the Human LSD1 Histone Demethylase. Mol. Cell (2006).

90. Metzger E, Wissmann M, Yin N, Müller JM, Schneider R, Peters AH, Günther T, Buettner R, Schüle R. LSD1 demethylates repressive histone marks to promote androgen-receptor-dependent transcription. Nature (2005).

91. Tochio N, Umehara T, Koshiba S, Inoue M, Yabuki T, Aoki M, Seki E, Watanabe S, Tomo Y, Hanada M, Ikari M, Sato M, Terada T, Nagase T, Ohara O, Shirouzu M, Tanaka A, Kigawa T, Yokoyama S. Solution structure of the SWIRM domain of human histone demethylase LSD1. Structure (2006).

92. Zibetti C, Adamo A, Binda C, Forneris F, Toffolo E, Verpelli C, Ginelli E, Mattevi A, Sala C, Battaglioli E. Alternative splicing of the histone demethylase LSD1/KDM1 contributes to the modulation of neurite morphogenesis in the mammalian nervous system. J. Neurosci. (2010).

93. Andrés ME, Burger C, Peral-Rubio MJ, Battaglioli E, Anderson ME, Grimes J, Dallman J, Ballas N, Mandel G. CoREST: A functional corepressor required for regulation of neural-specific gene expression. Proc. Natl. Acad. Sci. U. S. A. (1999).

94. Humphrey GW, Wang Y, Russanova VR, Hirai T, Qin J, Nakatani Y, Howard BH. Stable Histone Deacetylase Complexes Distinguished by the Presence of SANT Domain Proteins CoREST/kiaa0071 and Mta-L1. J. Biol. Chem. (2001).

95. Lee, M. G., Wynder, C., Cooch, N. & Shiekhattar, R. An essential role for CoREST in nucleosomal histone 3 lysine 4 demethylation. Nature (2005).

96. Garcia-Bassets I, Kwon YS, Telese F, Prefontaine GG, Hutt KR, Cheng CS, Ju BG, Ohgi KA, Wang J, Escoubet-Lozach L, Rose DW, Glass CK, Fu XD, Rosenfeld MG Histone Methylation-Dependent Mechanisms Impose Ligand Dependency for Gene Activation by Nuclear Receptors. Cell (2007).

97. Cai C, He HH, Gao S, Chen S, Yu Z, Gao Y, Chen S, Chen MW, Zhang J, Ahmed M, Wang Y, Metzger E, Schüle R, Liu XS, Brown M, Balk SP. Lysine-Specific Demethylase 1 Has Dual Functions as a Major Regulator of Androgen Receptor Transcriptional Activity. Cell Rep. (2014).

98. Toffolo E, Rusconi F, Paganini L, Tortorici M, Pilotto S, Heise C, Verpelli C, Tedeschi G, Maffioli E, Sala C, Mattevi A, Battaglioli E. Phosphorylation of neuronal Lysine-Specific Demethylase 1LSD1/KDM1A impairs transcriptional repression by regulating interaction with CoREST and histone deacetylases HDAC1/2. J. Neurochem. (2014).

99. Laurent B, Ruitu L, Murn J, Hempel K, Ferrao R, Xiang Y, Liu S, Garcia BA, Wu H, Wu F, Steen H, Shi Y. A Specific LSD1/KDM1A Isoform Regulates Neuronal Differentiation through H3K9 Demethylation. Mol. Cell (2015).

100. Wang J, Telese F, Tan Y, Li W, Jin C, He X, Basnet H, Ma Q, Merkurjev D, Zhu X, Liu Z, Zhang J, Ohgi K, Taylor H, White RR, Tazearslan C, Suh Y, Macfarlan TS, Pfaff SL, Rosenfeld MG. LSD1n is an H4K20 demethylase regulating memory formation via transcriptional elongation control. Nat. Neurosci. (2015).

101. Hino, S., Kohrogi, K. & Nakao, M. Histone demethylase LSD1 controls the phenotypic plasticity of cancer cells. Cancer Sci. (2016).

102. Nagasaka M, Tsuzuki K, Ozeki Y, Tokugawa M, Ohoka N, Inoue Y, Hayashi H. Lysine-specific demethylase 1 (LSD1/KDM1A) is a novel target gene of c-myc. Biol. Pharm. Bull. (2019).

103. Rusconi F, Paganini L, Braida D, Ponzoni L, Toffolo E, Maroli A, Landsberger N, Bedogni F, Turco E, Pattini L, Altruda F, De Biasi S, Sala M, Battaglioli E. LSD1 neurospecific alternative splicing controls neuronal excitability in mouse models of epilepsy. Cereb. Cortex (2015).

104. Hwang I, Cao D, Na Y, Kim DY, Zhang T, Yao J, Oh H, Hu J, Zheng H, Yao Y, Paik J. Far. Far Upstream Element-Binding Protein 1 Regulates LSD1 Alternative Splicing to Promote Terminal Differentiation of Neural Progenitors. Stem Cell Reports (2018).

105. Rusconi F, Grillo B, Ponzoni L, Bassani S, Toffolo E, Paganini L, Mallei A, Braida D, Passafaro M, Popoli M, Sala M, Battaglioli E. LSD1 modulates stress-evoked transcription of immediate early genes and emotional behavior. Proc. Natl. Acad. Sci. U. S. A. (2016).

106. Ramirez-Carrozzi VR, Braas D, Bhatt DM, Cheng CS, Hong C, Doty KR, Black JC, Hoffmann A, Carey M, Smale ST. A Unifying Model for the Selective Regulation of Inducible Transcription by CpG Islands and Nucleosome Remodeling. Cell (2009).

107. McCoy MT, Jayanthi S, Wulu JA, Beauvais G, Ladenheim B, Martin TA, Krasnova IN, Hodges AB, Cadet JL. Chronic methamphetamine exposure suppresses the striatal expression of members of multiple families of immediate early genes (IEGs) in the rat: Normalization by an acute methamphetamine injection. Psychopharmacology (Berl) (2011).

108. Jeanneteau F, Barrère C, Vos M, De Vries CJM, Rouillard C, Levesque D, Dromard Y, Moisan MP, Duric V, Franklin TC, Duman RS, Lewis DA, Ginsberg SD, Arango-Lievano M. The stress-induced transcription factor NR4a1 adjusts mitochondrial function and synapse number in prefrontal cortex. J. Neurosci. (2018).

Annex 2:

A bioinformatics approach reveals Nur77-regulated genes common to the nervous and immune systems

Montserrat Olivares-Costa[1¶*], Guillermo Parada[1,#a ¶], and María Estela Andrés[1#*]

[1] Department of Cellular and Molecular Biology, Faculty of Biological Sciences, Pontificia Universidad Católica de Chile.

[#a] Current Address: Wellcome Trust Sanger Institute, Wellcome Trust Genome Campus, Cambridge CB10 1SA, UK.

*Corresponding author: molivares1@uc.cl (MO); mandres@bio.puc.cl (MEA).

[¶] These authors contributed equally to this work.

Abstract

Neurons and immune cells have similar mechanisms for cell-to-cell communication. Moreover, an active crosstalk exists between neurons and immune cells. While neurotransmitters can activate or inhibit immune cells, cytokines modulate neuronal activity. The transcription factor Nur77 (NR4A1) is transiently induced by several stimuli both in neurons and T-lymphocytes, suggesting that Nur77 is involved in the coordination of gene expression response in the two cell types. By analyzing publicly available ChIP-seq and RNA-seq databases, we found Nur77 target genes common to the nervous and immune systems. Importantly, overrepresented functions as cell adhesion and cell anchoring appeared as processes regulated by Nur77 both in neurons and immune cells.

Introduction

Nur77 (also known as NGFI-B, TR3, and NR4A1)[1,2,3] is a transcription factor encoded by an immediate-early gene that belongs to the nuclear receptor superfamily. Along with Nurr1 and Nor1, they form a specific subgroup of orphan receptors, known as the Nur subfamily. Crystallographic studies have shown that Nur77, like Nurr1, naturally adopts a conformation related to active transcription, and it lacks the canonical ligand-binding pocket commonly present in ligand-inducible nuclear receptors[4,5]. Different oligomerization states have been described for this subfamily since all of them can bind DNA either as monomers when recruited to the Nerve-Growth-Factor Inducible gene B (NGFI-B)-responsive elements (NBRE) (A/TAAAGGTCA)[6,7] or as homodimers or heterodimers to Nur-Responsive Elements (NurRE) (AAATG/AC/TCA)[8]. Interestingly, Nur77 and Nurr1 can also form heterodimers with the retinoid x receptor (RXR) when targeting the genome on DR5 elements (GGTTCAnnnnnAGGTCA)[9].

Nur77 has been largely studied in the immune system for its functions of inducing apoptosis on auto-reactive immature lymphocytes T and of modulating the inflammatory response[10,11]. Nur77 is widely expressed in the Central Nervous System (CNS), particularly on brain nuclei that receive dopaminergic and noradrenergic neurotransmission, which then regulates its expression[12]. Remarkably, brain pathologies characterized by imbalances of catecholamines neurotransmission, such as anxiety, addiction, and schizophrenia, are associated with changes in the expression of Nur77[13,14]. Nur77 also seems to play a key role in neurodegenerative disorders, since in animal models of Parkinson's disease, Nur77 expression is significantly increased at the substantia nigra, where it appears to be involved

in the loss of dopaminergic cells given that the genetic disruption of NR4A1 gene reduced the loss of dopaminergic neurons induced by neurotoxins[15].

A close relationship between the nervous and immune systems has been reported. There are not only physical contacts between immune CNS-resident cells and nerve terminals that innervate peripheral immune organs[16], but there is also chemical communication between the two systems. For instance, inflammatory cytokines modulate neuronal functions through receptors present in neurons and glial cells[17,18]. On the other hand, neurotransmitters such as dopamine, glutamate, and serotonin that are released from neurons and immune cells, can activate or suppress T-cells in a context-dependent manner[19]. Accordingly, T-cells express receptors for many different neurotransmitters on their surface, and their expression is regulated over time by T cell receptor (TCR) activation[19,20]. In addition, neurons and immune cells share several features like the capacity to establish cell associations and to transmit information to neighboring cells through specialized cell-to-cell contacts, known as synapses in both systems[21].

In both the nervous and immune systems, Nur77 emerges as a key factor in the rapid signaling of cell-to-cell communication and in the genetic reprogramming that begins in the postsynaptic cell. In the CNS, the rapid and transient expression of Nur77 induced by neuronal activity regulates the distribution and density of dendritic spines in pyramidal neurons of the hippocampus[22], and it also impacts the metabolism of neurons by regulating mitochondrial energetic competence under chronic stimulation[23]. In T cells, Nur77 is an activity marker downstream of the TCR, the main receptor in immunological synapses[24,25]. Sekiya et al (2013) showed that strong TCR signals triggered by self-antigens induce Nur77 expression (and of the other Nur factors as well), which in turn control the transcription of Foxp3, thus driving T regulatory developmental programs[26]. Nur77 also modulates the inflammatory autoimmune response by regulating the metabolism and proliferation of T

cells[27]. Besides, Nur77 regulates the production of norepinephrine in macrophages by inhibiting the expression of tyrosine hydroxylase, limiting experimental autoimmune encephalomyelitis[28,29].

Given the role of Nur77 in the response and reprogramming of immune cells and neurons, we hypothesized that Nur77 regulates the expression of a set of genes common to the nervous and immune systems. To answer this question, we used bioinformatic approaches to find target genes of Nur77 common to both systems.

We used four different, publicly available databases. Our analysis reveals that there is a select group of common Nur77 target genes for the CNS and the immune system. The functions of cell adhesion and anchoring emerge as the processes regulated by Nur77 in both systems. We also characterized Nur77 binding sites throughout the genome, finding a significant distribution in strong enhancers and active promoters, supporting the function of Nur77 as a transcriptional activator in the CNS and immune systems.

Methods

Data acquisition

We downloaded the ChIP-Seq peaks from Gene Expression Omnibus (GEO) corresponding to EGFP-Nur77 in K562 (GSE31363)[30] and endogenous Nur77 in NSC (GSM1603270) and NC (GSM1603273)[31]. The microarray data was taken from the work published by Chen et al. in 2014 (GEO Accession; GSE76805)[22]. We used ENSEMBL gene annotation for human (hg19) and mouse (mm10), which were directly extracted as TxDb objects though GenomicGeutres and TxDb. Mmusculus.UCSC.mm10.ensGene R packages. Additional genomic annotations of different chromatin states and functional regions were extracted from UCSC Table browser, including the K562 Genome Segmentation by ChromHMM and Ensembl Regulatory Build.

Nur77 binding site characterization

The overlap between the different ChIP-Seq peaks and genomic features were calculated with the GenomicRanges R package using the function findOverlaps. We intersected the genomic coordinates with K562 Genome Segmentation by ChromHMM, and then we calculated the overlapping enrichment, by normalizing it by the total coverage of each chromatin state across the genome.

To obtain a list of possible Nur77 target genes, we used the annotation of TSS and proximal promoters provided by the Ensembl Regulatory build for human (hg19) and mouse (mm10). The annotated TSS and proximal promoters were assigned to transcripts ID from Ensembl annotation if they were located within 2000 nt upstream and 500 nt downstream from a transcript start coordinate. Then, the function findOverlaps from GenomicRanges was used to find Nur77 ChIP-Seq peaks that overlapped with TSS or proximal promoters

from the Ensembl Regulatory build. Finally, we used the biomaRt R package to find the common gene symbol associated with each of the Ensembl IDs that were assigned to each TSS and proximal promoter that overlapped with a Nur77 ChIP-Seq peak.

Microarray analyses

We analyzed the changes in gene expression after the overexpression of Nur77 in hippocampal pyramidal cells by analyzing publicly available microarray data published by Chen et al. in 2014 [22]. We computed the differential expression results from the microarray data to filter genes with an adjusted p-value lower than 0.05 and an absolute value of log2 fold change greater than one. We plotted the results using ggplot2 and highlighting the names of genes for which Nur77 peaks were detected in their promoters.

Ontology analysis

A list of common target genes of Nur77 in the neuronal and lymphatic systems was submitted to the Gene Ontology Consortium server (www.geneontology.org)[32,33] and then processed using default parameters with PANTHER analysis tool[34].

Results and discussions

Characterization of Nur77 binding sites throughout the genome.

To characterize Nur77 binding sites throughout the genome, we used a public database from the ENCODE project corresponding to a ChIP-Seq of overexpressing EGFP-tagged Nur77 (EGFP-Nur77) in the *chronic myelogenous leukemia* K562 cell line (GEO accession: GSE31363)[30]. The analysis of the coordinates of EGFP-Nur77 peaks, reported by ENCODE, with respect to the nearest transcription start site (TSS), revealed a high frequency of Nur77 binding events between +1000 and – 1000 nucleotides from TSS **(Figures 1A, B)**.

To further characterize the binding profile of EGFP-Nur77, we analyzed the enrichment of ChIP-Seq peaks across 15 chromatin states defined by Ernest et al. for the K562 cell line[35]. These chromatin states (numbered from 1 to 15) were obtained through the implementation of multivariate hidden Markov models, which integrates a wide range of epigenetic marks, including eight histone post-translational modifications, CTCF and the H2A.Z histone variant[35]. We calculated the overlap enrichment across the EGFP-Nur77 peaks and chromatin states for the K562 cell line, obtaining a significant enrichment of Nur77 peaks across chromatin states associated with active transcription.

An enrichment analysis using the human chromatin segmentation model generated by Ernst, (2011) shows a significant enrichment of Nur77 peaks in chromatin states associated with transcriptional regulatory regions, particularly in strong enhancers and active promoters **(Fig. 1C)**. Two of the chromatin states are described as strong enhancers (states 4 and 5), which differentiate in the occurrence of specific chromatin marks and distance to the TSS. The number 4 strong enhancer state displays a higher occurrence of

histone H3 lysine 4 trimethylation (H3K4me3) and histone H3 lysine 9 acetylation (H3K9ac), and it is closer to the TSS than the number 5 Strong enhancer state. Nur77 is enriched in both chromatin states described as strong enhancers, exhibiting a log2 enrichment greater than 4 in chromatin state 4 **(Fig. 1C)**. High enrichment of Nur77 binding is also observed in transcriptional transition states of chromatin. These areas have similar characteristics to transcriptional elongation areas, but they exhibit an increased presence of H4K20me1, H3K4me1, and more DNAse sensitivity[35], suggesting an intermediate state between the promoter activation and effective elongation. In contrast, we found a negative enrichment for Nur77 binding in transcriptional elongation areas. Nur77 is poorly enriched in states numbers 6 and 7; both described as weak enhancers, which differ in the occurrence of H3K4me2 and DNase sensitivity[35]. Finally, negative enrichment was observed in heterochromatin regions, indicating the absence of Nur77 in inactive chromatin territories **(Fig. 1C)**.

Altogether, these data indicate that Nur77 is mostly associated with active chromatin, which is consistent with the role of Nur77 as a transcriptional activator, also confirmed by the high presence of Nur77 in the TSS. Our data also shows that Nur77 binds transcriptional transition areas, suggesting that Nur77 is present in the promoters of its target genes independently of their state (active or inactive). On the other hand, the data suggests that the presence of Nur77 in enhancers would be limited to the active state.

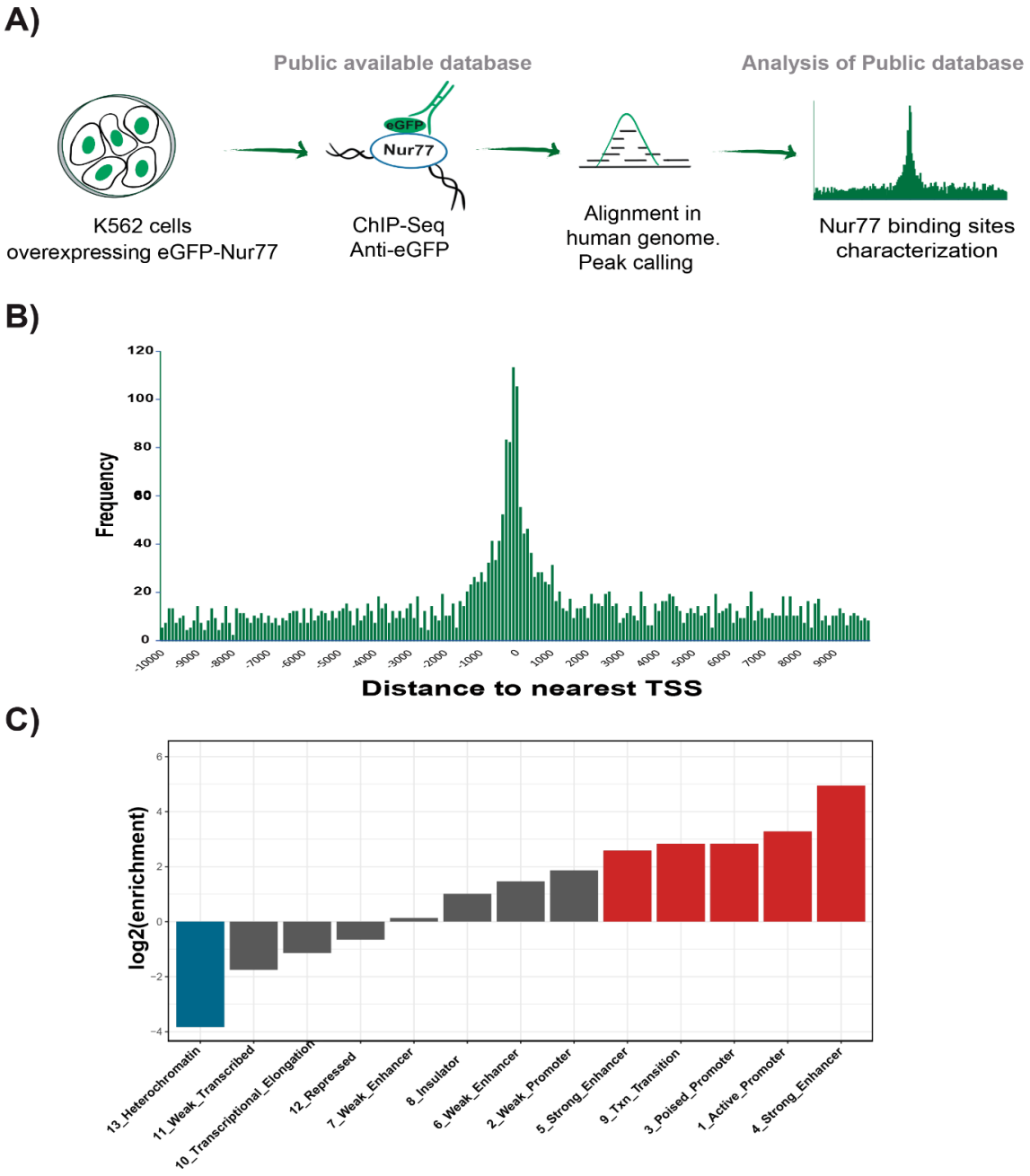

Figure1: Nur77 binds to active promoters and strong enhancers in K562 cells. Analysis of a publicly available database from the anti-EGFP ChIP-Seq experiment in the K562 cell line overexpressing EGFP-Nur77 [30]. A) Experimental procedure pipeline of the public database and bioinformatics analysis. B) The abundance of Nur77 binding events respect the nearest TSS location. C) Enrichment of Nur77 binding sites across different chromatin regions defined by Ernst et al. in 2011[35]. In red, log2 of enrichment ≥ 2. In blue, log2 of enrichment ≤ -2. *

Nur77 target genes in immune cells and neurons actively regulated by Nur77

. To identify target genes of Nur77 in the CNS and the immune system we analyzed published data sets. One set of data corresponded to the ChIP-Seq of overexpressed EGFP-Nur77 performed in the K562 cell line[30]. Second and third data sets corresponded to ChIP-Seqs of endogenous Nur77, of mouse neural stem cells (NSC) and NSC differentiated to neurons (NC) (GEO accession: GSM1603270 (NSC); GSM1603273 (NC))[31]. From these datasets, we identified genes that bind Nur77 in their promoters. To learn which Nur77 target genes are actively regulated by Nur77, we crossed them with mRNA microarray data obtained from mouse hippocampal pyramidal neurons overexpressing Nur77 (GEO Accession; GSE76805)[22] **(Fig. 2A).** The selected databases come from different sources, (NSC, NC, cultured hippocampal neurons and K562 cells), prompting us to take maximum precaution in selecting Nur77 target genes. We considered as Nur77 target genes, those that bind Nur77 in their promoters (- 2kb + 500 bp from TSS), thus reducing our list to the most probably target genes for Nur77.

The first analysis identified 58 genes that bind Nur77 in their promoters according to the ChIP-Seq of K562 cells, whose expression is modified in pyramidal neurons when Nur77 was overexpressed **(Table S.1)**. Of these 58 genes, 9 changed their expression twice or more (Log2 fold change ≥ 1) (identified with names in **Fig. 2B**). The second analysis identified 113 genes that bind Nur77 in their promoters according to the ChIP-Seq of NSC, whose expression is modified when Nur77 was overexpressed in pyramidal neurons (Table S.2). Of these 113 genes, 16 changed their expression twice or more (Log2 fold change ≥ 1) (identified with names in **Fig. 2C**).

The third analysis identified 116 genes that bind Nur77 in their promoters according to the ChIP-Seq of NC, whose expression changed when Nur77 was overexpressed in

pyramidal neurons **(Table S.3)**. Of these 116 genes, 17 changed their expression twice or more (Log2 fold change ≥ 1) (identified with names in **Fig. 2D**).

Although overexpression of EGFP-Nur77 in K562 cells resembles an active state, and therefore we cannot distinguish between the basal or induced recruitment of Nur77 to chromatin, our analyses suggest that Nur77 regulates an important number of genes that bind Nur77 in their promoters. This data also strengthens the idea that Nur77 is bound to the promoters of its target genes under basal conditions (NC and NSC), as it is shown in the previous analysis of the association of Nur77 to the different states of chromatin **(Fig. 1C)**.

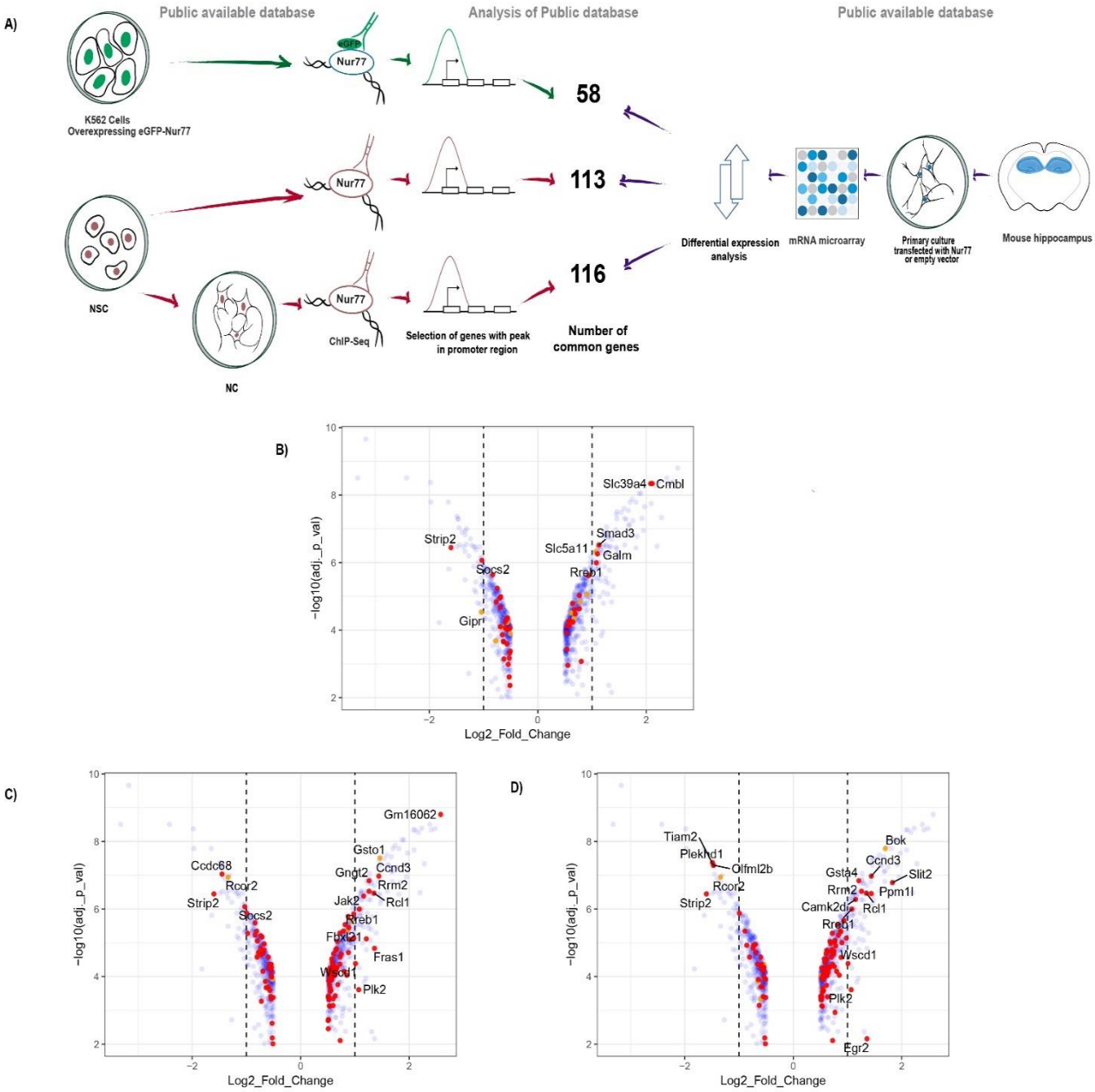

Figure 2: Nur77 target genes in neurons and immune cells. A) Pipelines of the experimental procedure of public databases [30,31] and of the analysis to select Nur77 target genes. B, C, D) Volcano plots representing genes that changed their expression when Nur77 was overexpressed in pyramidal neurons (blue), genes that also had a peak of Nur77 binding in their promoter (red dots) and TSS (orange dots) according to the ChIP-Seq from K562 cells (B), ChIP-Seq form NSC (C) and ChIP-Seq from NC (D). Positive numbers indicate upregulation and negative numbers down-regulation. The dotted lines demarcate Log2 Fold of Change = ±1.

Immune and nervous common Nur77 target genes

To find out whether Nur77 exerts a similar function in the nervous and immune systems, we searched for common target genes of Nur77 in neurons and immune cells. To this end, we selected genes that bind Nur77 on their promoters in both databases: (1) the ChIP-Seq of K562 overexpressing EGFP-Nur77[30], and (2) the ChIP-Seq of NC[31] **(Fig. 3A)**. We found 271 Nur77 target genes common to immune and neuronal ChIP-Seq **(Table S.4) (Fig. 3A)**. We are aware that subtle differences in ChIP-Seq protocols[30,31] could have limited the common results when crossing both databases. However, we selected these databases, given their high quality.

We carried out Gene Ontology (GO) analysis of these genes based on the three principal classifications, which are (1) molecular function, (2) cellular components, and (3) biological processes **(Fig. 3B and Table S.5)**. GO analysis showed an enrichment of Nur77 target genes in binding functions of the molecular function classification, which are: ribonucleoprotein complex binding (fold enrichment 5.2), cadherin bindings (fold enrichment 3.94), cell adhesion molecule binding (fold enrichment 3.05) and protein domain specific binding (fold enrichment 2.66) **(Fig. 3B)**. Regarding the cellular component classification, Nur77 target genes were enriched principally in categories of adhesion and junction which are: focal adhesion (fold enrichment 3.45), cell-substrate adherent junction (fold enrichment 3.43), cell-substrate junction (fold enrichment 3.39), adherens junction (fold enrichment 3.02), and anchoring junction (fold enrichment 2.93). Additionally, two categories of nuclear localization were enriched as well: nuclear speck (fold enrichment 3.33) and nuclear body (fold enrichment 2.86) **(Fig. 3B)**. Interestingly, many proteins encoded by Nur77 target genes, which are common to the nervous and immune system, are ribonucleoproteins and adhesion molecules. This fact is strengthened by the enrichment of Nur77 target genes in nuclear bodies and areas of adherents and anchoring junctions **(Fig. 3C)**.

In the biological process classification, Nur77 target genes were enriched in the regulation of the Endoplasmic-Reticulum-Associated protein Degradation (ERAD) pathway (fold enrichment 12.91) and regulation of response to endoplasmic reticulum stress (fold enrichment 8.01). Three GO terms related to interleukin signaling were also enriched: interleukin-12-mediated signaling pathway (fold enrichment 10.11) cellular response to interleukin-12 (fold enrichment 9.68) and response to interleukin-12 (fold enrichment 9.49). Nur77 target genes were also enriched in the regulation of protein autophosphorylation (fold enrichment 9.49) and cell aging (8.22) GO terms **(Fig. 3B)**.

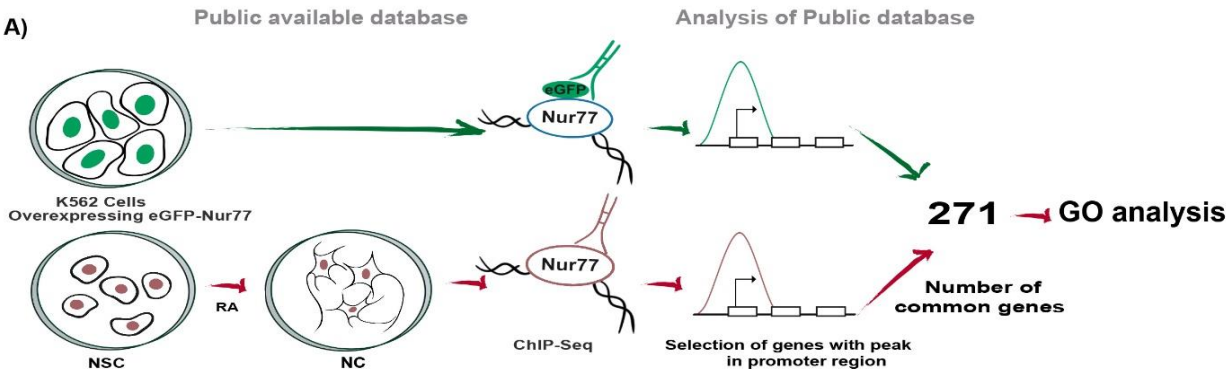
A)
Public available database
Analysis of Public database
eGFP
Nur77
K562 Cells
Overexpressing eGFP-Nur77
271
GO analysis
Nur77
RA
NSC
NC
ChIP-Seq
Number of
common genes
Selection of genes with peak
in promoter region

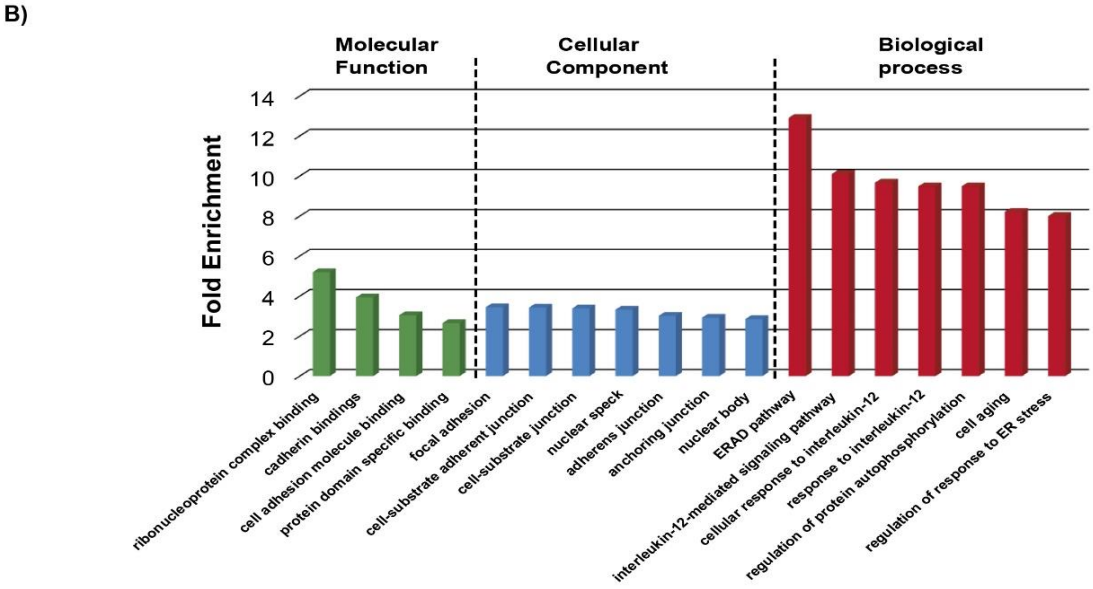
B)
Molecular
Function
Cellular
Component
Biological
process
Fold Enrichment
14
12
10
8
6
4
2
0
ribonucleoprotein complex binding
cadherin bindings
cell adhesion molecule binding
protein domain specific binding
focal adhesion
cell-substrate adherent junction
cell-substrate junction
nuclear speck
adherens junction
anchoring junction
nuclear body
ERAD pathway
interleukin-12-mediated signaling pathway
cellular response to interleukin-12
response to interleukin-12
regulation of protein autophosphorylation
cell aging
regulation of response to ER stress

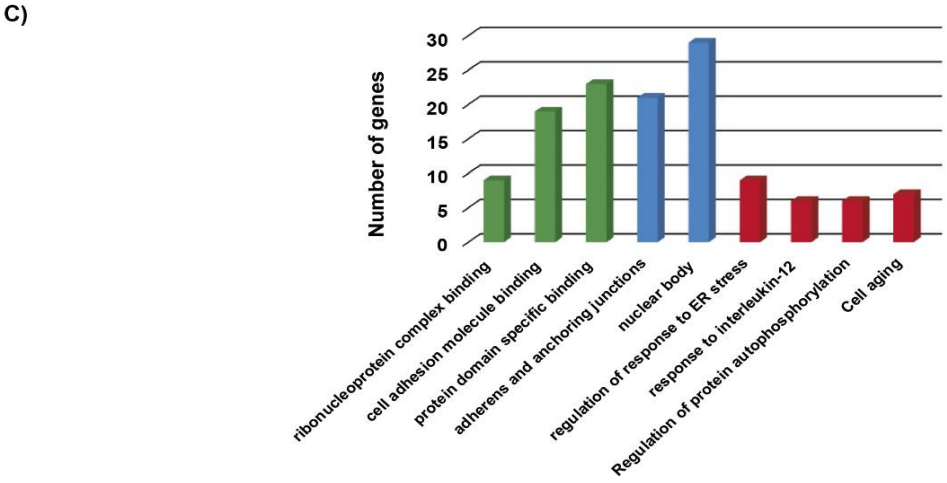
C)
Number of genes
30
25
20
15
10
5
0
ribonucleoprotein complex binding
cell adhesion molecule binding
protein domain specific binding
adherens and anchoring junctions
nuclear body
regulation of response to ER stress
response to interleukin-12
Regulation of protein autophosphorylation
Cell aging

Figure 3: GO analysis of common target genes for Nur77 among the immune and nervous systems A) Pipeline of experimental procedure of public databases, and corresponding GO analysis. B) Enriched GO terms (more than 2.5 fold of change). C) The number of genes classified in each GO terms category. Molecular function classification in green bars, cellular component classification in blue bars and biological process classification in red bars. Cell adhesion molecule binding category includes cadherin binding GO term genes. Adherens and anchoring junctions category includes genes of adherens junction, anchoring junction, focal adhesion, cell-substrate adherent junction, and cell-substrate junction GO terms. Nuclear body category includes genes of the nuclear speck GO term. Regulation of response to endoplasmic reticulum stress includes genes of regulation of ERAD pathway GO term. Response to interleukin-12 category includes genes of interleukin-12-mediated signaling pathways, cellular response to interleukin-12 and response to interleukin-12 GO terms (Table S.5).

The crossing of gene groups that bind Nur77 on their promoters both in the immune and nervous systems (271 genes), with the gene group that was modified by upregulating Nur77 in pyramidal neurons[22] resulted in a set of 9 genes: AGAP3, BIRC5, DYM, ITGB3, KIF21B, MORN5, RREB1, STRIP2, and WEE1. Previous evidence supports that Nur77 controls the expression of BIRC5 gene[36], validating our results. Further studies are required to fully validate Nur77's control over these genes, both in the nervous and immune systems.

In conclusion, our data analyses show that Nur77 is bound to the promoter of its target genes independently of their transcriptional state (weak, poised, or active). In addition, our data suggest that the presence of Nur77 in enhancers is limited to the active state. Therefore, we propose that Nur77 is constitutively present in promoters, but it only binds to enhancers when it is upregulated, hence, modulating transcription in response to stimuli.

Our analysis showed a strong participation of Nur77 target genes in anchoring and adhesion functions, which is consistent with the previously described roles of Nur77 in the modulation of neurite growth in neurons[23], and in the immune response[24,25], both processes that require interaction between cells and with the extracellular matrix.

Finally, the genes found in this work as common targets of Nur77 in the nervous and immune systems are novel, uncharacterized targets of this transcription factor. The work presented here is an approach pretending to guide the experimental focus regarding Nur77 investigation, partially solving the lack of knowledge of Nur77 target genes and presenting new functions that can be attributed to this transcription factor both in the immune and nervous systems.

References

1. Chawnshang C, Kokontis J, Shutsung L, Yijan C. Isolation and characterization of human TR3 receptor: A member of steroid receptor superfamily. J Steroid Biochem. (1989)
2. Hazel, T. G., Nathans, D. & Lau, L. F. A gene inducible by serum growth factors encodes a member of the steroid and thyroid hormone receptor superfamily. Proc. Natl. Acad. Sci. U. S. A. (1988)
3. Milbrandt, J. Nerve growth factor induces a gene homologous to the glucocorticoid receptor gene. Neuron (1988).
4. Flaig, R., Greschik, H., Peluso-Iltis, C. & Moras, D. Structural basis for the cell-specific activities of the NGFI-B and the Nurr1 ligand-binding domain. J. Biol. Chem. (2005).
5. Wang, Z. et al. Structure and function of Nurr1 identifies a class of ligand-independent nuclear receptors. Nature (2003)..
6. Wilson, T. E., Fahrner, T. J., Johnston, M. & Milbrandt, J. Identification of the DNA binding site for NGFI-B by genetic selection in yeast. Science. (1991).
7. Wilson, T. E., Fahrner, T. J. & Milbrandt, J. The orphan receptors NGFI-B and steroidogenic factor 1 establish monomer binding as a third paradigm of nuclear receptor-DNA interaction. Mol. Cell. Biol. (1993).
8. Philips, A. et al. Novel dimeric Nur77 signaling mechanism in endocrine and lymphoid cells. Mol. Cell. Biol. (1997).
9. Zetterström, R. H., Solomin, L., Mitsiadis, T., Olson, L. & Perlmann, T. Retinoid X receptor heterodimerization and developmental expression distinguish the orphan nuclear receptors NGFI-B, Nurr1, and Nor1. Mol. Endocrinol. (1996).
.10. McMorrow JP, Murphy EP. Inflammation: A role for NR4A orphan nuclear receptors? Biochemical Society Transactions. (2011)
11. Woronicz JD, Calnan B, Ngo V, Winoto A. Requirement for the orphan steroid receptor Nur77 in apoptosis of T-cell hybridomas. Nature. (1994).
12. Campos-Melo, D., Galleguillos, D., Sánchez, N., Gysling, K. & Andrés, M. E. Nur transcription factors in stress and addiction. Frontiers in Molecular Neuroscience (2013).
13. Lévesque, D. & Rouillard, C. Nur77 and retinoid X receptors: crucial factors in dopamine-related neuroadaptation. Trends in Neurosciences (2007)..
14. Xing, G., Zhang, L., Russell, S. & Post, R. Reduction of dopamine-related transcription factors Nurr1 and NGFI-B in the prefrontal cortex in schizophrenia and bipolar disorders. Schizophr. Res. (2006).
15. Rouillard, C. et al. Genetic disruption of the nuclear receptor Nur77 (Nr4a1) in rat reduces dopamine cell loss and L-Dopa-induced dyskinesia in experimental Parkinson's disease. Exp. Neurol. (2018).
16. Louveau A, Smirnov I, Keyes TJ, Eccles JD, Rouhani SJ, Peske JD, et al. Structural and functional features of central nervous system lymphatic vessels. Nature. (2015).
17. Galic MA, Riazi K, Pittman QJ. Cytokines and brain excitability. Frontiers in Neuroendocrinology. (2012).

18. Vezzani A, Viviani B. Neuromodulatory properties of inflammatory cytokines and their impact on neuronal excitability. Neuropharmacology. (2015)

19. Levite M. Neurotransmitters activate T-cells and elicit crucial functions via neurotransmitter receptors. Current Opinion in Pharmacology. (2008).

20. Ganor Y, Teichberg VI, Levite M. TCR Activation Eliminates Glutamate Receptor GluR3 from the Cell Surface of Normal Human T Cells, via an Autocrine/Paracrine Granzyme B-Mediated Proteolytic Cleavage. J Immunol. (2007).

21. Dustin ML, Colman DR. Neural and immunological synaptic relations. Science. (2002)

22. Chen Y, Wang Y, Ertürk A, Kallop D, Jiang Z, Weimer RM, Kaminker J, Sheng M. Activity-induced Nr4a1 regulates spine density and distribution pattern of excitatory synapses in pyramidal neurons. Neuron (2014).

23. Jeanneteau F, Barrère C, Vos M, De Vries CJM, Rouillard C, Levesque D, Dromard Y, Moisan MP, Duric V, Franklin TC, Duman RS, Lewis DA, Ginsberg SD, Arango-Lievano M. The stress-induced transcription factor NR4a1 adjusts mitochondrial function and synapse number in prefrontal cortex. J. Neurosci. (2018).

24. Cunningham NR, Artim SC, Fornadel CM, Sellars MC, Edmonson SG, Scott G, et al. Immature CD4 + CD8 + Thymocytes and Mature T Cells Regulate Nur77 Distinctly in Response to TCR Stimulation. J Immunol. (2006).

25. Moran AE, Holzapfel KL, Xing Y, Cunningham NR, Maltzman JS, Punt J, et al. T cell receptor signal strength in Treg and iNKT cell development demonstrated by a novel fluorescent reporter mouse. J Exp Med. (2011).

26. Sekiya T, Kashiwagi I, Yoshida R, Fukaya T, Morita R, Kimura A, et al. Nr4a receptors are essential for thymic regulatory T cell development and immune homeostasis. Nat Immunol. (2013).

27. Liebmann M, Hucke S, Koch K, Eschborn M, Ghelman J, Chasan AI, et al. Nur77 serves as a molecular brake of the metabolic switch during T cell activation to restrict autoimmunity. Proc Natl Acad Sci U S A. (2018).

28. Shaked I, Hanna RN, Shaked H, Chodaczek G, Nowyhed HN, Tweet G, et al. Transcription factor Nr4a1 couples sympathetic and inflammatory cues in CNS-recruited macrophages to limit neuroinflammation. Nat Immunol. (2015).

29. Wang LM, Zhang Y, Li X, Zhang ML, Zhu L, Zhang GX, et al. Nr4a1 plays a crucial modulatory role in Th1/Th17 cell responses and CNS autoimmunity. Brain Behav Immun. (2018).

30. Dunham, I. et al. An integrated encyclopedia of DNA elements in the human genome. Nature (2012).

31. Terranova C, Narla ST, Lee YW, Bard J, Parikh A, Stachowiak EK, et al. Global developmental gene programing involves a nuclear form of fibroblast growth factor receptor-1 (FGFR1). PLoS One. (2015)

32. Ashburner M, Ball CA, Blake JA, Botstein D, Butler H, Cherry JM, et al. Gene ontology: Tool for the unification of biology. Nature Genetics. (2000)

33. Carbon S, Douglass E, Dunn N, Good B, Harris NL, Lewis SE, et al. The Gene Ontology Resource: 20 years and still GOing strong. Nucleic Acids Res. (2019).

34. Mi H, Muruganujan A, Ebert D, Huang X, Thomas PD. PANTHER version 14: More genomes, a new PANTHER GO-slim and improvements in enrichment analysis tools. Nucleic Acids Res. (2019).

35. Ernst J, Kheradpour P, Mikkelsen TS, Shoresh N, Ward LD, Epstein CB, Zhang X, Wang L, Issner R, Coyne M, Ku M, Durham T, Kellis M, Bernstein BE. Mapping and analysis of chromatin state dynamics in nine human cell types. Nature (2011)

36. Yu C, Cui S, Zong C, Gao W, Xu T, Gao P, et al. The orphan nuclear receptor NR4A1 protects pancreatic β-cells from endoplasmic reticulum (ER) stress-mediated apoptosis. J Biol Chem. (2015).

Supporting information

Full extended tables are available at:

https://drive.google.com/drive/folders/14TD5g8wve9SfDd05hSpI24e5sGuGOGwf?usp=sharing

Table S.1: Nur77 target genes in the K562 cell line.

Genes that bind Nur77 on their promoters, according to the ChIP-Seq of K562 cells, whose expression is modified when Nur77 is overexpressed in pyramidal neurons. Columns correspond to gene name, gene description from wikigene database[1], Nur77 peak location according to the ChIP-Seq from K562 cells (GSE31363)[2], Log2 of the fold of change and p-value adjusted according to differential expression analysis of microarray from pyramidal neurons overexpressing Nur77 (GSE76805)[3] and gene identifier in the Ensembl database.

Table S.2: Nur77 target genes in NSC.

Genes that bind Nur77 in their promoters, according to the ChIP-Seq of NSC, whose expression is modified when Nur77 is overexpressed in pyramidal neurons. Columns correspond to gene name, gene description from wikigene database[1], Nur77 peak location according to the ChIP-Seq from NSC (GSM1603270)[4], Log2 of the fold of change and p-value adjusted according to differential expression analysis of microarray from pyramidal neurons overexpressing Nur77 (GSE76805)[3] and gene identifier in the Ensembl database.

Table S.3: Nur77 target genes in NC.

List of genes that bind Nur77 in their promoter regions, according to the ChIP-Seq of NC, whose expression is modified when Nur77 is overexpressed in pyramidal neurons. Columns correspond to gene name, gene description from wikigene database[1], Nur77 peak location according to the ChIP-Seq from NC (GSM1603273)[4], Log2 of the fold of change

and p-value adjusted according to differential expression analysis of microarray from pyramidal neurons overexpressing Nur77 (GSE76805) [22] and gene identifier in the Ensembl database.

Table S.4: Nur77 target genes common to lymphatic and neuronal systems

Nur77 target genes, common to the immune and neural systems. Only genes exhibiting Nur77 binding in their promoters are listed. This set of genes was used for GO analysis.

Table S.5: GO terms enriched in the analysis of Nur77 target genes.

GO terms enriched in the GO analysis and Nur77 target genes classified in each term. One table for each of the three principals GO categories is shown in separate sheets.

Supplementary reference

1. Hoffmann R. A wiki for the life sciences where authorship matters. Vol. 40, Nature Genetics. Nat Genet; (2008).
2. Dunham, I. et al. An integrated encyclopedia of DNA elements in the human genome. Nature (2012).
3. Chen Y, Wang Y, Ertürk A, Kallop D, Jiang Z, Weimer RM, Kaminker J, Sheng M. Activity-induced Nr4a1 regulates spine density and distribution pattern of excitatory synapses in pyramidal neurons. Neuron (2014).
4. Terranova C, Narla ST, Lee YW, Bard J, Parikh A, Stachowiak EK, et al. Global developmental gene programing involves a nuclear form of fibroblast growth factor receptor-1 (FGFR1). PLoS One. (2015)